An integrative study on the controls of mercury (Hg) in the sediments and food webs of thermokarst lakes on the Arctic Coastal Plain of Alaska

by

Samantha Burke

A thesis
presented to the University of Waterloo
in fulfilment of the
thesis requirement for the degree of
Doctor of Philosophy
in
Biology

Waterloo, Ontario, Canada, 2019

Examining Committee Membership

The following served on the examining committee for this thesis. The decision of the examining committee is by majority vote.

External Examiner:	Dr. Britt Hall University of Regina, Professor of Biology
Supervisor:	Dr. Heidi Swanson University of Waterloo, Associate Professor of Biology, University Research Chair
Internal Member:	Dr. Roland Hall University of Waterloo, Professor of Biology
Internal-external Member:	Dr. Simon Courtenay University of Waterloo, Professor of Environment, Canadian Water Network Scientific Director
Other Member(s):	Dr. Brian Branfireun Western University Professor of Biology, Canada Research Chair University of Waterloo Department of Biology Adjunct

Author's Declaration

This thesis consists of material all of which I authored or co-authored: see Statement of Contributions included in this thesis. This is a true copy of the thesis including any required final revisions as accepted by my examiners.

I understand that my thesis may be made electronically available to the public.

Statement of Contributions

While the research in this thesis is my own, multiple collaborators provided guidance and valuable input to each data chapter. The following contents of this thesis are part of a collaborative project with the United States Geological Survey in Alaska, to investigate the biological responses to increasing water temperatures in lakes of the Barrow/Atqasuk watershed, led by the Alaska Science Center Director, Dr. Christian Zimmerman. The objectives included in this thesis were developed primarily by myself with guidance from Dr. Heidi Swanson to fit within the larger objectives of the collaborative project. Details for specific contributions to each chapter are outlined below.

Chapter 2: Burke, S. M., Zimmerman, C. E., Branfireun, B. A., Koch, J. C., & Swanson, H. K. (2018). Patterns and controls of mercury accumulation in sediments from three thermokarst lakes on the Arctic Coastal Plain of Alaska. *Aquatic Sciences*, *80*(1), 1.

This paleolimnological investigation was not included in the scope of the original collaborative project and was my original idea. We applied for additional funds to complete this work, which were approved. The field work for this chapter was conducted by myself and Christian Zimmerman in the summer of 2014. The lab analyses were completed primarily by myself at the University of Waterloo and Biotron at Western University. The sediment core chronologies were developed by Johan Wiklund of the University of Waterloo Water lab, pigment analyses were completed in PEARL at Queen's University, and water chemistry was completed at the University of Alberta Biogeochemical Analytical Services

Laboratory. Data analysis and interpretation was completed by myself with guidance from Heidi Swanson. All coauthors provided insights and edits during manuscript preparation and publishing.

Chapter 3: Burke, S. M., Branfireun, B. A., Guernon, S., Laske, S.M. Zimmerman, C. E., Branfireun, B. A., Koch, J. C., & Swanson, H. K. (2019) Fish growth rates and lake sulphate control mercury levels in Ninespine stickleback (*Pungitius pungitius*) on the Arctic Coastal Plain of Alaska (In Prep.).

This paper addresses one of the main objectives of the collaborative study— to describe mercury transfer through the food webs of Arctic Coastal Plain lakes; however, the specific questions posited in the paper were developed by myself with guidance from Heidi Swanson following the results of Chapter 2. The field work for this chapter was a herculean effort during the summer of 2016 with a crew that included: Christian Zimmerman, Heidi Swanson, Leanne Baker, Sarah Laske, Josh Koch, Stéphanie Guernon, Alexandra Crichton, and myself. All of the invertebrate, plant, and fish prep and mercury analyses were completed by me at the University of Waterloo and Biotron (Western University). The zooplankton prep, analyses and community composition were completed by Stéphanie Guernon. Stable isotope analyses were completed by Environmental Isotope Laboratory all at the University of Waterloo. Fish aging was completed by Sarah Laske at the USGS in Anchorage. Water chemistry analysis was completed at the University of Alberta Biogeochemical Analytical Services Laboratory. The data analysis and interpretation were completed by myself with

guidance from Heidi Swanson. This manuscript is in preparation for submission to a journal, and coauthors are providing insight and guidance.

Chapter 4: Burke, S. M., Laske, S.M. Zimmerman, C. E.& Swanson, H. K. (2019) Parasitism of Ninespine stickleback (*Pungitius pungitius*): impacts on growth and mercury on the Arctic Coastal Plain of Alaska (In Prep.).

The idea for this chapter was born upon discovering how intense the *Schistocephalus* infection rate was among the study lakes. I developed the objectives addressed in this paper. The contributions for field sampling and lab analyses are the same as chapter two. In addition, bomb calorimetry was completed by myself and Amanda Soliguin in the Power lab at the University of Waterloo. All data analysis and interpretation were completed by me with guidance from Heidi Swanson. This manuscript is in the preparation for submission to a journal, and coauthors will provide insight and guidance.

Abstract

Arctic freshwater ecosystems are subject to profound climate-driven changes. Air temperatures are rising, leading to changes that include increased primary production and enhanced permafrost degradation. These and other climate-related effects interact to influence the accumulation of mercury in sediments and food webs of Arctic lakes. Mercury is a neurotoxin that is harmful to human and animal health, and in its methylated form, mercury can be taken up and biomagnified through food webs. The controls on mercury deposition, bioaccumulation, and biomagnification are complex and spatially variable. An area where especially little is known about spatial and temporal variability in mercury accumulation is in the food webs and sediments of lakes on the Arctic Coastal Plain of Alaska (ACP), a lake-rich region in northern Alaska.

Sediment cores were collected from three thermokarst lakes on the ACP and analyzed to understand changes in, and drivers of, Hg accumulation over the past ~100 years (Chapter 2). Mercury accumulation in two of the three lakes was variable and high over the past century (mean=37.4 μg/m^2/year and mean = 45.8 μg/m^2/year), and largely controlled by sedimentation rate. Mercury accumulation in the third lake was lower (mean = 6.5 μg/m^2/year), more temporally uniform, and was more strongly related to sediment Hg concentration than sedimentation rate. Sediment mercury concentrations were quantitatively related to measures of sediment composition and VRS-inferred chlorophyll-*a*, and sedimentation rates were related to various catchment characteristics. These results were compared to data from 37 previously studied Arctic and Alaskan lakes. Results from the meta-analysis indicate that lake thermokarst lakes have significantly higher and more

variable Hg accumulation rates than non-thermokarst lakes, suggesting that properties of thermokarst lakes, such as thermal erosion, thaw slumping, and low hydraulic conductivity likely make these lakes prone to high and variable Hg accumulation rates.

Following the observation that catchment influence varied spatially on the ACP, and that it affected the amount of, and pathways by which, mercury accumulated in lake sediments (Chapter 2), I hypothesized that catchment influence may also affect how mercury enters and accumulates in lake food webs on the ACP. In Chapter 3, six lakes were sampled across a physico-chemical gradient on the ACP to investigate variability in methylmercury levels ([MeHg]) in Ninespine stickleback (*Pungitius pungitius*), a fish species that was present in all lakes. Evidence suggested that bioaccumulation of MeHg through lake food webs was indirectly affected by degree of catchment influence. Methyl mercury concentrations in sediments and filter feeding invertebrates were higher in lakes that were inferred to be more autochthonous (less catchment influence), but higher in periphyton from lakes that were inferred to be more allochthonous (more catchment influence). Regardless of catchment influence, benthic invertebrates had higher MeHg levels than zooplankton. MeHg levels in Ninespine stickleback were significantly related to one tracer of catchment influence, sulphate concentration in lake water, and length-adjusted MeHg levels in Ninespine stickleback were best predicted by age-at-size, an indicator of growth ($p=0.030$). Together, lake sulphate concentration and fish age-at-size accounted for nearly all of the among-lake variability in length-adjusted [MeHg] in stickleback ($R^2=0.94$, $p=0.006$). It is likely that different sources of production (littoral macrophyte/biofilm vs pelagic phytoplankton) and food web structure (detrital vs grazing) affect rates of methylation and uptake of MeHg into the six lake food webs that were studied, but further research is necessary.

As growth was found to be the best biotic predictor of length-adjusted MeHg concentrations in fish (Chapter 3), the focus of Chapter 4 was to understand effects of parasitism on growth and mercury concentrations in stickleback. Parasites are an important and often poorly understood component of aquatic ecosystems. The cestode *Schistocephalus pungitii* is a parasite of Ninespine stickleback. Little is known about the effects of parasitism on the growth and ecology of Ninepsine stickleback, nor how parasitic infection affects MeHg concentration in this important prey fish species. Fish growth, MeHg concentrations, and incidence and intensity of parasitism in Ninespine stickleback were investigated using samples collected from six lakes on the Arctic Coastal Plain of Alaska. Comparisons were made between parasitized and unparasitized fish. In addition, differences between hosts and parasites in $\delta^{15}N$, [MeHg], and caloric density were investigated to assess potential implications of parasitism on mercury transfer through the food web. There were differences in infection rate (ranging between 8-98%) and parasitization indices (ranging from 12-23%) among lakes; however, in all lakes, cestode parasites had significantly lower $\delta^{15}N$ ($p<0.0001$) and [MeHg] ($p=0.001$) than their fish hosts, and tissue from parasitized stickleback had significantly higher [MeHg] than tissue from unparasitized stickleback ($p=0.05$). Higher MeHg concentrations ([MeHg)] in tissue from parasitized stickleback appears to be a result of decreased growth rates, as there was a positive relationship between infection rate (percent parasitized) and fish age-at-size ($p=0.04$), and it was previously shown (Chapter 3) that [MeHg] in stickleback is positively related to age-at-size. To predators, parasitized stickleback could actually represent a prey source with relatively lower [MeHg], because the relative mass and MeHg concentration of the parasite significantly lowers the overall mercury concentration of the "fish meal" ($p<0.01$). In addition, parasitized stickleback have a

similar caloric density to their unparasitized conspecifics (p=0.11). Because higher infection rates have been observed (>50%) in other Arctic lakes, and because the fecundity of *S. pungitii* is predicted to increase with climate warming, it is possible that cestode parasites could actually create an overall dilution of mercury through the simple food chains of shallow Arctic lakes.

This thesis represents the first in-depth analysis of mercury accumulation in lake sediments and mercury concentrations in food webs of lakes on the Arctic Coastal Plain of Alaska. Results of this research provide further evidence that mercury dynamics in lakes are complex and can be directly or indirectly influenced by several biotic and abiotic factors. It is clear that catchment characteristics play a significant, yet not fully understood, role in the deposition and accumulation of mercury in lake sediments, and that catchment characteristics also affect methylation and uptake of mercury into the food webs. Results from this research will ultimately help inform predictions of how fish mercury concentrations may respond to climate change.

Acknowledgements

I would like to begin by acknowledging my numerous funding sources for making this research possible. Thank you to the Arctic Landscape Conservation Cooperative of the US Fish and Wildlife Service, for providing the research funds to conduct all field work and analyses. Thank you to the Northern Scientific Training Program for multiple grants for northern field work. Finally, thank you to the Natural and Engineering Sciences Research Council of Canada, the W. Garfield Weston Foundation, and the Davis family for awarding me with personal scholarships.

The technical assistance that I was provided in both the lab and the field was invaluable, and the people who have helped me are far too numerous to list. Special thanks to the following labs that were *instrumental* in the analysis side of things: University of Alberta Biogeochemical Analytical Services Laboratory, Biotron at Western University, PEARL at Queen's University, the WATER lab, Power lab, and Environmental Isotope Laboratory all at the University of Waterloo, and the USGS Alaska Science Center.

During my PhD I was fortunate to be selected for the Global Lake Ecological Observatory Network (GLEON) Fellowship Program. I would like to thank Paul, Kathie, and Hilary for their mentorship, as well as the eleven other fellows in my cohort. This program provided such a great opportunity to learn how to conduct collaborative science, and to learn many techniques for sourcing and analyzing high frequency data.

Thank you to my incredible thesis committee Brian, Roland, and Chris. You have each brought so much unique and valuable knowledge and experience to this thesis. Brian, you have gone above and beyond the role of a committee member—you have dedicated a lot of time and energy to my professional development, and I truly appreciate it.

Leanne, thank you for being my friend, stats guru, and sounding board. I am so grateful for the time and emotional energy you have spent on helping me through this marathon. Being able to flip between discussing ecology and all of our other various common interests has been a joy.

Thank you to Heidi for being the mentor and friend that I needed on this journey. You are a brilliant scientist, who has taken on the (often thankless) task of training students at the expense of your personal research time. You are such an incredible role model, and have taught me *so much* during my time at UW. You have been patient and empathetic, all while maintaining that there are "no feelings in science". On countless occasions I have come to you with a problem, and left your office laughing and feeling confident. I am so grateful that you encouraged me to pursue professional development opportunities, even though they took time away from my primary research goals. I look forward to collaborating with you in the future.

Mom and Dad, thank you for fostering my curiosity of the natural world and acting as my first field assistants. You have both been so supportive of my endeavors (academic or otherwise) and have always encouraged me to believe that I can accomplish anything, while

providing tough love when necessary. Finally, thank you to Steve for keeping me grounded and providing much-needed support, comfort, laughter, and the occasional distraction; you have been my light at the end of the tunnel.

Table of Contents

List of Figures

List of Tables

1 General Introduction

Climate change is expected to have pronounced impacts on Arctic freshwater ecosystems (Rouse et al. 1997). Although it is widely accepted that the ecology and hydrology of these systems will be altered, it is difficult to predict specific effects at regional or local scales, due to an incomplete understanding of how climate-induced changes to freshwater ecosystems (e.g., warmer summer water temperatures, increased or decreased dissolved organic carbon and turbidity, etc) will interact and manifest to affect changes in ecosystem structure and function. Elevated air and water temperatures are causing degradation of permafrost and changes in the amount and location of primary production, composition of biotic assemblages, fish growth rates, and parasite infection rates (see Prowse et al. 2006). All of these factors, along with changes to lake catchments and water chemistry, can have profound impacts on mercury accumulation in Arctic lake systems.

1.1 Mercury

Mercury (Hg) is a heavy metal that can be harmful to human and animal health. In the methylated form (methylmercury (MeHg)), mercury is a neurotoxin, and can bioconcentrate in lower trophic levels before bioaccumulating and biomagnifying through food webs (see Kidd et al. 1995; Atwell et al. 1998; Lockhart et al. 2005). While there are natural sources of Hg (e.g., volcanoes, unweathered sediments, and forest fires), the majority of Hg emitted to the atmosphere originates from anthropogenic sources (AMAP, 2019). As of 2015, artisanal gold mining comprised nearly 40% of anthropogenic emissions of Hg, followed by coal combustion (~ 21%; AMAP, 2019). Gaseous elemental mercury (Hg(0)) has a relatively

long residence time in the atmosphere (6-9 months; Lindberg et al. 2007) and can thus travel around the globe on prevailing winds to areas that are remote from sources, including the Arctic (see AMAP, 2011). It has recently been shown that gaseous elemental mercury can be taken up directly by northern vegetation (Obrist et al. 2017). Hg(0) can also be oxidized in the atmosphere, and deposited onto lakes and landscapes (see Lindberg et al. 2007). In response to environmental regulations, declines in atmospheric mercury emissions have been observed in recent years in Europe and North America, while they continue to increase in South and East Asia (see AMAP, 2019). It is difficult to predict future mercury mobilization to aquatic ecosystems because of effects of climate change on mercury cycling. Even if anthropogenic emissions of Hg to the atmosphere are curtailed, it is possible that mercury deposition to lakes will continue to increase due to mobilization of 'legacy' mercury that is currently stored in soils and oceans (Corbitt et al. 2011). Recently, Schuster et al. (2018) found that there was a globally significant amount of mercury stored in Northern Hemisphere permafrost (~800 Gg Hg).

The methylation of mercury is a complex and not yet fully understood process, by which a methyl group is added to divalent mercury (see Lehnherr et al. 2014). Mercury methylation is often thought to occur primarily at the sediment-water interface (e.g., Korthals and Winfrey, 1987) in aquatic ecosystems; however, methylation can also occur in the water column (e.g., Watras et al. 1995a, Mauro et al. 2002), catchment (e.g., St. Louis et al. 1994), and in biofilms (e.g., Mauro et al. 2002). While sulphate-reducing bacteria (SRB) are the primary methylators in aquatic ecosystems (Compeau and Bartha, 1985), methanogenic archaea and iron-reducing bacteria have also been identified as methylators (see Lehnherr et

al. 2014). There are several factors that control rates of mercury methylation, including the amount of bioavailable inorganic mercury, presence of suitable methyl donors, and environmental conditions (see Lehnherr et al. 2014). Methylation is favoured in anoxic (e.g., Olson et al. 1974; Compeau and Bartha, 1985), low pH (e.g., Golding et al. 2007; Winch et al. 2008) conditions. Concentrations of both dissolved organic matter (DOM) and sulphate affect mercury methylation, but the effects are complex. Although DOM can act as a substrate for methylating microbes, DOM can also bind with mercury and make it less available for methylation (see Ravichandran et al. 2004). Similarly, sulphate can stimulate SRB, which results in higher methylation rates. However, a product of sulphate reduction is sulfide, which has a high affinity for/can complex with, divalent mercury - making it biologically unavailable for methylating microbes (see Lehnherr et al. 2014). Gilmour et al. (1992) suggest that 0.1-0.5 mM sulphate in sediment is optimal for methylation. Above this range, methylation is inhibited by sulfide, whereas below this range sulphate is limiting.

MeHg, whether it is derived from in-lake methylation or from the catchment (e.g., St Louis et al. 1994, Bravo et al. 2017), can enter the water column and bioconcentrate in phytoplankton, bacteria, and benthic algae (see Morel et al. 1998, Pickhardt and Fisher 2007). Many trace metals can bioconcentrate in algae and bacteria; however, MeHg not only bioconcentrates but also bioaccumulates and biomagnifies, which results in increasing portions of total mercury (THg) being comprised of MeHg as trophic level increases (e.g., Watras and Bloom, 1992). Fish can have concentrations of mercury that are one million times that of the water they inhabit (Linqvist et al. 1991). Bioconcentration of MeHg from water to primary producers represents an important step in this process, as phytoplankton often have more than

ten thousand times the concentration of mercury as ambient water (Pickhardt and Fisher 2007).

The majority (80-90%) of MeHg in fish comes from their diet, with the remaining fraction coming from water (Hall et al. 1997). Originally, it was thought that the efficient biomagnification of MeHg was due to its liposolubility (Boudou and Ribeyre, 1997); however, it was later identified that fish have a higher burden of mercury in muscle tissue than in fats (Boudou and Ribeyre, 1997), and that MeHg is bound to the amino acid cysteine (Harris et al. 2003). While MeHg is lipophilic enough to cross the cell membrane, it preferentially binds to proteins, which is why it accumulates more efficiently than inorganic Hg and is able to biomagnify (see Morel et al. 1998).

Since methylmercury biomagnifies through aquatic food chains, concentrations are highest in top predators, which are often fish. This can pose a risk for fish-eating wildlife and humans, and it is through eating fish that humans are primarily exposed to MeHg (AMAP, 2019). Effects of mercury toxicity can include lack of coordination, impaired cognition, deafness and blindness (see Rice at al. 2014). Because MeHg binds with cysteine, it is able to cross the blood-brain barrier and can cross the placenta in pregnant women, which poses a risk for neonates (see Tchounou et al. 2003). Some Indigenous communities are at an elevated risk of mercury exposure through diet, as they rely heavily on fish for subsistence (AMAP, 2019).

There are many biotic and abiotic factors that control concentrations of methylmercury in fish, including the amount of MeHg available for uptake into the food web, rates of

biomagnification through the food web, and fish ecology and life history (see Lehnherr et al. 2014). The amount of MeHg available for uptake into food webs is determined by the amount of MeHg delivered directly to lakes from catchments, as well as bioavailable THg, the activity of methylating bacteria in lakes, and demethylation rates (see Lehnherr et al. 2014). The bioaccumulation of mercury in fish can be affected by a myriad of factors including growth rates (Karimi et al. 2007), trophic position (Kidd et al. 2012), fish age (Scott et al. 1972), and life history (Swanson et al. 2011); whereas the biomagnification of mercury through a food web can be impacted by variations in primary production (Pickhardt et al. 2002), and other physico-chemical factors (e.g., Kidd et al. 2012).

There is considerable uncertainty regarding effects of climate change on mercury magnification and accumulation in Arctic lake food webs (AMAP 2011). Climate change may affect the pool of available MeHg and its transfer through lake food webs through various mechanisms, one of which is increases in sediment mercury accumulation. Since one of the primary locations for mercury methylation is in sediment porewaters, the delivery of bioavailable THg can facilitate methylation. Results of paleolimnology studies reveal that Hg accumulation in Arctic lake sediments increased pre- (ca ~ 1850) to post-industry (see Landers et al. 1998). Anthropogenically derived mercury can be stored in catchment soils for years (see Grigal, 2002), and later deposited to lakes. This is of particular concern for lakes with permafrost soils in their catchments, as permafrost soils store nearly twice the amount of mercury as the atmosphere, oceans, and all other soils combined (Schuster et al. 2018), and permafrost is degrading at an accelerated rate (see Grosse et al. 2013).

Permafrost degradation, or thermokarstic activity, can result in mass amounts of catchment sediment and soil entering a lake (Grosse et al. 2013). These sedimentation events can lead to the release and downstream transport of stored THg and MeHg (e.g., Hinzman et al. 2005; Obrist et al. 2017; St. Pierre et al. 2018), as well as solutes like SO_4 (e.g., Roberts et al. 2017), and organic matter (e.g., Hinkel et al. 2012) to lakes and lake sediments. With continued climate change, further increases in sedimentation events are expected to result from permafrost degradation (see Grosse et al. 2013). Another climate-related mechanism that could influence mercury accumulation in sediments is increased primary production. Warmer air temperatures will lead to earlier ice-off in northern lakes, and consequently more light availability and higher primary production (see Prowse et al. 2006). Warmer temperatures are also expected to lead to increases in precipitation in the Arctic (Trenberth et al. 2011), resulting in greater nutrient deposition and higher primary production (Paerl and Huisman, 2008). Outridge and colleagues (2007) found a strong link between mercury accumulation in Arctic lake sediments and increases in lake primary production, and suggested that because algal-derived carbon has a high affinity for Hg, increases in production result in greater scavenging of mercury from the water column to sediments. Not only can increases in phytoplankton production enhance scavenging and thus availability of THg for methylation, but higher primary production can also stimulate methylation in sediments (Bravo et al. 2017).

Determining net effects of climate-related changes on mercury accumulation in Arctic lakes is exceedingly complex, as there are many ecological interactions through which a change in an environmental variable, such as lake temperature or primary production, may result in

either an increase or decrease in mercury concentrations in biota. For example, while higher primary production may increase mercury accumulation via algal scavenging of Hg from the water column and increased methylation rates, increased primary production may also decrease mercury accumulation through either bloom dilution or growth dilution. Following the observation that there were fish in oligotrophic lakes with much higher mercury concentrations than conspecifics in more productive lakes, Pickhardt et al. (2002) experimentally found that increasing algal biomass decreases the mercury concentration of individual algal cells, and termed the phenomenon 'bloom dilution.' 'Growth dilution' refers to the phenomenon by which faster growth rates in individual fish lead to lower concentrations of mercury (Karimi et al. 2007), and fish growth rates are expected to increase in the Arctic due to both warming water temperatures and increases in primary production (Reist et al. 2006b). Warming lake temperatures may also increase incidence and severity of parasitism (e.g., Marcogliese, 2001; Lv et al. 2006), however, which can lead to decreases in fish growth (e.g., Schultz et al. 2006). The complexity of direct and indirect effects that may either increase or decrease fish mercury concentrations in Arctic lakes makes it difficult to make predictions. This is especially true in regions with little data, such as the Arctic Coastal Plain of Alaska (AMAP, 2011).

1.2 The Arctic Coastal Plain of Alaska

The Arctic Coastal Plain of Alaska (ACP) is a lake-rich region of northern Alaska that extends from the foothills of the Brooks Range (69.4°N) to the Beaufort and Chukchi seas (71.3°N) within a zone of continuous permafrost. Approximately 40% of the ACP is covered in shallow, small isothermal lakes and ponds (Clilverd et al. 2009). Summer water temperatures range from 7 to 13°C (Hinkel et al. 2012), and waterbodies shallower than ~2m freeze to the bottom whereas deeper lakes without bedfast ice can become anoxic over winter (Clilverd et al. 2009). During the summer months, these lakes are well-mixed, and there is a strong positive relationship between air and water temperatures (Shuter and Post, 1990, Arp et al. 2011).

Lakes on the ACP are defined as 'thermokarst' or 'thaw' lakes, as they were formed through the degradation of ground ice. Many of the lakes on the ACP formed during the transition between the Pleistocene and Holocene, after the last Thermal Maxima (Grosse et al. 2013). These lakes are underlain by permafrost, and while thickness of the active layer (top layer of soil that seasonally thaws) typically varies between 0.6 and 0.8 meters deep (Hinkel et al. 2012), there is evidence that the active layer is deepening as a result of rising air temperatures (e.g., Jorgensen and Shur, 2007; Plug and West, 2009). Thermokarst events, or permafrost degradation, are expected to increase in frequency and magnitude with a warming climate in this region, and will result in thermal erosion, catastrophic lake drainages, and retrogressive thaw slumps, as well as a deeper active layer (see Grosse et al. 2013). Many of these processes can result in increased catchment-derived inputs of sediment and soil to lakes, and mobilization of legacy mercury stored in catchment soils.

Lakes on the ACP have been defined as ultraoligotrophic (Clilverd et al. 2009, often having chl-*a* concentrations <3µg/L (Hinkel et al. 2018). As in other Arctic regions, however, it is expected that these lakes will become more productive with rising air temperatures (see Prowse et al. 2006). Elevated air temperatures will lead to thinning lake ice (e.g., Arp et al. 2012) and longer ice-free seasons (e.g., Dibke et al. 2011), consequently leading to more light availability and increased primary production (Huisman et al. 1994). Warmer air temperatures may also result in greater thermal stability (MacIntyre et al. 1999; Verburg and Hecky, 2009) and anoxia, which can cause limiting nutrients (e.g., phosphorous) to regenerate more rapidly and foster a subsequent increase in production (Wagner and Adrian, 2009). There have been multiple climate-related studies on the ACP, including one on changing ice regimes (Arp et al. 2012), and another on lake expansions and drainages (Hinkel et al. 2007). Most of these studies have focussed on changes to the physical landscape and hydrology; however, Lougheed et al. (2011) resampled a series of tundra ponds on the ACP that was originally investigated in the 1970's. The authors found that there were increases in water temperature, nutrients, and primary production (Lougheed et al. 2011). To date, there have been no studies completed on effects of these changes on mercury in sediments, water, or biota.

The food webs of ACP lakes are simple, and contain few fish species (e.g., Carey and Zimmerman, 2014; Laske et al. 2018). The most common fish species are Ninespine stickleback (*Pungitius pungitius*) and Alaska blackfish (*Dallia pectoralis*). Ninespine stickleback are a small freshwater fish species from the family Gasterostidae that is found

throughout the circum-Arctic, and primarily feeds on zooplankton and dipteran larvae (Hynes, 1950). Alaska blackfish, a member of the Esocidae family, is another small-bodied fish species found in Arctic Alaska, Siberia, and the Bering Strait Islands that primarily feeds on zooplankton and invertebrates (Ostdiek and Nardone, 1959). Both of these fishes can tolerate low oxygen (e.g., Lewis et al. 1972, Crawford, 1974), and stickleback can also tolerate high salinities (Nelson, 1968). It is the ability of both of these species to tolerate winter conditions (e.g., low oxygen, high salinity) that explains their ubiquity in ACP lakes (Haynes et al. 2014). Less common fish species in lakes on the ACP of Alaska include Arctic grayling (*Thymallus arcticus*), Broad whitefish (*Coregonus nasus*), and Least cisco (*Coregonus sardinella*) (Carey and Zimmerman, 2014). It is possible that fish community composition on the ACP could change with rising air temperatures. An ongoing northward range shift in some cool-water fishes (e.g., Northern pike (*Esox lucius*), Yellow perch (*Perca flavescens*), Walleye (*Sander vitreus*)) could lead to resource competition with native taxa (see Reist et al. 2006b). These range shifts and the concomitant changing community composition, will change food web structure and likely mercury dynamics; however, data characterizing these effects are sparse.

Growth of fishes on the ACP may also change with a warming climate. It has been well established that, within a species, fish grow faster at the warmer extent of their range, as long as thermal optima are not exceeded (e.g., Lagler et al. 1977). Climate change will likely increase fish growth directly via warming lake temperatures (Hill and Magnuson, 1990, Reist et al. 2006b), but if previously well-mixed lakes begin to stratify, growth of fishes, especially cold-water fishes, may decrease via temperature-related changes in habitat use, including

exclusion from the warmest epilimnetic and benthic habitats (e.g., Guzzo et al. 2016). As mercury is often higher in pelagic food chains than in benthic food chains (Power et al. 2002), climate-induced changes in habitat use will likely affect bioaccumulation of Hg in fishes, but predictions are poorly constrained at present.

Fish growth, food web structure, energy flow, and thus, Hg accumulation, in northern lakes can be substantially altered by the presence and ecology of parasites. Parasites play an important but under-researched role in aquatic food webs (Lafferty et al. 2008). They can increase food chain length and the amount of omnivory, consequently altering overall structure and function of the food web (Lafferty et al. 2008; Thieltges et al. 2013). Fish parasites that live inside their hosts are referred to as endoparasites, whereas those that live on external body surfaces are referred to as ectoparasites. Since many endoparasites divert nutrients from their host organisms, infection can lead to a reduction in fish growth rate (e.g., Shultz et al. 2006). There are several expected direct and indirect effects of climate change on freshwater parasites. Longer growing seasons and higher temperatures should lead to more annual generations of parasites (Marcogliese, 2001). Previous research has shown that infection rates of both eye-dwelling diplostomatid trematodes (Höglund and Thulin, 1990) and intestinal acanthocephalans (Eure, 1976) are substantially greater in fish from waters warmed by industrial cooling water. More recently, a study found that the cestode parasite *Schistocephalus solidus* that infects Three-spined stickleback (*Gasterosteus aculeatus*), had higher plerocercoid (larval parasite) growth rates in elevated water temperatures (Macnab and Barber, 2012). In fact, plerocercoids from fish reared in 20°C were on average four times the weight of those from hosts reared in 15°C, which is especially concerning because

there are direct relationships between plerocercoid weight and fecundity (Macnab and Barber, 2012). In the same study, the authors found that infection by *S. solidus* causes Three-spined stickleback hosts to seek out warmer microhabitats, which increases the rate of life-cycle completion (Macnab and Barber, 2012). To my knowledge, no research has been conducted on the effects of *Schistocephalus* infections on the energy flow and contaminant dynamics in Arctic Alaska; however, since they affect fish growth and food web structure, they will likely affect Hg accumulation in ways that we do not yet understand.

1.3 Study Area

To address gaps in understanding of the complex interactions that affect Hg accumulation in shallow thermokarst lakes in the Arctic, I chose to study several lakes on the Arctic Coastal Plain of Alaska, and examine various aspects of Hg delivery from catchments, lake physico-chemistry, food web structure, fish growth rates, and parasitism. The lakes in this study were selected from a group of lakes monitored by the Circumarctic Lake Observation Network (CALON; Fig 1), and represent three regions on the ACP: the Barrow Region (BRW), the Atqasuk Region (ATQ) and the Reindeer Camp Region (RDC; Fig 1). Utqiagvik (previously known as Barrow) is located on the coast of the Beaufort and Chukchi seas and is located in the BRW region. It is the largest community on the Arctic Coastal Plain, and the northernmost settlement in the United States of America. The Iñupiat have lived in Utqiagvik for the past 1500 years, and of its current population of ~ 4000 people, greater than 60% are Indigenous (Census of Population and Housing, 2013). Atqasuk, located in the ATQ region, is a community south of Utqiagvik with a population of ~250, with nearly 95% of the population being Indigenous. The Iñupiat historically are hunter-gatherers and still rely heavily on hunting and fishing for subsistence. There are no communities in or near the RDC region.

As mentioned above, little is known about the deposition and accumulation of mercury in sediments, or the uptake and bioaccumulation of mercury in the food webs of lakes on the Arctic Coastal Plain of Alaska. However, we do know that air temperatures in this region are rising at an accelerated rate (Przybylak et al. 2007), and that concomitant changes, including increased precipitation (Hinzman et al. 2005), and warming permafrost (~3°C; Clow and

Urban, 2002) are occurring. All of these changes could have implications for mercury accumulation. As such, I sought to characterize patterns and understand drivers of mercury in the sediments and food webs of lakes on the Arctic Coastal Plain of Alaska, and interpret results in the context of a changing climate.

1.4 Thesis Structure and Research Objectives

The overarching goal of this research was to identify patterns and understand drivers of mercury in the sediments and food webs of lakes on the Arctic Coastal Plain of Alaska. Using a variety of techniques and approaches, including paleolimnology, stable isotope analysis, and bomb calorimetry, I investigated and compared transport and accumulation of mercury among several lakes.

In Chapter 2, I employed a paleolimnological approach to investigate mercury accumulation rates in sediments of 3 lakes during the past ~ 100 years. I explored drivers of within- and among-lake variation, and placed results in a larger landscape context by performing a meta-analysis. Specifically, I aimed to:

a. Characterize patterns of Hg accumulation during the past ~ 100 years in sediments from three lakes that represented the Barrow, Atqasuk, and Reindeer Camp regions;
b. Identify environmental variables (e.g., chl-*a* concentration, organic matter content, sedimentation rate) that influence temporal patterns of sediment Hg accumulation within lakes, and compare effects of environmental drivers among the three study lakes; and,
c. Collate mercury accumulation and other sediment proxy data from previously published studies on Arctic and sub-Arctic lakes, and interpret sediment Hg accumulation rates in the context of thermokarst landscape types.

In Chapter 3, I aimed to investigate biotic and abiotic controls of mercury in food webs of six lakes on the Arctic Coastal Plain of Alaska. The lakes represented the Atqasuk and Reindeer Camp regions. I determined levels of methyl mercury in fish and lower trophic level organisms, and compared concentrations among lakes and between regions. I explored causes of among-lake and between-region variability by relating mercury levels to a suite of relevant covariates. In this chapter, my objectives were to:

a. Determine if differences in lake physico-chemistry between the Atqasuk and Reindeer Camp regions were consistent with inferences generated by the paleolimnological study (Chapter 2);
b. Test whether there were differences in MeHg between regions and/or among lakes in abiotic (i.e., water, sediment) and biotic (i.e., bulk zooplankton, periphyton, benthic invertebrates, and fish) ecosystem compartments that were consistent with predictions generated by analyses of sediments and lake physico-chemistry; and,
c. Examine causes of variability in MeHg concentrations in biota by relating MeHg concentrations to a suite of abiotic and biotic covariates.

Building on the results of Chapter 3, I endeavoured to understand the effects of parasitism on growth and mercury concentrations in Ninespine stickleback (*Pungitius pungitius*) in Chapter 4. I determined the prevalence and intensity of parasitism in each of six study lakes that represented the Atqasuk and Reindeer Camp regions, and investigated effects of parasitism on growth, mercury concentrations, and energy density in Ninepspine stickleback. In this study, I aimed to:

a. Determine if there were differences in the magnitude of *Schistocephalus pungitii* infections in Ninespine stickleback among the six study lakes and between the two regions;
b. Further elucidate the trophic ecology of *S. pungitii* parasites by comparing the trophic position ($\delta^{15}N$) and MeHg concentrations between parasite and host; and,
c. Examine effects of parasitism on Ninespine stickleback growth, energy density, and MeHg concentration.

Results from Chapters 2-4 are synthesized in Chapter 5, in which I propose a conceptual model for the mercury dynamics of lakes on the Arctic Coastal Plain and discuss implications of results in the context of a rapidly changing climate.

1.5 Research Approaches

Completion of this research required integration of several different approaches, and included application of a variety of paleo and contemporary techniques used in limnology and aquatic ecology. A paleolimnological approach was used to address the objectives in Chapter 2. Paleolimnology involves the reconstruction of past limnological conditions using chemical, physical, and biological information that is preserved in lake sediments, and is particularly useful when long-term monitoring data are unavailable and/or insufficient (Smol, 2009). Through radiometric dating techniques, approximate dates can be attributed to sections of a sediment core, and related to changes in numerous biological and chemical indicators. Paleolimnology has been used extensively to describe environmental change in the Arctic (e.g., Wolfe et al. 2002; Vadeboncoeur et al. 2003; Smol et al. 2005; Quinlan et al. 2005; Michelutti et al. 2005). In Chapter 2, I used concentrations of chlorophyll-*a* in sectioned sediment cores to infer past primary production, and calculated sedimentation rates (through radiometric dating) and measured Hg concentrations in sediments to calculate past Hg mercury accumulation.

A variety of laboratory techniques and methods were applied to contemporary samples that were collected in support of the studies conducted in Chapters 3 and 4. Stable isotope ratios of nitrogen (N; $\delta^{15}N$) and carbon (C; $\delta^{13}C$) were used to quantify trophic position and carbon source, respectively, of Ninespine stickleback, zooplankton, benthic invertebrates, and *S. pungitii*. Stable isotope analysis (SIA) is a robust and commonly used tool to examine food web structure and basal sources of production. Organismal $\delta^{15}N$ values exhibit stepwise enrichment between trophic levels, which allows for the estimation of relative trophic

position (Minagwa and Wada, 1984). Conversely, enrichment of $\delta^{13}C$ is negligible with each trophic transfer through the food web, and thus can be used to infer origins of dietary carbon (Rounick and Winterbourn, 1986; Peterson and Fry, 1987; Cabana and Rasmussen, 1996). I used stable isotope ratios to infer food web structure in the study lakes, to investigate possible causes of among-lake and between-region variability in biotic mercury concentrations, and to examine trophic ecology of an under-studied parasite, *S. pungitii.*

While results from stable isotope analysis can lend insight into food web structure and predator-prey relationships, complementary application of bomb calorimetry can help further elucidate prey quality (i.e., energy density) and energy flow in food webs (e.g., Gaye-Siessegger et al. 2004). In oxygen bomb calorimetry, heat produced from the combustion of an organic compound is measured under constant pressure in the presence of excess oxygen. Results can be used to calculate caloric density. Estimates of caloric density of fishes are required to parameterize bioenergetics models, to quantify importance of distinct predator-prey linkages, and to draw inferences on energy flow that results from different habitats (e.g., Cummins and Wuycheck, 1971; Hartman and Brandt, 1995). I used bomb calorimetry to quantify the caloric density of stickleback and their cestode parasites *S. pungitii*, and to determine whether there were energy differences between parasitized and unparasitized fish.

1.6 Figures

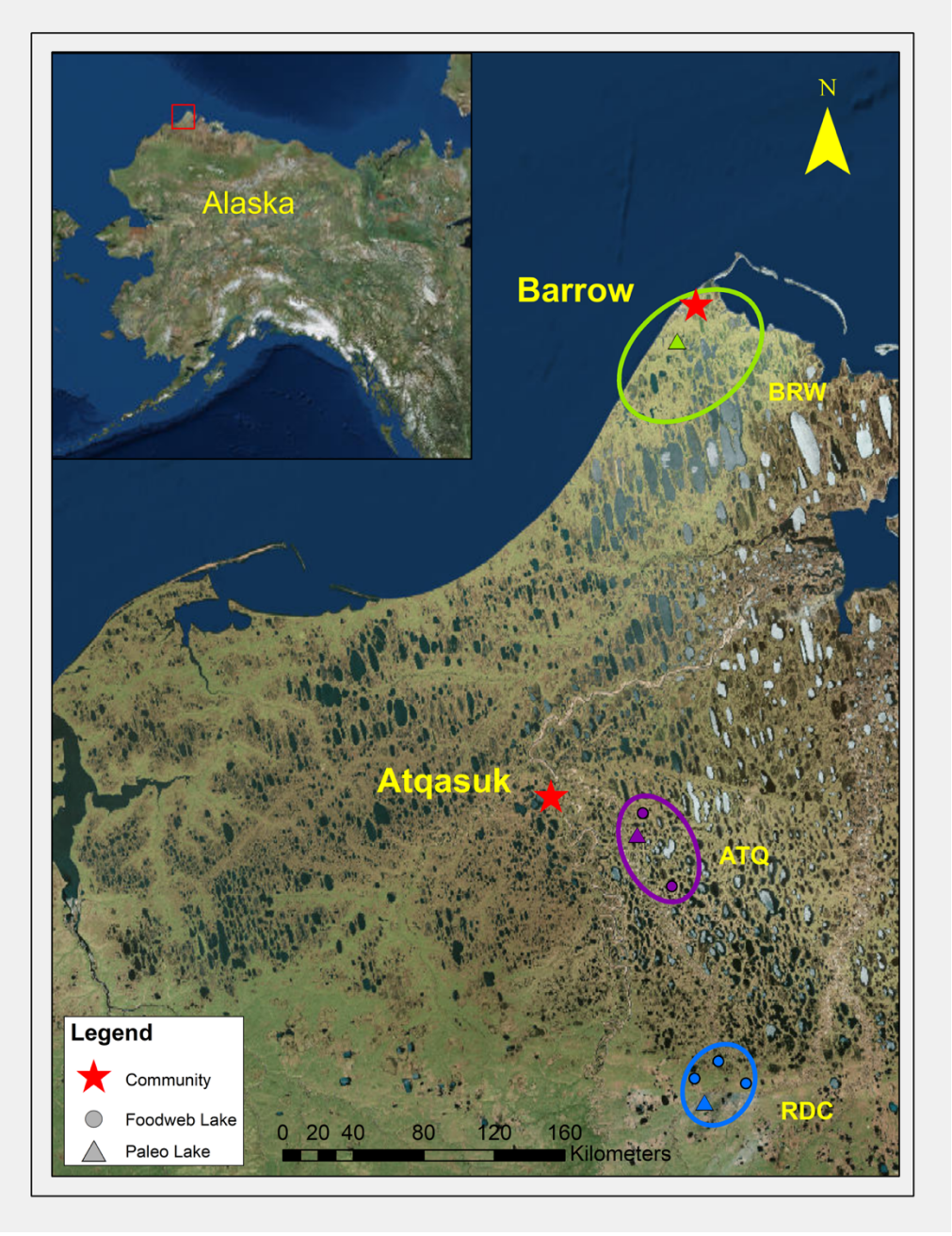

Figure 1.1. Map of study lakes on the Arctic Coastal Plain of Alaska. Blue symbols represent the Reindeer Camp (RDC) region, purple symbols represent the Atqasuk (ATQ) region, and green symbols represent the Barrow (BRW) region; triangles represent lakes that were included in the paleolimnological study (Chapter 2) whereas circles represent lakes that were included in the food web studies (Chapters 3 and 4).

2 Patterns and controls of mercury accumulation in the sediments of three thermokarst lakes on the Arctic Coastal Plain of Alaska

2.1 Introduction

Mercury (Hg), in an organic, methylated form (monomethylmercury; MeHg), is a neurotoxicant that bioaccumulates and biomagnifies through aquatic food webs (see Kidd et al. 1995; Atwell et al. 1998; Lockhart et al. 2005), and can reach concentrations in fish that can be harmful to fish-eating wildlife and humans. Post-industrial (ca.1850) increases in Hg emitted to the atmosphere can largely be attributed to the combustion of coal (Driscoll et al. 2013). In North America, Hg emissions from the power sector have decreased from their peak in the 1980s due to emissions controls (Slemr et al. 2003); however, there have been recent increases in coal combustion (and thus, Hg emissions) for electricity production in other regions, including Asia. In addition, other industrial activities, such as artisanal gold mining, are emerging as significant contributors to the global atmospheric pool of Hg (see AMAP, 2011), thus making the future of Hg emissions unclear. Changes in Hg deposition, and the degree to which anthropogenic emissions have contributed to the pool of Hg in aquatic ecosystems, are often assessed using paleolimnological approaches, as lake sediments can act as a natural archive preserving information in the absence of an instrumental record.

In combination with sedimentation rates, mercury concentrations in dated lake sediment cores are used to produce reliable records of historical Hg accumulation rates (e.g., Biester et al. 2007). Numerous studies have reconstructed historical Hg accumulation rates in lake sediments (e.g., Yang et al. 2003; Fitzgerald et al. 2005; Drevnick et al. 2012), and found near ubiquitous increases in Hg accumulation rates from pre-industry (pre ca. 1850) to

present. Ratios of modern to pre-industry Hg concentrations (termed enrichment factors), or Hg accumulation rates (termed flux ratios), are often used to assess anthropogenically driven changes in lake sediment Hg (e.g., Landers et al. 1998; Bindler et al. 2001). Studies conducted at temperate latitudes have reported a large range of Hg flux ratios in lake sediments; 2.1-6.9 in Vermont and New Hampshire (Kamman et al. 2002), 3.6-9.8 in Minnesota (Engstrom et al. 2007), and 1.6-5.7 (Lorey and Driscoll, 1999) and 3-30 (Bookman et al. 2008) in New York. Variability in flux ratios among these temperate lakes can largely be explained by distance from point sources of Hg emissions.

Results from studies conducted on sediment cores from Arctic lakes indicate that increases in Hg flux have occurred from ~1850 to modern times, and that these increases are in general more modest (a mean flux ratio of 3) than many of those observed in temperate systems (see Landers et al. 1998) – reflecting greater distance from point sources. Increases in Hg flux from pre-industry to modern times (a flux ratio >1) have been described for 53 of 56 Arctic lakes reported in eight different primary and synthesis publications (Hermanson et al. 1998; Landers et al. 1998; Bindler et al. 2001; Outridge et al. 2007; Muir et al. 2009; Drevnick et al. 2012; Deison et al. 2012; Drevnick et al. 2016). Reported modern Hg fluxes for lakes in the aforementioned studies varied by ~30-fold (mean of 14 $\mu g/m^2$/year), while Hg concentrations for these same lakes varied ~3-fold (mean of 150 ng/g).

Although increases in the global atmospheric pool of Hg since pre-industry have resulted in increases in Hg accumulation in the vast majority of lakes studied, the degree of increase varies, and some of this variation is due to among-lake differences in physical and biological

characteristics of lakes and catchments. Relative catchment size affects the rate at which atmospherically derived Hg is delivered to both Arctic (see Drevnick et al. 2012) and temperate (Grigal et al. 2002) lakes. Lakes that have greater catchment to lake area ratios (relative catchment sizes) have been found to respond to changes in atmospheric Hg emissions more slowly than those with smaller catchment to surface area ratios, due to the storage and gradual release of "legacy" Hg in catchment vegetation, litter, soil and groundwater (see Grigal, 2002; Harris et al. 2007). Catchment soil composition also affects delivery of Hg to lakes and lake sediments. Mercury (either anthropogenic or natural) that is retained in catchment soils is often strongly sorbed to organic matter (OM), and thus the amount of OM and the rate of OM decomposition can affect the magnitude and timing of release of Hg from catchments to downstream lakes (see Grigal, 2002). In thermokarst lakes that receive drainage from OM-rich peats, Hg delivery to lakes can also be affected by degradation of permafrost.

The potential contribution of legacy Hg (stored in the catchment) to lake sediments is particularly large for Arctic thermokarst lakes. 'Thermokarst' refers to the process by which ice-rich permafrost soils degrade, causing land subsidence, water impoundment, and the formation and expansion of surface water bodies, such as lakes. Over 20% ($3.6 \times 10^6 km^2$) of the northern permafrost region is characterized as thermokarst landscape (Olefeldt et al. 2016). Recently, Olefeldt et al. (2016) delineated the areal extent of three different categories of thermokarst landscape - hillslope, lake, and wetland – using a conceptual modeling framework that accounted for presence of distinct thermokarst landforms and other landscape characteristics, such as ground ice content, terrestrial ecoregion, and presence of

permafrost peat soils (histels). ‘Lake thermokarst’ landscapes are characterized by lake initiation, expansion, drainage, and drainage basin formation (Olefeldt et al. 2016). ‘Wetland thermokarst’ landscapes are characterized by landforms such as thermokarst bogs, fens, and shore fens, and ‘hillslope thermokarst’ landscapes by active layer detachment slides, retrogressive thaw slumps, thermal erosion gullies, beaded streams, and thermokarst water tracks (Olefeldt et al. 2016).

Rising temperatures resulting from climate change affect the frequency and magnitude of thermokarstic processes (e.g., thermal erosion, catastrophic drainages, and retrogressive thaw slumps; see Grosse et al. 2013), and thus Hg delivery to lakes. Thermokarst lakes are formed through degradation of ground ice, and once a thermokarst lake is formed, it tends to grow laterally through thermal and mechanical erosion into adjacent ice-rich permafrost deposits and soils, which can lead to shoreline collapse (Jorgenson and Shur, 2007; see Grosse et al. 2013). When a lake expands via thermal erosion, large amounts of soil or sediment, which contain bound Hg, are mobilized and deposited into the lake (see Grosse et al. 2013). The amount of Hg deposited is largely dependent on soil and sediment characteristics, and the degree of interaction with atmospherically-deposited Hg over time (Oswald et al. 2014). Thermokarstic events that affect catchments with soils rich in organic matter (OM) may result in relatively high Hg delivery to lakes, as soil OM generally has higher total Hg (Oswald et al., 2014) and a greater proportion as MeHg (see Bravo et al. 2017), whereas thermokarstic events that affect catchments with soils rich in minerogenic matter could result in Hg concentrations being diluted in lake sediments (Deison et al. 2012).

Rising temperatures can also influence the delivery of Hg to lake sediments by increasing lake primary production (Outridge et al 2007). In previous studies, a large portion of post-industrial increases in Hg in Arctic lake sediments has been attributed to increases in autochthonous primary production and algal scavenging (Outridge et al. 2007; Stern et al. 2009). The 'algal-scavenging hypothesis' originated from observed positive relationships between sediment Hg concentration and S2 carbon (the algal-derived component of organic carbon). Kirk et al. (2011) found, however, that in 7 of 14 Arctic lakes, the relationship between sediment Hg concentration and algal S2 carbon content was not significant, suggesting that changes in sediment Hg concentrations and fluxes could not be attributed to changes in primary production alone.

The Arctic Coastal Plain of Alaska is a 'lake thermokarst' region that stretches from the Brooks Range (68°N) to the Arctic Ocean (71°N), and covers an area of approximately 300 000 km^2. There is a paucity of information (i.e., no down-core studies) on Hg accumulation in sediments for lakes on the Arctic Coastal Plain compared to other regions in Alaska and the Arctic. Studies of temporal patterns in Hg accumulation have been completed on higher relief lakes further south in Alaska that are not formed or affected by thermokarst processes (e.g., Allen-Gil et al. 1997; Engstrom et al. 1997; Landers et al. 1998; Fitzgerald et al. 2005). Fitzgerald et al. (2005) found that Hg accumulation rates in foothills lakes near the Brooks Range (64°N, 147°W) had increased three-fold since ca. 1850, indicating anthropogenically driven increases in Hg delivery to these lakes. Based on the finding that pre-industrial Hg accumulation rates in sediment were higher than those found in other Arctic lakes, Fitzgerald et al. (2005) also concluded that erosional inputs of Hg to lakes in the Brooks Range were

relatively more important than in other Arctic lakes. Concentrations of Hg and other metals have been found to be naturally elevated in sediments of Arctic Alaskan lakes relative to uncontaminated lakes in other Arctic and temperate regions, due to mineral rich soils (Allen-Gil et al. 1997). The importance of erosional inputs of naturally derived Hg to thermokarst lakes on the Arctic Coastal Plain is unknown.

Our overall objective was to consider dominant controls on, and variability among, sediment Hg accumulation rates in Arctic and subarctic lakes. Specifically, we aimed to: 1) characterize patterns of Hg accumulation during the past ~100 years in sediments of three Arctic Coastal Plain lakes in Alaska; 2) identify factors (e.g., Chl-*a* concentration, organic matter content, sedimentation rate) that influenced patterns of sediment Hg accumulation, and compare results among the three study lakes; and, 3) collate mercury accumulation and other sediment proxy data from previously-published studies on Arctic and sub-Arctic lakes (n=37), and interpret sediment Hg accumulation rates in the context of thermokarst landscape types. Results were interpreted in the context of evaluating how changing climate could affect Hg accumulation rates in Arctic thermokarst lakes.

2.1 Methods

Study area

The three lakes for which primary data were collected for this study are located on the Arctic Coastal Plain of Alaska, an area that extends north from the foothills of the Brooks Range (68°N) to the Chukchi and Beaufort Seas (71°N). The lakes are located on low-relief tussock Tundra within a zone of continuous permafrost, and span a distance of three degrees of latitude. Selected from a larger set of lakes monitored by the Circum-Arctic Lakes Observation Network (http://arcticlakes.org), the lakes are (north to south) Barrow 100 (BRW 100), Atqasuk 206 (ATQ 206), and Reindeer Camp 312 (RDC 312; Fig. 2.1). These lakes are representative of other thermokarst lakes in the northern permafrost region, as they occupy depressions formed by the degradation of ground ice and rely on snowmelt and summer rainfall to maintain a water balance (Grosse et al. 2013). Specific location and physiographic information about the study lakes is in Table 2.1.

Sample collection and preparation

In August 2014, sediment cores were collected in duplicate (to provide sufficient mass for future analyses) from each of the three lakes, using a Glew gravity corer fitted with a Lucite tube (7.6 cm internal diameter). Sediments were extruded into 0.5 cm segments with a Glew extruder, placed in 4oz Whirl-pak® bags, and kept in the dark at 4°C while in transit to the laboratory at the University of Waterloo (Waterloo, Ontario, Canada). Samples were then stored in the dark at 4°C before ~0.5 g subsamples of each core segment were analyzed for loss on ignition (LOI) to quantify percent organic matter (%OM) and percent mineral matter

(%MM). LOI analyses were completed at the WATER lab at the University of Waterloo, following methods from Dean (1974).

Sediment dating and sedimentation rates

Freeze-dried subsamples of sediment from 1 cm intervals were analyzed from one core from each lake to determine total and supported ^{210}Pb activity using an Ortec co-axial HPGe Digital Gamma Ray (Ortec GWL-120-15) Spectrometer interfaced with Maestro 32 software (version 5.32; Ortec, 2006) at the University of Waterloo's WATER Lab.

Chronologies for each sediment core were developed using the constant rate of supply model (Appleby, 2001), which assumes that the flux of ^{210}Pb from the atmosphere is constant and adjusts for variations in sedimentation rate (see Figure S2.1-S2.3, Appendix A). Sedimentation rates were calculated using ^{210}Pb dates and cumulative dry mass. All subsequent analyses were completed on sediment from the one core in each lake for which chronologies were developed.

Total mercury analysis

Total mercury analysis was completed on homogenized freeze-dried sediment at 1 cm intervals (beginning at 0.5 cm) at the Biotron Centre for Experimental Climate Change Research at Western University (London, Ontario, Canada). Sample sizes were approximately 50 mg. Analyses were completed on a Milestone® DMA-80 Direct Mercury Analyzer in accordance with U.S. EPA method 7473 (U.S. EPA, 2007). A certified reference material (MESS-3; Marine Sediment Certified Reference Materials from the National Research Council, Ottawa, Ontario) was analyzed at the start of each run and after every 10

samples (mean recovery: 109.9% ± 15.3 SD, *n*=9). Blanks were analyzed at the start of each run and after every 10 samples (*n*=4). All Hg concentrations are expressed as ng/g dry weight.

VRS-inferred chlorophyll-a analysis

Chlorophyll-*a* (Chl-*a)* concentrations were inferred using visual reflectance spectroscopy (VRS) at the Paleoecological Environmental Assessment and Research Lab (PEARL) at Queen's University (Kingston, Ontario, Canada). The VRS method provides a means to infer changes in whole lake primary production, as it detects chlorophyll-*a* and its derivatives, which negates the need to account for pigment diagenesis (Michelutti et al. 2010). Briefly, sediments (from intervals alternate to those used for Hg analyses) were freeze-dried and sieved to 125 μm to homogenize the samples and improve replication. Following this, sediment from each interval was analyzed using a FOSS NIRS (Near Infrared Spectrophotometer) system Model 6500 rapid content analyzer to obtain sediment reflectance. For each interval, chlorophyll-*a* concentrations were inferred based on the measured amplitude of a trough in percent reflectance at 650-700nm wavelengths (the red portion of the spectrum; Wolfe et al. 2006).

Aerial imagery analysis

Historical aerial imagery was obtained from the United States Geological Survey EarthExplorer https://earthexplorer.usgs.gov/ (USGS, 2016). These images were geo-referenced using the ArcGIS™World Imagery Basemap (ESRI, 2014). The geo-referenced lakes were manually converted into polygons, and their surface areas were calculated to

quantify changes in lake surface area over time. Surface area of Arctic Coastal Plain lakes tends to increase in spring and early summer due to snow melt. We therefore chose to quantify and compare lake surface areas between 1948 and 2005, as images in these years were captured on Aug 2nd and Aug 1st, respectively. Obvious physical changes within the catchment were also noted using all images. All aerial imagery analyses were completed using ArcMap™10.2.2 (ESRI, 2016).

Comparisons with other Arctic and subarctic lakes

To provide further context for results, and to compare Hg accumulation rates from our study to other studies, a literature search for available published down-core data from other Alaskan and Arctic lakes was conducted. Overall, data were compiled for 37 additional lakes (33 Arctic, 4 Alaskan subarctic; Fig. 2.1, Table 2.2; see Table S2.1, Appendix A). If accumulation rates were not reported, sedimentation rate and mercury concentration were used to calculate them. Where raw or tabular data were not available, values were extracted from published figures using WebPlotDigitizer v3.10 (Rohatgi, 2016). To account for in-lake matter transfer and to strengthen among-lake comparisons, focus-corrected accumulation rates were used when focusing factors were available. Uncorrected rates were used when focusing factors were not available. All lakes, including the three lakes sampled, were assigned a landscape type (hillslope thermokarst, lake thermokarst, non-thermokarst) based on their coordinates and the maps generated by Olefeldt et al. (2016); a lake was assigned a designation if the dominant landscape type had moderate (10-30%) or high (30-60%) coverage of a particular landscape type. All data and metadata are located in the Table S2.1 (Appendix A).

Data analysis

Statistical tests were completed using R Studio v 1.0.136 with the core packages in addition to 'Kendall' (McLeod, 2015). Figures were generated using either SigmaPlot v11.0 (Systat, 2008) or ArcMap™10.2.2 (ESRI, 2016). To determine if there were significant temporal monotonic trends in Hg accumulation, Hg concentration, and chlorophyll-*a*, Mann-Kendall tests were completed for the entire core of each of the three study lakes. Mann-Kendall tests were also completed on Hg accumulation rates for each of the 37 lakes for which data were compiled from the literature. Mercury accumulation rates were calculated as the product of sedimentation rate and Hg concentration. To determine which variable accounted for more of the variability in Hg accumulation rate, Hg accumulation rates were related to each of sedimentation rate and Hg concentration using simple linear regressions. To determine if chlorophyll-*a* concentrations and/or %OM explained variability in Hg concentrations, sediment Hg concentrations from each lake were related to VRS-inferred chlorophyll-*a* concentrations and %OM using simple linear regressions. Finally, to assess how Hg accumulation rates varied among thermokarst landscape types, mean Hg accumulation rates for all 40 lakes (3 sampled in this study, 37 from literature) were compared among lake thermokarst, hillslope thermokarst, and non-thermokarst, landscapes (determined from Olefeldt et al. 2016) with an ANOVA and post-hoc Tukey's test.

2.3 Results

Historical changes in lake sediment mercury and primary production

The sediment core used in this study from BRW 100, the northernmost study lake, was 16 cm long. The bottom of the core was dated to 1942, suggesting a relatively high rate of sediment accumulation (mean 0.04 ± 0.02 g/cm^2/year). Mercury concentrations ([Hg]) in the BRW 100 core decreased from 101 ng/g to 81 ng/g between 1942 and 2014, and this trend was significant (Fig. 2.2; Mann-Kendall: S=-61, τ=-0.58, p=0.002). A significant increase in VRS-inferred Chl-*a* also occurred between 1942 and 2014 (Fig. 2.2; Mann-Kendall: S=117, τ=0.77, p=0.0001), suggesting that primary production has increased in BRW 100 since 1942. Mercury accumulation rates were variable (mean = 37.4 ± 14.7 μg/m^2/year), and no significant monotonic trend was detected (Mann-Kendall: S= -29.0, τ=-0.28, p=0.17); however, episodic increases in Hg accumulation occurred in ca. 1972, 1983, and 1995, with concomitant increases in sedimentation rate (Fig. 2.2).

The sediment core collected from the latitudinally intermediate lake, ATQ 206, was longer than the core from BRW 100; the deepest section was 23.5 cm from the surface, and dated to 1878. Sedimentation rate was lower than that observed in BRW 100 (mean 0.01 ± 0.01 g/cm^2/year). In contrast to the significant and gradual decrease in sediment [Hg] observed in BRW 100, a gradual increase in [Hg] from 28 to 81 ng/g was observed between the early 1880s and the early 1990s, followed by a subsequent decrease to 61 ng/g by 2013; a significant positive trend overall was detected (Fig. 2.3; Mann-Kendall: S= 136, τ=0.648, p<0.001). Similar to BRW 100, a significant increase in VRS-inferred Chl-*a* occurred

between 1878 and 2014 in ATQ 206 (Fig. 2.2; Mann-Kendall: S=125, τ=0.47, p=0.001). Mercury accumulation rates (mean 6.5 ± 1.6 μg/m^2/year) increased significantly between the 1880s and 2014, more than doubling from 3.0 to 7.0 μg/m^2/year (Fig. 2.3; Mann-Kendall: S= 107, τ=0.42, p=0.04). Although there were overall increases in both [Hg] and Hg accumulation between the top and bottom of the core, sedimentation and accumulation rates inferred from the ATQ 206 core were less variable and appreciably lower (sedimentation rates ~3-4-fold lower, Hg accumulation rates ~ 5.5-6.5-fold lower) than those from either BRW 100 or RDC 312 (Figs 2.2, 2.3, 2.4).

The southernmost lake, RDC 312, was dated to 1912 at the bottom of the 12.5 cm core, indicating a sediment accumulation rate (mean 0.08 ± 0.07 g/cm^2/year) of similar magnitude to BRW 100 and >4-fold higher than ATQ 206. Mercury concentration increased significantly between the early 1900s and 2014, from 41 ng/g to 60 ng/g (Fig. 2.4; Mann-Kendall: S= 46, τ=0.70, p<0.001). Unlike the other two lakes, there was not a significant monotonic increase in Chl-*a* over time in RDC 312 (Mann-Kendall: S= 38, τ=0.36, p=0.07). Mean mercury accumulation rate (45.8 ± 40.5 μg/m^2/year) was more similar to BRW 100 (37.4 μg/m^2/year) than to ATQ 206 (mean 6.5 μg/m^2/year), and similar to BRW 100, Hg accumulation was variable with no significant monotonic trend (Mann-Kendall: S= 4.0, τ=0.61, p=0.84). A periodic increase in Hg accumulation in ca. 1943, along with smaller increases in ca. 1971 and ca. 1986, were coincident with increases in sedimentation rate (Fig. 2.4). The smaller increases in Hg accumulation in RDC 312 occurred at similar times as two of the events identified in BRW 100 (ca. 1972 and ca. 1983).

Controls on mercury accumulation and concentration

Mercury accumulation rate (μg/m^2/year) is the product of sedimentation rate and Hg concentration. To determine which of these variables was the dominant control, Hg accumulation rates were related to both sedimentation rate and [Hg] using linear regressions applied to data from each of the three lakes. In both BRW 100 and RDC 312, nearly all (97% and 99%, respectively) of the variability in Hg accumulation rate was explained by sedimentation rate (simple linear regression, $F_{(1,13)}$=400.75, $p<0.001$, R^2= 0.97; Fig. 2.2 (BRW 100); $F_{(1,10)}$=1628, $p<0.001$, R^2= 0.99; Fig. 2.4 (RDC 312). In ATQ 206, Hg concentration explained more of the variability in Hg accumulation ($F_{(1,21)}$=8.75, $p<0.001$, R^2= 0.29; Fig. 2.3) than sedimentation rate ($F_{(1,21)}$=1.47, $p=0.24$, R^2= 0.07).

Controls on Hg concentration varied among lakes. In ATQ 206, where Hg accumulation was more strongly related to [Hg] than sedimentation rate, there were significant positive relationships between [Hg] and both %OM (R^2=0.70) and Chl-*a* (R^2=0.28) (simple linear regression, $F>_{(1,20)}\geq$16.52, $p<0.001$). These positive relationships indicate that Hg delivered to ATQ 206 is primarily bound to allochthonous and/or autochthonous organic matter; while we can clearly identify the contribution of autochthonous OM-bound Hg via the relationship between [Hg] and Chl-*a*, %OM represents both autochthonous (quantifiable) and allochthonous (not quantifiable with these data) contributions. In RDC 312, where Hg accumulation was more strongly related to sedimentation rate, [Hg] concentration was also significantly and positively related to %OM (R^2=0.66) and Chl-*a* (R^2=0.87) ($F>_{(1,10)}\geq$19.14, $p\leq0.001$). In contrast, there were significant negative relationships between [Hg] and both %OM (R^2=0.50) and Chl-*a* (R^2=0.40) in BRW 100 ($F\geq_{(1,13)}\geq$13.18, $p\leq0.003$), but a

significant and positive relationship between %MM and [Hg] (R^2=0.47, $F_{(1,13)}$=13.18, p=0.003). These results indicate that Hg in BRW 100 sediments is likely associated more with mineral matter than with organic matter. The negative relationships between primary production and [Hg] were likely driven by increases in Chl-*a* and OM from ~1999-2014, and indeed when these years were excluded from the analysis, no significant relationship existed between [Hg] and %OM ($F_{(1,10)}$=4.03, p=0.07, R^2= 0.29). The negative relationship between [Hg] and Chl-*a* was weaker, although still significant ($F_{(1,20)}$=5.27, p=0.03, R^2= 0.21).

To identify potential causes of episodic sedimentation events (with associated increases in Hg accumulation) in BRW 100 and RDC 312, historical aerial images were analyzed. It appears that there were increases in lake surface area in both lakes between 1948 and 2005; surface areas of BRW 100 and RDC 312 increased by 12.7% and 5.4%, respectively, during this time period (Fig. 2.5, Table 2.1). In contrast, there was a negligible change in the surface area of ATQ 206 (0.3%) during this same time period (Fig. 2.5, Table 2.1). Other notable changes in lake morphometry and catchment characteristics can be discerned from the aerial imagery series. In BRW 100, an access road was constructed at some point between 1955 and 1973 (Fig. 2.5). An article outlining a funding proposal for this road narrows the window of road construction to between 1967 and 1973 (Tundra Times, 1966), which is coincident with a sedimentation event that occurred in ca. 1972 (Fig. 2.2).

Visual interpretation of aerial imagery suggests that catchment hydrology could have contributed to the sedimentation events observed in the sediment profile for RDC312. RDC 312 has the largest relative catchment size of the three lakes (Table 2.1), and unique

hydrological features, including an up-gradient lake complex to the south and southeast (Fig. 2.5). It is also evident that a shoreline collapse occurred along the eastern bank of the lake at some point (Fig. 2.5); however, this event predates available aerial imagery.

Comparison of mercury accumulation with other Arctic and subarctic lakes

Of the eleven additional Alaskan lakes for which data were available, the majority (8) had mean Hg accumulation rates that were most similar to that observed for ATQ 206 (6.5 ± 1.6 $\mu g/m^2$/year); that is, much lower (mean Hg accumulation= 4.8 ± 3.3 $\mu g/m^2$/year) and more uniform (mean temporal standard deviation= 1.4 ± 0.6) than what we observed in either BRW 100 (37.4 ± 14.7 $\mu g/m^2$/year) or RDC 312 (45.8 ± 40.5 $\mu g/m^2$/year; Table 2.2). When the additional 33 Arctic lakes with available data, including the seven aforementioned Alaskan lakes, and lakes from Canada, Greenland, and Norway (Fig. 2.1; Table 2.2) were separated by landscape type (lake thermokarst, hillslope thermokarst, and non-thermokarst), significant differences were found in both mean Hg accumulation (ANOVA, $F_{(2,37)}$=17.64 , $p<0.0001$) and temporal variability (standard error, ANOVA, $F_{(2,37)}$=18.83, $p<0.0001$; Fig. 2.6). Post-hoc Tukey's tests indicated that lakes in lake thermokarst landscapes had significantly higher mean Hg accumulation than lakes in non-thermokarst landscapes and hillslope thermokarst landscapes ($p<0.01$), and that Hg accumulation in lakes from lake thermokarst landscapes was significantly more temporally variable than that in hillslope thermokarst landscapes (<0.0001) or non-thermokarst landscapes ($p<0.0001$). The lakes that fall in the lake thermokarst landscape category include the three lakes from this study and two lakes (2A and 2B) in the Mackenzie Delta Uplands from Deison et al. (2012). Similar to BRW 100 and RDC 312, sedimentation rate in these two Deison et al. (2012) lakes explained

almost all of the variability in Hg accumulation rate (simple linear regression $R^2 \geq 0.94$, $F_{(1,5)} \geq 97.75, p < 0.002$).

Mercury accumulation rates increased significantly (similar to ATQ 206) in 28 of the 37 lakes for which data were acquired from the literature (Mann-Kendall, Table 2.2). No significant monotonic trends were observed in 7 of the lakes (Mann-Kendall, Table 2.2), and a significant decrease was observed in one lake in the Mackenzie River delta (Mann-Kendall, Table 2.2). Including the lakes from this study, 14 of 16 (88%) non-thermokarst lakes displayed a significant increase in Hg accumulation, whereas Hg accumulation increased in 14 of 19 (74%) 'hillslope thermokarst' lakes and 2 of 5 (40%) 'lake thermokarst' lakes (see Table S2.1, Appendix A).

2.4 Discussion

Controls on Hg accumulation

Of the three lakes sampled for this study, two had variable and non-directional temporal trends in Hg accumulation (BRW 100 and RDC 312) rates that were driven by sedimentation rate, and one lake (ATQ 206) had a significant (2.4-fold) temporal increase in Hg accumulation rate that was driven by Hg concentration. Analyses conducted on additional data collated from 37 subarctic and Arctic lakes revealed that two to three-fold increases in Hg accumulation since preindustrial times have been widely observed in lakes in the Northwest Territories (see Muir et al. 2009), Nunavut (Hermanson et al. 1995), Norway (Drevnick et al. 2012), Greenland (Bindler et al. 2001), and Alaska (Fitzgerald et al. 2005). Observations of no directional change (see Muir et al. 2009) and/or decreases (Deison et al. 2012) in Hg accumulation were less common. Several features of BRW 100 and RDC 312 and their catchments may explain the relatively high and variable sedimentation rates observed, and the lack of temporal trend in Hg accumulation rate. These interpretations may be applicable to the similar trends in sedimentation and Hg accumulation rates observed for lakes 2A and 2B from Deison et al. (2012), and allow for more informed predictions and understanding of Hg accumulation rates in lakes in lake thermokarst regions (Olefeldt et al. 2016) that have similar physical characteristics.

BRW 100 is a typical example of a thermokarst lake on the Arctic Coastal Plain; it is elliptical in shape, and oriented to the northwest (see Grosse et al. 2013). An access road was constructed to BRW 100 between 1967 and 1973, which aligns with one of the major sedimentation events (ca 1972). Aside from possible land use change-related sediment

inputs, the high and variable sedimentation rate may also reflect thermokarstic activity or surface runoff events associated with low soil hydraulic conductivity. Thermokarst lakes are subject to several shoreline erosive processes, including thermal erosion and mechanical erosion via wave action (see Grosse et al. 2013). The silty, ice-rich catchment sediments of the thermokarst lakes of the Arctic Coastal Plain make them prone to enhanced shoreline erosion (see Grosse et al. 2013), which likely contributed to lateral growth in BRW 100 (12.7% since 1948), and sedimentation events not related to road construction. Sedimentation events could also reflect pulses of material delivered to BRW 100 during spring snowmelt or large precipitation events; previous data indicate that the catchment soils of BRW 100 are poorly drained (Jorgensen and Grunblat, 2013), and thus more prone to pulses rather than gradual and continuous sediment delivery.

While visual analysis of aerial imagery indicates that thermal shoreline erosion could have contributed to the variable and high sedimentation rate in RDC 312, as it too appears to have expanded (to a lesser extent, 5.4% since 1948), it is likely that erosive processes related to terrestrial catchment hydrology (i.e., relative catchment size and presence of up-gradient lake complex) had a greater influence on sedimentation rate and thus Hg accumulation. RDC 312 is not a typical thermokarst lake; although it is in a zone of continuous permafrost and in a lake thermokarst region, lake morphology and catchment composition are distinctly different from BRW 100. For example, BRW 100 is surrounded by polygonal ground indicative of degrading ground ice, which is absent from the area surrounding RDC 312. RDC 312 is also at a higher elevation than low-relief BRW 100 (as it borders Brooks Range), and has a smaller area, but larger relative catchment size. Its proximity to Brooks Range exposes it to

higher storm intensities than are typical near the coast (Miller, 1963). Finally, RDC 312 is located in the Arctic silty lowland, where soils are silty with a thick organic-rich surface layer. Previous data indicate that these soils likely have an even lower hydraulic conductivity than the catchment soils of BRW 100 (Jorgensen and Grunblat, 2013). Large relative catchment size (compared to BRW 100), and low hydraulic conductivity could facilitate overland flow and pulses of sediment (and Hg) from surface erosion. Since two of the major sedimentation events in each of BRW 100 and RDC 312 occurred around the same time (early 1970s and mid 1980s) it is possible that they were triggered by regional weather events (e.g., high precipitation, abnormally warm or windy year), although the 1972 BRW 100 event was almost certainly driven by the road construction. BRW 100 and RDC 312 had variable and high sedimentation and Hg accumulation rates, and we suggest that this is largely due to a combination of thermokarst activity and runoff over catchment soils with low hydraulic conductivity. We suspect that similar factors explain the variable and high sedimentation and Hg accumulation rates in lakes 2A and 2B from Deison et al. (2012).

Compared to the other four lakes located within a lake thermokarst region, ATQ 206 had relatively low and consistent Hg accumulation rates that were more similar to those observed further south in Arctic Alaska. There was a significant increase over time in Hg accumulation in ATQ 206, and the magnitude of this increase was similar to what was observed in the five Alaskan lakes near the Toolik Field Station originally investigated by Fitzgerald et al. (2005). These five lakes collectively showed a ~2.5-fold increase in Hg accumulation rates since preindustrial times (before ca.1850), which the authors attributed to a combination of increases in atmospheric deposition and enhanced erosion of soils

(Fitzgerald et al. 2005). While the sediment core from ATQ 206 did not quite extend to pre-industrial times (pre-1850), a similar 2.4-fold increase was observed in Hg accumulation between 1883 and 2013. Although the lakes studied by Fitzgerald et al. (2005) are much smaller in surface area than ATQ 206, the Fitzgerald et al. (2005) lakes have several physical attributes that are similar to ATQ 206 (e.g., relatively small catchment to surface area ratio, coarse catchment sediments) and that could explain why sedimentation and Hg accumulation rates in these lakes were dissimilar to those observed in BRW 100 and RDC 312.

Relatively high hydraulic conductivity in ATQ 206 and in the Fitzgerald et al. (2005) lakes may partially explain the relatively low and invariable sedimentation rates and the relatively low Hg accumulation rates in these lakes. The Fitzgerald et al. (2005) lakes and ATQ 206 have catchment soils with a greater fraction of sands (Fitzgerald et al. 2005; Jorgensen and Grunblat, 2013). These coarse catchment sediments likely have higher hydraulic conductivity; hydraulic conductivity tests on soils near ATQ 206 in the Arctic sandy lowland, and on soils near RDC 312 in the Arctic silty lowland, indicated that soils near ATQ 206 were twice as conductive as those near RDC 312 (J. Koch, unpublished data). While conductivity tests were not performed near BRW 100, catchment conductivity is likely low (relative to ATQ 206), since it is located in the Arctic peaty-sandy lowland, where soils in swales are poorly drained (Jorgenson and Grunblat, 2013). We suggest that the relatively low sedimentation and Hg accumulation rates in ATQ 206 and the Fitzgerald lakes (when compared to BRW 100 and RDC 312) can be explained by a combination of high hydraulic conductivity, small relative catchment sizes, and an absence of catchment land-use

disturbance and appreciable thermokarst activity (e.g., thermal erosion/lateral expansion, or slumping).

Mercury accumulation rates were more strongly related to Hg concentration than sedimentation rates in ATQ 206, and Hg concentration was positively related with both %OM and VRS-inferred Chl-*a* in both ATQ 206 and RDC 312. In BRW 100, Hg concentration was negatively related to both %OM and VRS-inferred Chl-*a*. Positive relationships between Hg concentration and indicators of lake primary production (%OM and VRS-inferred Chl-*a*) in ATQ 206 and RDC 312 can be explained by the affinity of the oxidized Hg species, Hg(II), for reduced complexes in organic matter (e.g., thiols; see Ravichandran et al. 2004). This complexation can occur in (but is not restricted to) the lake or in the catchment, and as such the transfer of OM from the terrestrial catchment can be an important source of Hg. Since we did not quantify the proportion of OM originating from the terrestrial catchment (allochthony) versus the lake (autochthony) it is difficult to disentangle the positive relationships between Hg concentration and %OM; however it is likely that both allochthonous and autochthonous sources contributed to the OM in each of the lakes. Many researchers have attributed post-industrial increases in Hg accumulation to a form of autochthonous complexation termed "algal scavenging" (Outridge et al. 2007; Stern et al. 2009). Algal scavenging could explain the positive relationship between Hg concentration and Chl-*a* observed in ATQ 206 and RDC 312. The negative relationship between Hg concentration and primary production in BRW 100 is less straightforward. Unlike ATQ 206, RDC 312, and many temperate lakes, the Hg in this lake is not primarily associated with organic, but rather minerogenic matter, as evidenced by the significant

positive relationship with %MM. Although Hg can be deposited directly onto lakes, it is clear from the strong relationship between sedimentation rate and Hg accumulation that catchment contributions have historically been important in Hg delivery to BRW 100. The negative relationship between %OM and Hg concentration was driven by samples that represent the time period 1999-2014, when an increase in autochthonous primary production (indicated by Chl-*a*) was observed. Since Hg is more closely associated with minerogenic matter in this lake, it is possible that the increase in number of algal cells resulting from greater primary production decreased the Hg concentration in each algal cell (and consequently the sediment), via a similar mechanism to bloom dilution (Pickhardt et al. 2002). This inference is supported by the fact that when the years 1999-2014 (when a noticeable increase in Chl-*a* was observed) are excluded from the analysis, there is no relationship between [Hg] and %OM.

The future of Hg accumulation in thermokarst lakes

Results from this study allow for some predictions about future trends in Hg concentration and accumulation in thermokarst lakes. As temperatures continue to rise, growing seasons will lengthen, and there will likely be a continued increase in autochthonous primary production (i.e., more algal cells) in Arctic lakes (Prowse et al. 2006). Additionally, rising temperatures are expected to result in increases in thermokarstic activity (e.g., thermal erosion, thaw slumping; see Grosse et al. 2013), and enhanced runoff (Barnett et al. 2005), which could increase the amount of terrestrial organic matter entering lakes from catchment sources. As the data from this study indicate, each of these climate-affected processes could have disparate effects on sediment Hg concentration depending on the fraction (i.e., organic

matter or minerogenic matter) with which the Hg in a given lake is most closely associated, and the composition/conductivity of catchment soils. Our results suggest that an increase in primary production could lead to an increase in sediment Hg concentration in both ATQ 206 and RDC 312 due to complexation with organic matter (i.e., algal scavenging), and a decrease in sediment Hg concentration in BRW 100 due to dilution of minerogenic sediments. There is also potential for an increase in sediment Hg concentration in RDC 312 due to either increased runoff or enhanced thermokarstic activity, as its catchment has a thick organic surface layer. Since Hg concentration was the dominant driver of Hg accumulation in ATQ 206, if sedimentation rates in this lake remain low and steady, an increase in Hg accumulation could be expected with increased primary production. Conversely, if sedimentation rates in BRW 100 and RDC 312 remain high and variable, an increase in primary production (and concomitant increases and decreases in Hg concentration in RDC 312 and BRW 100, respectively) would likely not have a notable impact on Hg accumulation in these lakes, since sedimentation rate is the dominant driver of Hg accumulation.

Predicted temperature-driven increases in primary production and thermokarstic activity in Arctic regions are well documented; however, these processes are not always collinear. Longer ice-free seasons should lead to an increase in phytoplankton production, as seen in BRW 100 and ATQ 206 in this study (e.g., Prowse et al. 2006); however, thermokarstic events such as retrogressive thaw slumps (prominent in hillslope thermokarst landscapes) have been found to decrease phytoplankton production (Thienpont et al. 2013). Although the temporal scale and resolution of aerial photograph coverage precluded the direct assessment of thaw slump activity in this study, it is important to consider the potential mechanisms thaw

slumping could drive. A thaw slump results in a massive amount of permafrost soil entering a lake. Permafrost soils have comparatively higher ionic concentration than the overlying active layer due to persistent leaching, so concentrated solutes enter the system with the sediment (Kokelj and Burn, 2003). Base cations facilitate the absorption and flocculation of humic substances (coloured dissolved organic matter), and although the inundation of ion-rich minerogenic soils from a thaw slump may temporarily limit light, it can lead to greater water clarity in the long term (Thompson et al. 2008). This increased clarity can lead to increased macrophyte growth, and potentially a shift away from phytoplankton dominance (Thompson et al 2008), which could decrease sediment [Hg] by reducing the capacity for "algal-scavenging". Of the three study lakes, RDC 312 is the only lake that is currently macrophyte-dominated; however, it is unclear how long it has been in this state. Additionally, thaw slumping itself can lead to a dilution of Hg in surface sediments (Deison et al. 2012). Thus, effects of rising temperatures on Hg accumulation and concentration in thermokarstic lake sediments will depend on catchment size and catchment sediment composition, as well as a variety of variables that control primary production, and frequency and magnitude of thermokarstic events

Future Hg accumulation rates in the study lakes could also reflect changes in atmospheric deposition (Fitzgerald et al. 2005). Although the lakes studied here have not historically displayed a distinct atmospheric Hg signal (increase to peak Hg concentrations in 1970s followed by recent decrease; e.g., Engstrom et al. 1997), it is possible that this could change. Legislation has led to a decrease in Hg emissions by the power sector in North America since the 1980s (Slemr et al. 2003); however, since this legislation is not globally applicable and

Arctic Alaska receives considerable Hg inputs from Asia and Russia (see AMAP, 2011), future emissions are unpredictable. If emissions were to continue to decline, it could have an impact on Hg concentration and accumulation in the Arctic Coastal Plain lakes. Changes in emissions would likely be detected first in lakes with small relative catchment sizes, like ATQ 206 and BRW 100, before lakes with large relative catchment sizes, like RDC 312, due to the important and longer-term influence of Hg (both anthropogenic and natural) stored in catchment soils (see Grigal, 2002; Fitzgerald et al. 2005; Harris et al. 2007). Further research is required to effectively predict the timeframe and magnitude of the impact of reduced atmospheric emissions on Hg in lake sediments.

Thermokarst landscapes cover more than 20% of the northern permafrost region (Olefeldt et al. 2016), and available data from this study and previously published work suggest that the highest and most variable Hg accumulation rates occur in lakes in thermokarst regions. We suggest that low hydraulic conductivity and thermokarstic processes (e.g., thermal erosion, retrogressive thaw slumps) lead to high and variable Hg accumulation rates. Available data cover only a fraction of the global thermokarst landscape (i.e., lake thermokarst and hillslope thermokarst); however, the vast majority of this landscape is located in Arctic Russia, where presumably lakes with variable and high Hg accumulation rates also exist.

2.5 Conclusions

Results of this study demonstrate that lakes on the Arctic Coastal Plain of Alaska have variable Hg accumulation histories with different underlying controls. Sedimentation rate drove Hg accumulation in the lakes where it was found to be high and variable, and high and variable sediment and Hg accumulation rates were more prevalent in lakes on thermokarst landscapes than on non-thermokarst landscapes. It can be inferred that Hg accumulation in other lakes with similar characteristics (i.e., ice rich catchment sediments, large relative catchment size, and low hydraulic conductivity) on 'lake thermokarst' or 'hillslope thermokarst' landscapes could also be driven by sedimentation rate. Conversely, Hg accumulation rates in lakes with small relative catchment sizes and conductive catchment soils could be driven more by factors that control Hg concentration, such as primary production and organic matter inputs. It is imperative that variability in landscape setting and lake physical characteristics, such as relative catchment size, catchment soil composition (grain size, ice content), and hydraulic conductivity, are reflected in predictions of future Hg accumulation in Arctic lakes.

2. 7 Figures

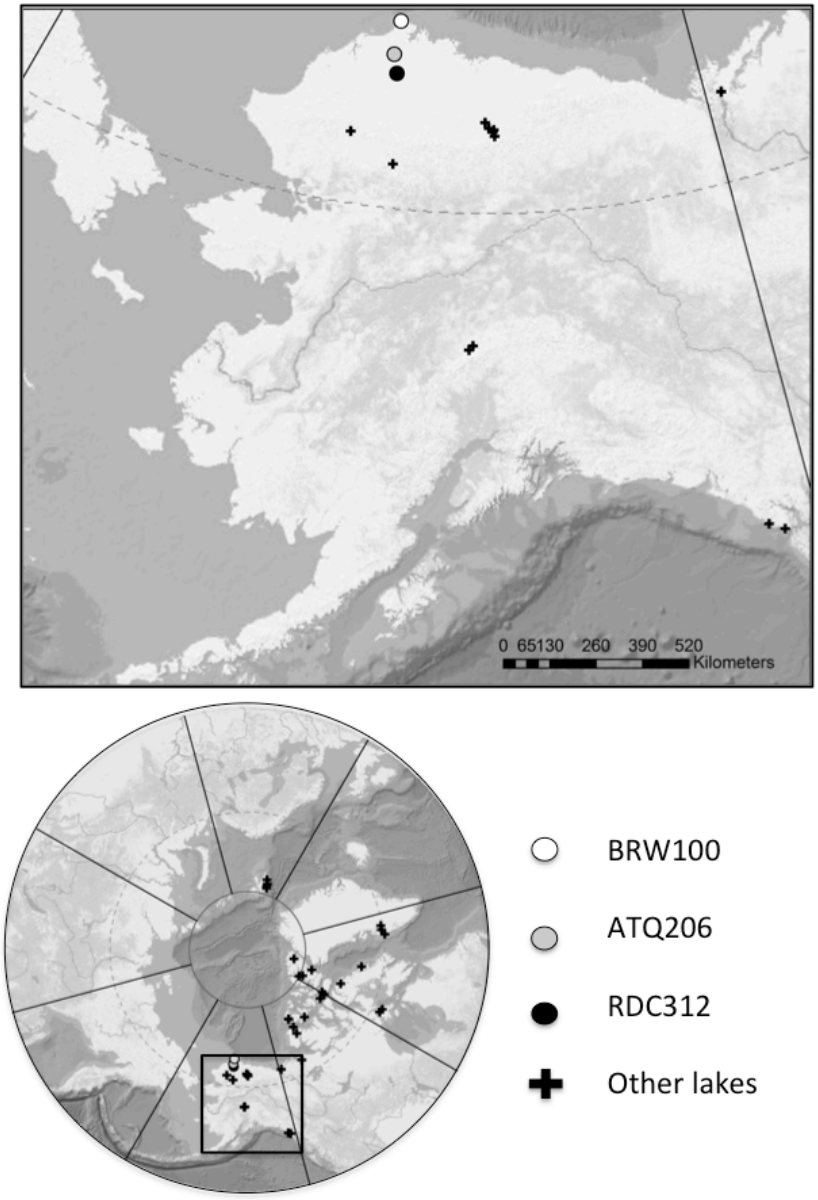

Figure 2.1. Study lakes on the Arctic Coastal Plain of Alaska (BRW 100, ATQ 206, RDC 312) and other lakes with published sediment Hg accumulation data; circles represent lakes in this study, crosses represent comparison lakes.

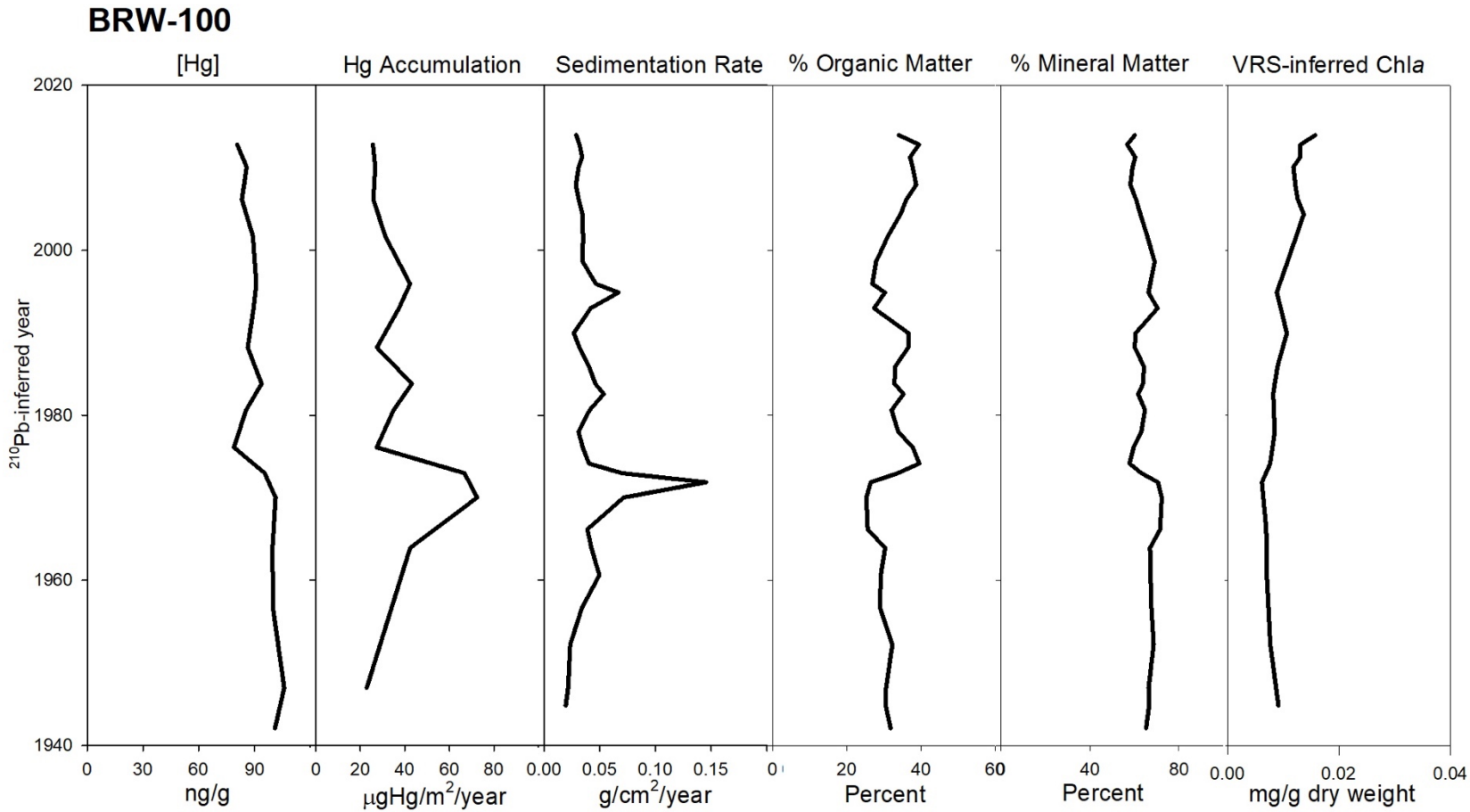

Figure 2.2. Temporal profiles of sediment mercury concentration, accumulation rate, sedimentation rate, percent organic matter, and percent mineral matter, and VRS-inferred chlorophyll *a* for lake BRW100 on the Arctic Coastal Plain of Alaska sampled in August 2014.

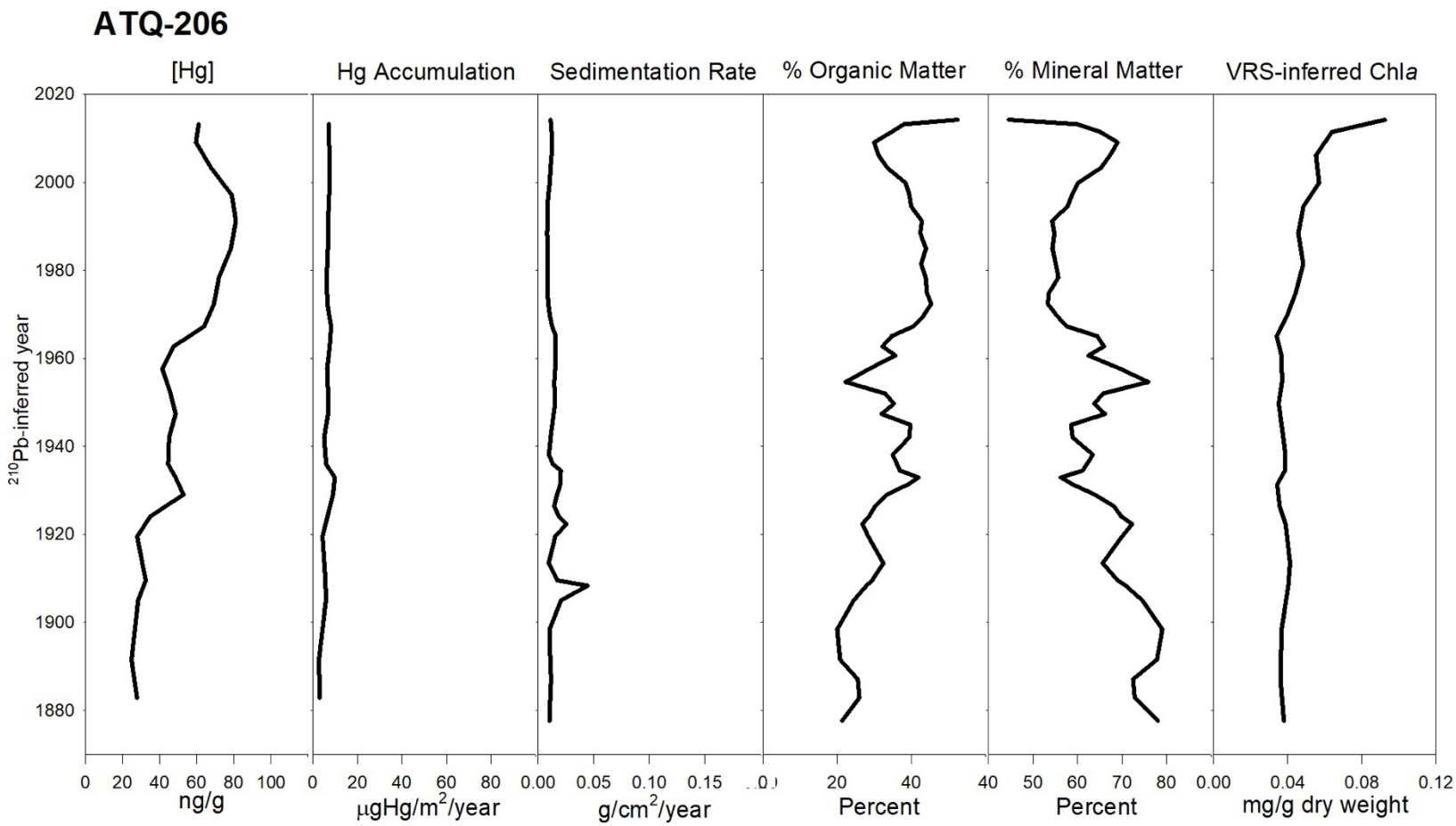

Figure 2.3. Temporal profiles of sediment mercury concentration, accumulation rate, sedimentation rate, percent organic matter, and percent mineral matter, and VRS-inferred chlorophyll a for lake ATQ206 on the Arctic Coastal Plain of Alaska sampled in August 2014.

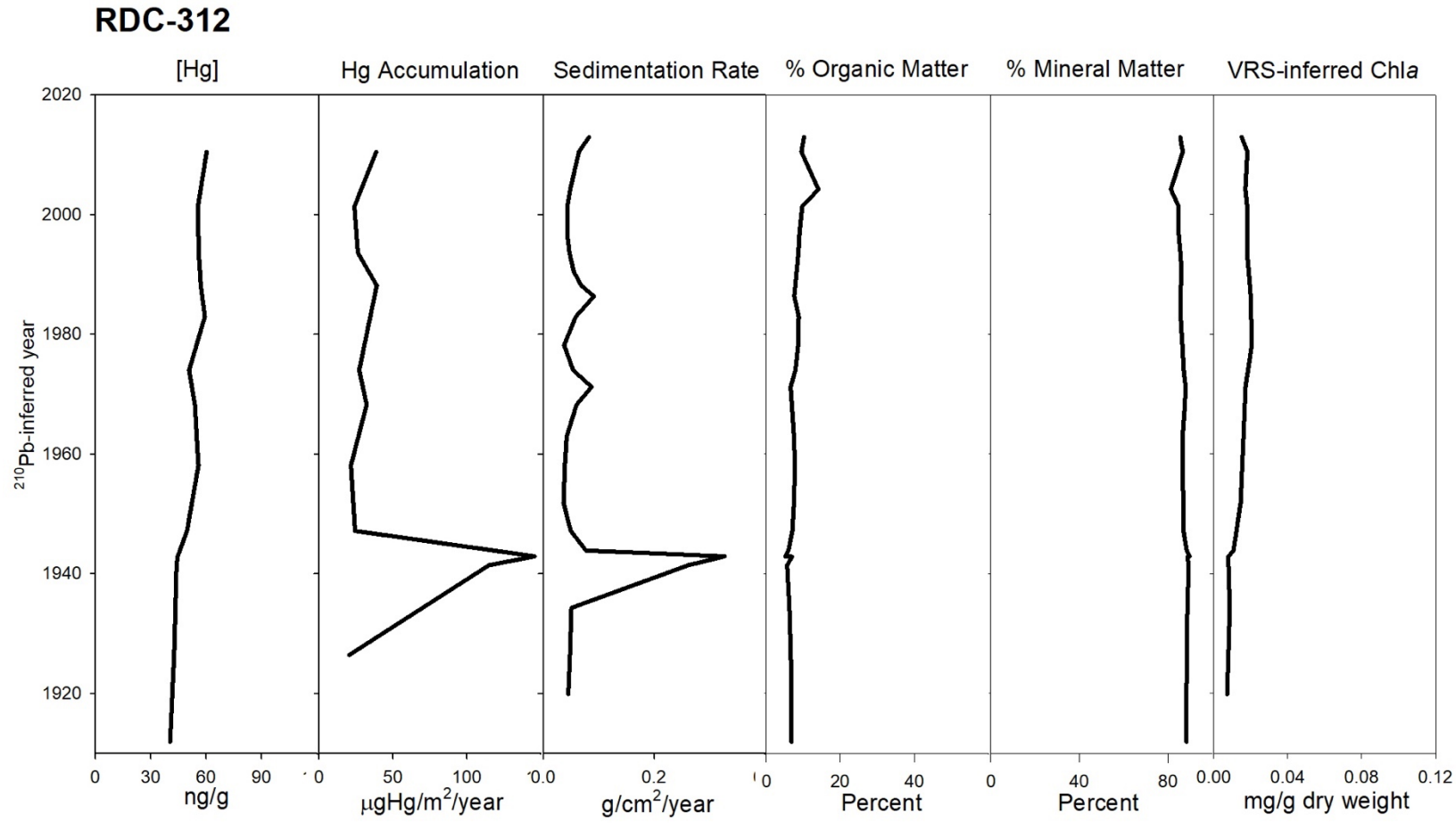

Figure 2.4. Temporal profiles of sediment mercury concentration, accumulation rate, sedimentation rate, percent organic matter, and percent mineral matter, and VRS-inferred chlorophyll a for lake RDC312 on the Arctic Coastal Plain of Alaska sampled in August 2014.

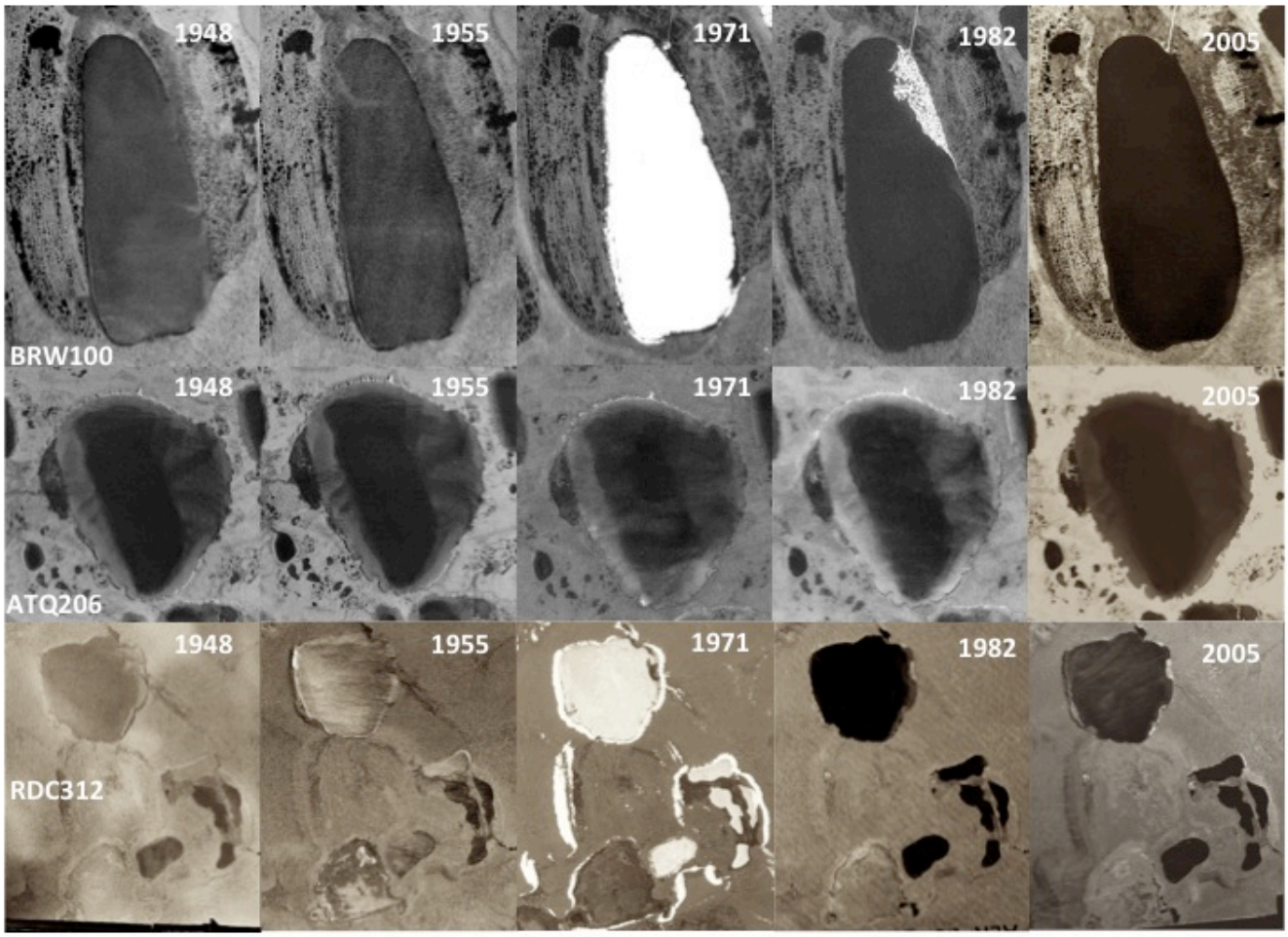

Figure 2.5. Historical aerial images from 1948, 1955, 1971, 1982, and 2005 of three study lakes (BRW 100, ATQ 206, and RDC 312) on the Arctic Coastal Plain of Alaska; the imagery is property of the United States Geological Survey (USGS, 2016).

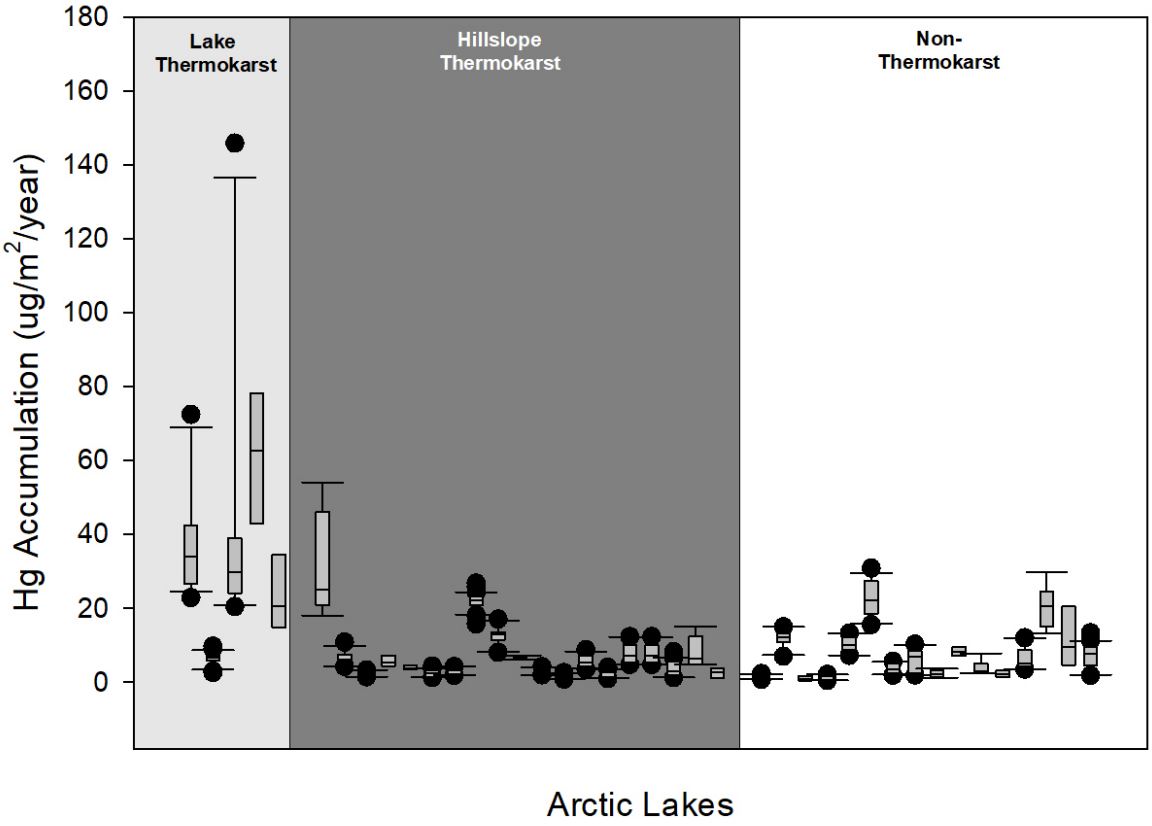

Figure 2.6. Box and whisker plots for mercury accumulation rates for 36 circumarctic and 4 subarctic Alaskan lakes on different landscape types, as defined in Olefeldt et (2016). The range bars 95% confidence intervals; boxes show the inter-quartile ranges (25%-75%), the horizontal line indicates the median. The lakes in 'lake thermokarst' panel represent, in order: BRW 100, ATQ 206, and RDC 312 (this study), and lakes 2A, and 2B (data from Deison et al. 2012). Accumulation rates are significantly higher and more variable in Lake Thermokarst lakes than Non-thermokarst lakes and hillslope thermokarst lakes. Accumulation rates are focus-corrected when data were available (see Table S2.1, Appendix A).

2.8 Tables

Table 2.1. Physical characteristics and summary Hg accumulation results of the three study lakes (BRW 100, ATQ 206, RDC 312) on the Arctic Coastal Plain of Alaska; Hg accumulation trends were assessed using Mann-Kendall tests (a p value <0.05 denotes a significant temporal trend and the Kendall's tau denotes the direction and magnitude of the relationship; McLeod, 2015); catchments were delineated, and percent growth was calculated using ArcMap™10.2.2 (ESRI, 2016).

	BRW 100	**ATQ 206**	**RDC 312**
Latitude (decimal degrees)	71.24163	70.41557	69.95348
Longitude (decimal degrees)	-156.77391	-156.98128	-156.63817
Surface area (km^2)	1.7	1.8	0.7
Catchment area (km^2)	24.0	22.8	29.9
Catchment to surface area ratio	13.7	12.8	41.0
Growth since 1948 (%)	12.7	-0.3	5.4
Landscape type	lake thermokarst	lake thermokarst	lake thermokarst
Mean Hg accumulation ($\mu g/m^2$/year)	37.4	6.5	45.8
Standard deviation	14.7	1.6	40.5
Hg accumulation trend	no trend	positive	no trend
Kendall's tau (τ)	0.28	0.42	0.61
Mann-Kendall p value	0.17	0.04	0.84

Table 2.2. Mean Hg accumulation and Mann-Kendall results for thirty-seven previously studied Arctic and subarctic lakes; landscape types were designated using the maps generated by Olefeldt et al 2016; further lake information available in appendix A.

Lake	Country	Landscape Type	Mean Hg Accum. ($\mu g/m^2/year$)	σ	Trend	τ	p
2-A	Canada	lake	62.23	18.04	neg	-0.71	0.019
2-B	Canada	lake	23.88	13.58	pos	0.91	0.007
Amituk	Canada	non-thermokarst	1.34	0.56	pos	0.70	0.02
AX-AJ	Canada	hillslope	32.55	13.79	pos	0.94	<0.001
BI-02	Canada	hillslope	6.53	1.86	pos	0.39	0.047
BK-AH	Canada	hillslope	2.73	0.59	n/a	-0.39	0.062
Brady	USA	non-thermokarst	11.84	2.30	pos	0.46	0.033
Burial	USA	hillslope	5.69	1.45	pos	0.71	0.019
CF-11	Canada	non-thermokarst	1.07	0.62	pos	1.00	0.009
Char	Canada	non-thermokarst	1.49	0.62	pos	0.89	0.0001
Daglet	USA	non-thermokarst	10.23	1.99	pos	0.78	0.002
Daltjørna	Norway	non-thermokarst	22.70	4.81	pos	0.78	0.0001
DV-E	Canada	hillslope	4.02	0.66	n/a	0.67	0.308
Efficient	USA	hillslope	2.44	0.91	pos	0.64	<0.0001
Forgetful	USA	hillslope	3.16	0.83	pos	0.49	0.013
Hazen	Canada	hillslope	21.91	2.29	n/a	-0.10	0.442
Lake 53	Greenland	non-thermokarst	3.69	1.32	pos	0.86	<0.0001
Lake 70	Greenland	non-thermokarst	6.23	3.00	n/a	0.41	0.127
Matacharak	USA	non-thermokarst	2.33	1.00	pos	0.83	0.002
MB-AC	Canada	hillslope	12.56	2.56	pos	0.84	<0.0001
MB-S	Canada	hillslope	6.77	0.40	n/a	0.00	1
Mcleod	USA	hillslope	2.65	0.70	pos	0.48	0.006
North	Canada	hillslope	1.35	0.53	pos	0.82	0.0003
Nunatak	Greenland	non-thermokarst	8.24	1.62	pos	0.81	0.016
Ossian Sarsfjellet	Norway	non-thermokarst	4.00	1.86	pos	0.72	0.009
Perfect	USA	hillslope	5.85	1.61	pos	0.88	<0.0001
Relaxing	USA	hillslope	2.48	0.99	pos	0.85	<0.0001
Rocky Basin	Canada	non-thermokarst	2.35	1.00	pos	1.00	0.03
Romulus	Canada	hillslope	7.77	2.65	pos	0.78	0.002
Rummy	Canada	hillslope	6.80	0.94	n/a	0.62	0.072
SHI-L4	Canada	non-thermokarst	6.46	3.03	pos	0.82	<0.0001
SHI-L7	Canada	non-thermokarst	20.34	5.61	n/a	0.17	0.602
Surprise	USA	hillslope	3.83	2.10	pos	0.90	<0.0001
Vassauga	Norway	non-thermokarst	7.30	3.35	pos	0.93	0.002
West	Canada	hillslope	8.21	4.13	pos	0.76	0.006
Wonder	USA	hillslope	2.59	1.26	pos	0.93	0.002
Yterjørna	Norway	non-thermokarst	12.21	9.69	pos	0.84	<0.0001

3 Fish growth rates and lake sulphate explain variation in mercury levels in Ninespine stickleback (*Pungitius pungitius*) on the Arctic Coastal Plain of Alaska

3.1 Introduction

Mercury (Hg) is a neurotoxin, and in its methylated form (methyl mercury; MeHg) it can biomagnify and bioaccumulate in aquatic food webs (see Kidd et al. 1995; Atwell et al. 1998; Lockhart et al. 2005), often reaching concentrations that are high enough to affect the health of humans and fish-eating wildlife (e.g., Lockhart et al. 2005). There are several interrelated physical, biogeochemical, and ecological variables that can influence the methylation, uptake, and bioaccumulation of Hg in aquatic ecosystems and food webs. Ultimately, MeHg concentrations ([MeHg]) in fish are governed by the amount of available MeHg at the base of the food web, the rate of biomagnification through the food web, and the rate of accumulation in individual organisms (see Lehnerr et al. 2014).

The amount of MeHg available at the base of lake food webs is controlled by the amount of bioavailable inorganic Hg and the activity of methylators, typically sulphate-reducing bacteria (SRB; Compeau and Bartha, 1985; King et al. 2000). Several environmental variables interact to affect rates of mercury methylation, including concentrations of SO_4 (Gilmour et al. 1992) and dissolved organic matter (DOM; Graham et al. 2012; Graham et al. 2013), as well as temperature, redox conditions, and pH (see Ullrich et al. 2001).

Elevated sulphate concentrations can stimulate SRB; however, there is an optimum above which sulphate can inhibit methylation, as sulphate reduction produces sulfide which can

bind with inorganic Hg making it less bioavailable (Gilmour et al. 1992). Similarly, DOM can stimulate SRB, because microbes can use OM as an energy source (see Ravichandran et al. 2004). In some cases, however, high concentrations of DOM can inhibit methylation, because the formation of Hg-DOM complexes results in a decrease in the amount of bioavailable Hg (see Ravichandran et al. 2004; Paranjape and Hall, 2017). This is less likely to occur in acidic waters, where the charge on the DOM-sulfide binding site is weaker. Sulphate reduction, and consequently methylation, is also favoured in environments with low oxygen (see Ullrich et al. 2001) and warmer temperatures (Bisogni and Lawrence, 1975; Korthals and Winfrey, 1987). It was traditionally thought that mercury methylation primarily occurred in lake sediment pore-waters (Korthals and Winfrey, 1987); however, more recently it has been found to occur in the water column (Watras et al. 1995a, Mauro et al. 2002), in biofilm associated with macrophyte beds (Mauro et al. 2002), and in the catchments (St. Louis et al. 1994; Bravo et al. 2017) of lakes.

Authors of a recent study investigated the effects of organic matter composition on methylation rates and MeHg concentration in boreal lake sediments (Bravo et al. 2017). Overall, bacterial activity and methylation rates were higher in sediments with autochthonous (phytoplankton-derived) organic compounds. Lake sediments that were dominated by allochthonous (terrestrial-derived) organic compounds had lower methylation rates, but higher overall MeHg concentration. The results suggested that allochthonous OM is less labile, and not as bioavailable for bacterially mediated methylation *in situ*, and thus that significant methylation was occurring in lake catchments (Bravo et al. 2017). This work illustrated that the origin and composition of organic matter has important implications for

mercury methylation rates and concentrations, and should be considered in predictions of effects of climate-induced change on mercury bioaccumulation.

Once methylated, the uptake of Hg into lake food webs and accumulation in fish is influenced by several factors, including primary production (Pickhardt et al. 2002), fish growth rates (Karimi et al. 2007), age, condition (Scott et al. 1972), trophic position (Kidd et al. 2012), and life history (Swanson et al. 2011). Although increases in primary production can lead to greater scavenging of Hg from the water column (Outridge et al. 2007) and higher methylation rates, high primary production can also decrease the amount of MeHg entering the food web through bloom dilution (Pickhardt et al. 2002). Primary production also affects growth and feeding ecology of fish, and Hg concentrations are generally higher in slower growing (Karimi et al. 2006), older fish (Scott et al. 1972), and fish that feed at higher trophic positions (e.g., Kidd et al. 2012).

Although mercury emissions to the atmosphere are generally decreasing globally (Slemr et al. 2003; see AMAP, 2019), a rapidly changing climate is leading to complex effects on methylation and bioaccumulation of mercury in aquatic ecosystems. For example, while increases in lake primary production may be expected as a result of warmer water temperatures (Michelutti et al. 2005), increases in primary production can act to either increase or decrease fish Hg concentration via different mechanisms (as stated above). Warmer temperatures can also increase methylation rates (see Ullrich et al. 2001) and mobilization of bioavailable THg from northern lake catchments (Rydberg et al. 2010).

Climate change is also affecting fish growth rates (Reist et al. 2006b) and food web structure (Perrson et al. 1996), both of which can affect fish Hg concentration.

Predicting effects of climate-induced change on mercury methylation, uptake, and bioaccumulation in aquatic food webs is especially urgent in the Arctic, where warming is occurring at an accelerated rate (IPCC, 2007). Indigenous communities rely heavily upon fish consumption for subsistence, and current fish mercury levels affect the health of fish-eating wildlife, such as loons (Scheuhammer et al. 2008; Evers et al. 2014). There is a particular paucity of mercury data for the Arctic Coastal Plain of Alaska (ACP), as identified in a review of temporal trend studies that have been conducted in the circum-Arctic (AMAP, 2011). The ACP is a lake-rich region in northern Alaska that stretches from the foothills of the Brooks Range (68°N) to the Beaufort and Chukchi Seas (71°N). Many lakes on the ACP are developed from the degradation of ground ice (i.e., thermokarst lakes), and thermokarstic processes that shape the development and succession of these lakes (e.g., thermal erosion, catastrophic drainages, and retrogressive thaw slumps) are increasing in frequency and magnitude with rising air temperatures (see Grosse et al. 2013).

Increased frequency and prevalence of thermokarst activity can affect Hg accumulation in Arctic freshwater ecosystems in several ways (e.g., Deison et al. 2012; Chapter 2, 2018). Direct effects include mass transport of Hg, such as when retrogressive thaw slumps occur, and Hg bound to catchment materials is transported to downstream lakes and streams. Indirect effects include potential reductions in algal scavenging of Hg; this can occur when thermokarst activity results in increased turbidity and corresponding decrease in

phytoplankton biomass (Thienpont et al. 2013). Methylation rates can also be affected by thermokarstic activity, as a result of increased inputs of OM and SO_4 from the catchment (Kokelj et al. 2009).

As part of a study on the accumulation of Hg in sediments of lakes on the ACP, (Chapter 2) conducted a meta-analysis on published data from the circum-Arctic and found that sediment mercury accumulation was higher and more variable in thermokarst lakes than non-thermokarst lakes. Additionally, these authors identified that the mercury accumulation in the sediments of some thermokarst lakes on the ACP are more influenced by their catchment than others (Chapter 2). The "higher catchment influence" lakes were found to have high and variable sediment Hg accumulation rates, while the "lower catchment influence" lakes were found to have relatively low and consistent sediment Hg accumulation rates. In the "higher catchment influence" lakes, primary production (inferred from sediment Chl-*a*) was lower and sediment Hg accumulation was linked to sedimentation events, while in the "lower catchment influence" primary production was higher and related to Hg concentration, which was driving Hg accumulation (Chapter 2).

Earlier work indicated that primary production and sedimentation events are both a product of catchment characteristics, and are spatially variable on the Arctic Coastal Plain of Alaska. Both primary production (including source of organic matter, Bravo et al. 2017) and sedimentation events have the potential to affect the methylation and uptake of mercury into the food web. Since primary production and sedimentation events can be climate-mediated, it is especially pertinent to understand the controls of MeHg concentration in the fishes and

other biota of ACP lakes with different levels of catchment influence. On the ACP, the Reindeer Camp (RDC) region is an area with lakes that likely have higher catchment influences (e.g., larger relative catchment sizes, lower hydraulic conductivity), while the Atqasuk (ATQ) region is an area with lakes that have lower catchment influence (e.g., small relative catchment sizes, high hydraulic conductivity; Chapter 2). As such, the primary objectives of this study were to: 1. Determine if there are physico-chemical differences in water chemistry between lakes in the Reindeer Camp and Atqasuk regions that are consistent with differences in catchments outlined in Chapter 2. Determine if there are differences between the Atqasuk and Reindeer Camp regions in MeHg concentrations in sediment, periphyton, zooplankton, invertebrates, and fish; and, 3. Identify drivers of MeHg in different food web components by relating MeHg concentrations in sediment, periphyton, invertebrates, and fish to possible explanatory variables, including water chemistry variables, and stable isotope ratios of carbon and nitrogen. I predicted that the lakes from the Atqasuk region, which have lower catchment: lake area ratios (outlined in Chapter 2) would be relatively more autochthonous than those in the Reindeer Camp region, which have higher catchment : lake area ratios. If true, we expected that MeHg concentrations in fish and lower trophic level biota would be higher in the more allochthonous lakes than in the more autochthonous lakes, due to higher inputs of Hg, OM, and ions in the allochthonous lakes. We further expected that differences in mercury concentrations between regions would be related to variables that indicate source and amount of primary production (e.g., Chl-*a*, DOC).

3.2 Methods

Study area

The six lakes in this study are located on the Arctic Coastal Plain (ACP) of Alaska (Fig 3.1), which extends north from the Brooks Range (68°N) to the Beaufort and Chukchi Seas (71°N). The six study lakes are located within a zone of continuous permafrost on Tussock Tundra, and were selected from a larger set of lakes monitored by the Circum-Arctic Lakes Observation Network (http://arcticlakes.org). Two regions are represented by the selected lakes, the Atqasuk (ATQ) region (lakes: ATQ 200, ATQ 201, ATQ 206), and the Reindeer Camp (RDC) region (lakes: RDC 308, RDC 309, RDC 311). The lakes in this study are shallow (2-4 m), small (0.5-2.5 km^2), well-mixed, and do not strongly stratify. The food webs of ACP lakes are simple, and contain few fish species (e.g., Carey and Zimmerman, 2014; Laske et al. 2018). The most common fish species are Ninespine stickleback (*Pungitius pungitius*) and Alaska blackfish (*Dallia pectoralis*). The ACP is a heterogeneous landscape, and as such, there are hydrological and other physical differences between the ATQ and RDC regions; briefly, catchments in the ATQ region are small relative to lake areas, and are characterized by sandy, well-drained soils with high hydraulic conductivity (Chapter 2; Koch, unpublished data, 2015). Based on the results of Chapter 2, I *a priori* classified these lakes as "lower catchment influence." Catchments in the RDC region are larger relative to lake area than catchments in the ATQ region (Chapter 2), and are located in the ACP foothills transition zone, which is an area where topography and ice-rich soils lead to bank erosion and shoreline subsidence (Hinkel et al. 2012). Catchment soils in the RDC region are silty with a thick organic-rich surface layer (Jorgensen and Grunblat, 2013), and have a lower hydraulic conductivity (Koch, unpublished data, 2015) than those in the ATQ

region (Chapter 2); this makes them prone to higher overland flow. I *a priori* classified the RDC lakes as "higher catchment influence." Visual assessment revealed that lakes in the RDC region have much greater macrophyte cover (~>75%) in their littoral zones than those in the ATQ region (~<10%). Select physico-chemical data on each of the lakes are presented in Table 3.1.

Sample collection and preparation

In August 2016, a variety of biotic (i.e., fish, macroinvertebrates, zooplankton, macrophytes, periphyton/biofilm) and abiotic (water and sediment) samples were collected from each of the six study lakes. Fish were collected using a combination of fyke nets and minnow traps. Upon collection, fish were sacrificed, measured for fork length and weight, and frozen whole at -20°C for future analyses of stable isotope ratios and mercury (total mercury for all fish, methyl mercury for a subset; more details below). The only fish species collected from all lakes was Ninespine stickleback (*Pungitius pungitius*). As such, further analyses focused on this species. No piscivorous fish were collected from any of the study lakes; however, Arctic grayling (*Thymallus arcticus*; ATQ 200, ATQ 206) and Alaska blackfish (*Dallia pectoralis*; ATQ 206, RDC 309, RDC 311) were found in a subset of lakes. Benthic macroinvertebrates were collected using a combination of dip-netting and Ekman dredging (250 µm mesh). After collection, invertebrates were sorted, identified to taxonomic Family, and frozen at -20°C for future analyses of stable isotope ratios and total (where possible) and methyl mercury concentrations. Bulk zooplankton samples were collected from the pelagic zone of each lake by pumping 60 L of water through 53 µm mesh. A sub-sample was preserved in ethanol, and this was used to determine taxonomic resolution, and to estimate zooplankton abundance

(individuals/L; Guernon, 2019). A second sub-sample was frozen -20°C for analyses of stable isotope ratios and total and methyl mercury concentrations.

Water samples were collected from the approximate centre of the lake. Secchi depth was estimated, and *in situ* measurements of lake temperature and dissolved oxygen (profiles) were taken with a YSI Professional Plus Handheld meter, along with measurements of conductivity and pH. Grab water samples were collected for nutrients, turbidity, and ions. Several liters of water were collected in brown Nalgene bottles and filtered onshore using ethanol-rinsed 0.42 μm filters. Unfiltered water samples for Hg analysis were collected via a surface grab using the 'clean hands-dirty hands' technique (U.S. EPA, 1996). Filtered water samples for Hg analysis were collected by using a peristaltic pump and an acid-washed Teflon line that was deployed slightly below surface. Water samples were filtered through quartz QMA filters that had been muffled at 450°C for 20 minutes and stored in acid-washed petri dishes. Filters were mounted in acid-washed re-usable cartridges. All water samples were preserved with ultra-trace HCl at a concentration of 1% by volume. Following collection of filtered water for Hg analysis, the same filtering apparatus was used to collect samples for analyses of DOC and DIC.

After water samples were collected, sediment samples were collected from the same approximate mid-lake location using an Ekman dredge. The top 2 – 3 cm of sediment was collected using an acid-washed Teflon spoon before being frozen at -20°C prior to analysis of total and methyl mercury concentrations. Periphyton samples were collected by hand and by

syringe from algal mats and macrophyte beds, and frozen prior to stable isotope and total and methyl mercury analyses.

Laboratory analysis

All biological samples (fish, invertebrates, zooplankton, biofilm) and sediment samples were freeze-dried using a LabConco FreeZone operated at -54°C and 0.014 mBar for 48 hours. Freeze-dried samples were ground to a uniform powder using scissors inside borosilicate scintillation vials or a mortar and pestle. Prior to freeze-drying, whole stickleback had their otoliths and guts removed, and macroinvertebrates were sorted by family and removed from shells where applicable (i.e., mussels, snails).

Total Hg analysis on 260 fish (mean=44±12 (s.d.)/lake) was completed at the University of Waterloo, Waterloo, Ontario, Canada, using an Ohio Lumex PYRO-915+ (100-240V, 50/60Hz, 700W; Burger et al. 2004). Approximately 10-15 mg of dry tissue was used for THg analysis. The mean method detection limit was 0.02 ± 0.01 μg/g (dry weight). The mean relative percent difference between duplicate samples was 9.5±5.6% (n=28), and the mean percent recovery of certified reference material was 95.9±7.4% (n=33; DORM-4, National Research Council of Canada 2012). Results from method blanks (n=38) were consistently below the method detection limit.

Analyses of methylmercury (MeHg) concentrations on fish, zooplankton, benthic invertebrates, periphyton, and sediment were completed at the Biotron Analytical Services Laboratory at Western University, London, Ontario, Canada. Briefly, a potassium hydroxide

solution (KOH) was added to sample tissues prior to hot block digestion (Bloom and Fitzgerald, 1988), and the resulting extracts were speciated by gas chromatography and analyzed using cold vapor atomic fluorescence spectroscopy on a Tekran 2700 Automated MeHg Analysis System following U.S. EPA method 1630 (U.S. EPA, 1998). Ten to 15 mg of tissue from a subset (10%) of Ninespine stickleback were analyzed for methylmercury whereas all invertebrates, zooplankton, sediment, and periphyton samples were analyzed for methylmercury. The method detection limit was 0.009 ng/g (dry weight). Mean relative percent difference between duplicates was 9.6±9.5% (n=28), and mean percent recovery of certified reference material was 85.5±14.4% (n= 24; DORM-4, National Research Council of Canada 2012). Results from method blanks (n=27) were consistently below the detection limit.

Analyses for stable carbon and nitrogen isotope ratios were completed on the fish, invertebrates and zooplankton at the Environmental Isotope Laboratory at the University of Waterloo, Ontario. Stable isotope ratios are expressed as delta values ($\delta^{13}C$, $\delta^{15}N$) in parts permil (‰) relative to international standards (Pee-Dee Belemnite and N_2 gas, respectively). Analytical error for $\delta^{13}C$ and $\delta^{15}N$ never exceeded 0.3 and 0.2‰, respectively, based on measurements of standardized reference materials cross-calibrated to the international standards, and standardized reference materials comprised no less than 20% of samples. The mean relative percent difference between duplicate samples was 1.2±1.8% (n=104) for $\delta^{13}C$ and 6.4±8.3% (n=104) for $\delta^{15}N$.

To estimate fish age, one sagittal otolith from each fish was submerged in water and photographed (Leica Application Suite version 4.0.0, Leica Microsystems [Switzerland] Limited) at 40x magnification under a dissecting microscope (Leica M60) at the USGS Alaska Science Center, Anchorage, Alaska. Two independent readers counted visible annuli under reflected light (Jones and Hynes 1950; DeFaveri et al. 2014). If results from the two readers did not agree, a third reader provided an independent estimate (< 7%).

Water samples were analyzed for a suite of standard water chemistry parameters (e.g., nutrients, ions, dissolved organic carbon) at the University of Alberta Biogeochemical Analytical Service Laboratory in Edmonton, Alberta. Total and methyl mercury analyses in water were completed at the Biotron Analytical Services Laboratory at Western University, London, Ontario. Water samples were analyzed for SUVA (the UV absorbance at 254 nm, normalized for DOC concentration). The $SUVA_{254}$ was quantified using the methods outlined in Weishaar et al. (2003) with a Spectramax® M2 spectrophotometer (Molecular Devices Corp., Sunnyvale, CA, USA) in the Watershed Hydrology Group Laboratory at McMaster University, Ontario, Canada.

Data analysis

All statistical analyses were completed using R Studio v 1.0.136 and R v 3.5.1 with core packages, as well as "lsmeans" (Lenth et al. 2016) and "vegan" (Oksanen et al. 2018) packages. Figures were generated using Sigmaplot v 11.0 (Systat, 2008) or Arcmap™10.2.2 (ESRI, 2016). As mentioned above, MeHg analyses were completed on a subsample of fish (10%) that were analyzed for total mercury. A mean ratio of [MeHg] to [THg] was calculated

for stickleback in each lake, and this ratio was used to convert all of the THg concentrations in stickleback to estimated MeHg concentrations; MeHg concentrations were then used in all other data analyses (Table S3.1 Appendix B). When data were not normally distributed a, $\log_e$ transformation was applied, and for all significance testing, alpha was set to 0.05.

To address objective 1 and determine if there were physico-chemical differences in water chemistry between regions on the ACP consistent with those outlined in Chapter 2, a principal components analysis on lake chemistry variables was generated. Additionally, t-tests were used to compare other water chemistry variables including DOC : Chl-*a*, THg, and MeHg.

To address objective 2 and determine if there were differences between the ATQ and RDC regions in MeHg concentrations in sediment, periphyton, zooplankton, and invertebrates, t-tests were used. For the zooplankton MeHg, values presented are from a bulk sample, and for the invertebrate MeHg concentrations, values presented represent a mean across all taxa present in each lake; community composition data can be found in Table S3.2 (Appendix B). Because mercury is known to increase with fish length (e.g., Bodaly et al. 1993), an ANCOVA was used to assess regional differences in fish MeHg, with the $\log_e$ of length as a covariate and lake as the categorical variable to standardize for fish length, and a least-squares mean of fish [MeHg] was calculated for each lake, henceforth referred to as LSmean [MeHg]. The LSmean [MeHg] were then used as a responding variable for further data analyses (i.e., correlation analyses and general linear models).

To address objective 3 and identify drivers of MeHg in different ecosystem components in this region, a combination of analyses was used. To identify potential drivers of mercury methylation, Pearson's product-moment correlations were used to identify significant relationships between water chemistry covariates (SO_4, DIC, Cl, DOC, DOC : Chl-*a*, TN, TP, pH, Turbidity, Chl-*a*) and %MeHg (a proxy for methylation) in sediment and periphyton. General linear models were then used to model %MeHg by statistically significant and ecologically relevant covariates. To better understand the trophic ecology of each region, t-tests were used to compare zooplankton abundance and carbon and nitrogen stable isotope ratios in biota between regions. Finally, to identify drivers of fish [MeHg], Pearson's product-moment correlations were used to identify significant relationships between fish LSmean [MeHg] and biotic (e.g., age-at-size) and abiotic variables (SO_4, DIC, Cl, DOC, DOC : Chl-*a*, TN, TP, pH, Turbidity, Chl-*a*). General linear models were then used to model fish LSmean [MeHg] by the variables with a significant correlation with fish LSmean [MeHg].

3.3 Results

Lake Chemistry

Physico-chemical properties of the lakes differed between the two regions (Table 3.1). The RDC lakes had higher concentrations of dissolved inorganic carbon (DIC), dissolved organic carbon (DOC), sulphate (SO_4), and chloride (Cl) than the ATQ lakes, indicating relatively stronger catchment influences in the RDC lakes. The ATQ lakes had comparatively higher Chl-*a* concentrations indicating higher autochthonous production (Table 3.1). Additionally, the RDC lakes had higher SUVA, indicating that organic carbon in these lakes is more aromatic (Table 3.1). Results of a principal components analysis conducted on the water chemistry data (Fig 3.2) further illustrate differences between regions. PC1 explained 67% of the variability in water chemistry among the study lakes, and appears to reflect a gradient of allochthony to autochthony; variables associated with terrestrial/catchment influence (i.e., DIC, DOC, Cl, SO_4) have negative loadings on PC1 (Fig. 3.2), whereas indicators of higher autochthonous production (i.e., Chl-*a*, TP and turbidity) have positive loadings on PC1 (Fig. 3.2). All of the ATQ lakes had positive PC1 loadings, indicating greater autochthony, whereas all of the RDC lakes had negative PC1 loadings, indicating greater allochthony, (Fig 3.2). There was a significant difference between PC1 scores of the RDC lakes and the ATQ lakes (T-test; t=4.29, p=0.01, df= 3.98). Additionally, the RDC lakes had a significantly higher mean DOC : Chl-*a* ratio than the ATQ lakes, further indicating the greater importance of allochthonous inputs to the RDC lakes (T-test; t=3.83, p=0.04, df=2.68; Fig 3.3).

Methyl mercury concentrations in water, sediment, and periphyton

As results from water chemistry analyses revealed significant differences between regions in several variables that affect mercury accumulation and methylation, total and methyl mercury

concentrations in water, sediment, and periphyton were compared between the ATQ and RDC regions before being related to possible covariates (e.g., pH, DOC). There were no significant differences in concentrations of total (T-test, t=1.44, p=0.29, df=2.02) or methyl mercury (T-test, t=1.20, p=0.35, df=2.0) in unfiltered water samples. Concentrations of total and methyl mercury in filtered water could not be statistically compared between regions because several values of MeHg were less than the method detection limit (MDL=0.006 ng/L). While there was no significant difference between regions in [THg] in sediment (T-test; t=2.03, p=0.16, df=2.31; Fig 3.4a-c), mean [MeHg] (T-test; t=15.69, p<0.01, df=2.02; Fig 3.4a-c) and mean percent MeHg (of total Hg) were significantly higher in the ATQ region than in the RDC region (T-test; t=8.56, p<0.01, df=2.35 Fig 3.4a-c). Similarly, although there was no significant difference in [THg] in periphyton between regions (T-test; t=1.06, p=0.38; Fig 3.4a-c), both mean periphyton [MeHg] (T-test; t=3.02, p=0.04, df=3.79; Fig 3.4a-c) and mean percent MeHg differed significantly between the regions (T-test; t=2.79, p=0.05, df=4.0 Fig 3.4a-c). Whereas [MeHg] and %MeHg in sediment were significantly higher in the ATQ region, [MeHg] and %MeHg in periphyton were significantly higher in the RDC region. These results indicate that while methylation in lake sediments is higher in ATQ lakes, methylation in littoral periphyton and associated biofilms is higher in the RDC lakes. To investigate the relative importance of different methylation sites in the study lakes, %MeHg in sediment was compared to %MeHg in periphyton for lakes within each region. There was no significant difference between %MeHg in sediment and % MeHg in periphyton in the ATQ lakes (Paired t-test; t=0.62, p=0.59, df=2); however, in the RDC lakes, %MeHg in periphyton was significantly higher than %MeHg in sediment (Paired t-test; t=0.12.77, p=0<0.01, df=2, Fig 3.4c).

To further investigate the cause of differences between regions in %MeHg, %MeHg in sediment and periphyton for each lake were correlated with relevant water chemistry variables, including major ions, DOC, pH, nutrients, and chlorophyll-*a*. Percent MeHg in sediment was significantly and negatively correlated with several catchment-associated variables, including SO_4, Cl, DOC, and DOC : Chl-*a*, whereas percent MeHg in periphyton was significantly and positively correlated with some of these same variables, including SO_4 and Cl (Table 3.2). Since the positive correlations between %MeHg in periphyton and the catchment indicator variables could represent a causative methylation mechanism, %MeHg in periphyton was related to SO_4 concentrations in the water column (as the correlation with SO_4 was the strongest, and because SO_4 was significantly correlated with Cl; Pearson product-moment correlation, r= 0.84, p=0.03). SO_4 concentration explained >75% of the variability among lakes in %MeHg in periphyton (Linear regression, R^2=0.77, $F_{(1,4)}$=17.75, p=0.01, Fig 3.5).

Methyl mercury concentrations in zooplankton and benthic invertebrates

As zooplankton are typically exposed to water column MeHg (diffused from sediments) via phytoplankton, I expected that [MeHg] in zooplankton would be higher in the ATQ lakes than in the RDC lakes. MeHg concentrations in zooplankton ranged between 4.65-16.31 ng/g dry weight (Fig 3.6) and, unlike concentrations in sediment and periphyton, did not differ significantly between regions (T-test, t=0.79, p=0.51, df=2.08). To aid in interpreting results of stable isotope analyses on fish, zooplankton abundance was compared between regions. Although statistically insignificant (T-test, t=0.28, p=0.80, df=3.99), there were obvious differences between regions in zooplankton abundance, which ranged from 1 to 98 individuals/L in the study lakes.

Similar to the results for zooplankton, MeHg concentrations in benthic invertebrates did not mirror the regional patterns found for either sediment or periphyton, and there was no significant difference between region (T-test, t=1.69, p=0.17, df=3.82). Mean [MeHg] in benthic invertebrates (mean of all taxa) for each lake ranged from 26.9-50.7 ng/g dry weight (Fig 3.6), which was between 2.2-8.5 times higher than bulk zooplankton MeHg concentrations (Fig 3.6).

Benthic invertebrate community composition was not assessed, nor was benthic invertebrate abundance quantified. Presence/absence of invertebrate taxa are presented in Table S3.2 (Appendix B). Only a few macroinvertebrate taxa were common between regions and captured in all lakes. Taxa that were collected in all lakes, and which had enough mass for analytical comparison between regions included Sphaeridae, Chironomidae, and Tanypodinae. Methyl mercury concentrations in Sphaeridae, a type of filter-feeder, were significantly higher in ATQ lakes than in RDC lakes (T-test, t=2.45, p=0.04, df=4, Fig 3.7); however, there were no significant differences in [MeHg] between regions in Chironomidae (collector-gatherers; t-test, t=1.33, p=0.27, df=3.15; Fig 3.7), or Tanypodinae (predator-engulfers; t-test, t=0.31, p=0.78, df=2.50; Fig 3.7).

Trophic Ecology

In light of the regional differences in [MeHg] in some ecosystem components, as well as the regional differences in primary production, inter-lake variability in zooplankton abundance, and qualitative observations of variability in types and abundance of benthic invertebrate taxa, mean stable C and N isotope ratios of zooplankton, invertebrates, and fish were compared between regions to assess energy pathways and trophic structure. In both regions,

the fish were ^{15}N-enriched by ~4-5 ‰ compared to the primary consumers (zooplankton and invertebrates), indicating that, as expected, they are feeding at a higher trophic position (Fig 3.8). The fish fell between zooplankton and benthic invertebrates in carbon isotope space in both regions (Fig 3.8). Separation of benthic invertebrates and zooplankton in carbon isotopic space was greater in the RDC lakes than in the ATQ lakes (Fig 3.8). There were differences in $\delta^{13}C$ between the regions, which is indicative of differences in basal carbon sources. Fish (T-test, t=2.86, p=0.05, df=3.71) and benthic macroinvertebrates (T-test, t=5.19, p=0.02, df=2.35) had significantly depleted ^{13}C in the RDC lakes compared to the ATQ lakes. Zooplankton also had more negative $\delta^{13}C$ in the RDC lakes than in the ATQ lakes, but the difference was not statistically significant (T-test, t=1.38, p=0.23, df=3.13).

Mercury concentrations in Ninespine stickleback

Because there were differences between regions in [MeHg] in sediment and periphyton, and because lakes in the RDC region appeared to be more influenced by their catchments and the food webs to have different basal resources, I expected [MeHg] in stickleback to differ among lakes, and to be higher in the RDC region. MeHg concentrations in stickleback differed significantly among lakes and were significantly related to fish length. In addition, the relationship between [MeHg] and fish length differed significantly among lakes (i.e., interaction term was significant; ANCOVA, R^2=0.78 $F_{(11,248)}$=84.14, p<0.0001). Least-squares mean (at the mean length; 50 mm) [MeHg] did not differ significantly between regions, however (T-test, t=1.05, p=0.35, df=3.98), since one lake from the ATQ region (ATQ 201) had relatively high LSmean [MeHg], while one lake from the RDC region (RDC 309) had relatively low LSmean [MeHg] (Fig 3.9).

To determine drivers of among-lake variability in LSmean [MeHg] in stickleback (at the mean length of 50mm), relevant biotic and abiotic covariates were related to LSmean stickleback [MeHg] using Pearson's product-moment correlation (Table 3.3). Contrary to the expectation that mercury concentrations in fish would be most closely related to variables that indicate source of production (allochthonous vs autochthonous), neither DOC nor Chl-*a* were significantly correlated to LSmean [MeHg] in stickleback (Table 3.3). There was, however, a significant positive correlation between LSmean [MeHg] in stickleback and LSmean age (at the same standardized size of 50 mm; generated from an ANCOVA relating age to lake and loglength; R^2=0.76, $F_{(11,237)}$=70.78, p<0.0001) (Pearson's product-moment correlation, r=0.85, t= 3.29, p=0.030, df=4 Fig 3.10a). Additionally, there was a significant positive correlation between lake SO_4 concentration and LSmean [MeHg] in stickleback (Table 3.3, Fig 3.10b). Stickleback age-at-size and lake logSO_4 concentration were not significantly correlated (Pearson's product-moment correlation, r=0.47, t=1.07, p=0.35, df=4). No other variables, either biotic or abiotic, were significantly related to LSmean [MeHg] in stickleback (Table 3.3). A general linear model including both SO_4 concentration and stickleback age-at-size (interaction term not significant, p>0.05) accounted for 94% of the variability in length-adjusted mean [MeHg] in stickleback (R^2=0.94, $F_{(2,3)}$=41.87, p=0.006).

3.4 Discussion

Lake Chemistry

Based on the results from Chapter 2, I predicted that water chemistry data would reflect relatively greater autochthony in the ATQ (low catchment influence) lakes, and relatively more allochthony in the RDC (high catchment influence) lakes. This prediction was supported by results from the multivariate analysis of water chemistry, which showed that lakes in the RDC region were associated with variables that indicate higher catchment influence, including higher concentrations of ions and DOC. In contrast, the ATQ lakes were associated with variables that indicate higher autochthonous production, including concentrations of chlorophyll-*a* and total phosphorous. In addition, RDC lakes had higher DOC : Chl-*a* ratios; as Chl-*a* is a proxy for in-lake production, a lower DOC : Chl-*a* ratio indicates a larger proportion of autochthonous production (see Rose et al. 2015).

The physico-chemical differences in lakes between the ATQ and RDC regions were first addressed in Chapter 2, where I found that Hg accumulation in lake sediments was heavily influenced by catchment processes (i.e., sedimentation rate) in an RDC lake, and in-lake processes (i.e., primary production) in an ATQ lake. The higher catchment influence in the RDC lakes was inferred to be a product of catchment soils and hydrology. The ATQ lakes are located on sandy well-drained soils, have high hydraulic conductivity, and small relative catchment sizes (Chapter 2; Koch, unpublished, 2015). In contrast, the RDC lakes have much larger relative catchment sizes (Chapter 2), are located on silty catchment soils with a thick organic-rich surface layer (Jorgensen and Grunblat, 2013), and have a lower hydraulic conductivity (Koch, unpublished, 2015). Based on the results of chlorophyll-*a* analyses

completed in this study, along with anecdotal visual observations (aerial) of macrophyte extent, I suspect that differences in degree of catchment influence have led to phytoplankton dominance in the ATQ lakes, while in-lake production of RDC lakes is macrophyte-dominated. Studies have shown that in lakes with high sediment inputs, such as those with thermokarstic activity (Mesquita et al. 2010; Chapter 2), primary production is dominated by macrophytes, since inputs of minerogenic soils can result in ionic-organic compounds precipitating from water column, which leads to greater water transparency and establishment of emergent vegetation (Stabel, 1986; Kalff, 2001).

Differences in lake water chemistry between regions were not reflected in differences in water column [THg] or [MeHg], or in the [THg] of sediment or periphyton. However, there were differences between regions in [MeHg] and %MeHg in both sediment and periphyton, suggesting that lake physico-chemistry does influence the location and rates of mercury methylation. Percent MeHg can be used as a proxy for net methylation rates, such that a higher %MeHg indicates higher net methylation (Drott et al. 2007). As rates of methylation and demethylation were not directly quantified, %MeHg (of total) was used an indicator of net methylation. I thus infer higher net methylation rates in sediments of the more autochthonous ATQ lakes, and higher net methylation rates in periphyton in the more allochthonous RDC lakes.

Autochthonous primary production was higher in the ATQ lakes than the RDC lakes. Greater autochthonous production can impact mercury methylation in multiple ways. Higher algal densities increase the capacity for elemental mercury to be scavenged from the water

column and delivered to the sediment porewaters (e.g., Outridge at al. 2007); however, a negative relationship between primary production and mercury delivery to the sediments has also been found (Kirk et al. 2011). Although water column mercury concentrations were not significantly different between regions, fluxes of mercury to sediments in the ATQ lakes may thus be greater because of algal scavenging; however, if this were the case, I would expect higher THg in the sediments of the ATQ lakes, which was not observed. Primary production can also impact methylation by increasing the amount of bioavailable organic matter. I suggest that the higher inferred methylation rates in the sediments of the ATQ lakes are likely a product of greater autochthony increasing methylation rates, which is consistent with the work of Bravo et al. (2017) on boreal lakes. These authors found that in lakes where the organic matter was dominated by phytoplankton-derived compounds, the sediment Hg methylation rates were higher, since this carbon is more labile and available to be used as a substrate for methylating bacteria (Bravo et al. 2017). The higher specific ultraviolet absorbance (SUVA) values in RDC lakes provide further evidence that carbon could be less bioavailable in those lakes. SUVA represents the UV absorbance of a water sample at 254 nm, normalized for DOC concentration. There is a significant positive correlation between SUVA at 254 nm and the aromaticity of carbon (Weishaar et al. 2003), and it is humic (allochthonous) substances that comprise the aromatic fraction of DOC (Weishaar et al. 2003). Therefore, although the more allochthonous RDC lakes have larger catchment inputs (e.g, sediments, ions), the organic matter entering the systems is on average more recalcitrant, and subsequently less bioavailable to bacteria and other organisms.

Net methylation appears to be higher in periphyton of the RDC lakes than in periphyton of the ATQ lakes or in sediment of the RDC lakes. This result is unsurprising because although the majority of mercury methylation is thought to occur in anoxic sediment porewaters (Gilmour et al. 1992), there is recent evidence that beds of macrophytes provide an environment ideal for dense periphyton growth – the biofilms that characterize periphyton include sulphate reducing bacteria, and can be methylation "hot spots" (Mauro et al. 2001). Results from various studies on waterbodies in Brazil (Mauro, 2001), Florida (Mauro et al. 2002), and Wisconsin (Mauro et al. 2002) indicate that methylmercury production was elevated in periphyton associated with macrophyte beds. In this study, not only is periphyton far more abundant (qualitative, anecdotal observation) in the RDC lakes due to macrophyte dominance, but it also likely receives greater inputs of sulphate and bioavailable Hg(II) from the catchment. Percent MeHg in periphyton was positively correlated with both SO_4 and Cl (catchment indicators), whereas %MeHg in sediment was negatively correlated with these and other catchment indicators. This further supports my inference that the level of catchment influence is driving methylation location and rate in the study lakes. While inferred methylation rates in the ATQ lake sediments were higher than those in the RDC sediments, and this is consistent with the findings of Bravo et al. (2017), inferred methylation rates in periphyton were higher in the RDC lakes and related to catchment indicators. This suggests that effects of catchment influence on MeHg accumulation in shallow Arctic thermokarst lakes may be mediated by presence and extent of littoral macrophyte beds and associated periphyton.

The significant positive relationship between water column SO_4 concentrations and %MeHg in periphyton suggests that sulphate is likely affecting methylation rates in the periphyton. Elevated sulphate concentrations can stimulate sulphate-reducing bacteria (Gilmour et al. 1992; Branfireun et al. 1999), which are the primary methylators in many freshwater systems (Compeau and Bartha, 1985). Gilmour and Henry (1991) suggested that there is an optimal sulphate concentration for methylation, above which methylation is inhibited and below which sulphate is limiting. Although I do not have a full suite of data on periphyton or sediment chemistry, the water column sulphate concentrations were relatively low in these lakes, so I infer that sulphate was likely limiting in all of these systems. Bacterial sulphate reduction is often sulphate-limited, and under sulphate-limiting conditions, methanogenesis is the primary pathway of terminal carbon metabolism (Capone and Kiene, 1988). Thus, increased sulphate loading can result in a greater proportion of carbon flow through sulphate respiration (Regnell, 1990).

Once mercury is methylated in either the sediments or the periphyton in these lakes, it is taken up by organisms feeding at the sediment-water interface or on the macrophyte biofilms, or it is diffused into the water column where it can be assimilated by phytoplankton and subsequently consumed by grazers. I expected that organisms grazing in the water column or at the sediment water interface would have higher MeHg concentrations in the ATQ lakes than the RDC lakes, and that organisms feeding in/on the biofilm would have higher MeHg concentrations in the RDC lakes. A comparison of [MeHg] in bulk zooplankton revealed no differences between regions. Analyses on individual taxa would have likely been more revealing; however, due to sample size limitations, we were unable to complete analyses on

individual taxa (zooplankton were live-sorted into Cladocerans and Copepods, see Guernon, 2019) in every lake, so comparisons were made using bulk samples. Using bulk samples could have affected the analysis in several ways. First, the community composition of zooplankton in each lake is different (Guernon, 2019), and previous authors have reported that certain zooplankton taxa (i.e., Daphnia spp.) have higher MeHg concentrations because they are efficient grazers (Chétalat and Amyot, 2009). In addition, MeHg in bulk samples of zooplankton from the ATQ lakes could be diluted by the more abundant phytoplankton, which are comparatively lower in MeHg and which were not removed from bulk samples. It was also unsurprising that in general, zooplankton abundance was higher in the ATQ lakes since zooplankton abundance is governed by basal resources and tends to increase with lake trophic state (McCauley and Kalff, 1981). I suggest that the ATQ lakes better support a grazing food web than the RDC lakes.

Benthic macroinvertebrates had appreciably higher [MeHg] than bulk zooplankton in all of the study lakes, and there was no regional difference detected in the mean macroinvertebrate [MeHg]. This may be due to regional differences in the composition of benthic invertebrate communities (Table S3.2, Appendix B), but quantitative data are not available to test this assertion. Since the habitats (e.g., extent of macrophyte cover) and invertebrate communities likely differ between regions in ways I did not quantify, the comparison of mean MeHg in benthic invertebrate taxa was coarse. Three taxa were collected in high enough numbers to permit taxa-specific comparisons of [MeHg] among lakes: Sphaeridae, Chironomidae, and Tanypodinae. I expected that bivalves would have higher [MeHg] in the ATQ lakes than in the RDC lakes, which I did find: Sphaeridae had significantly higher [MeHg] in the ATQ

lakes than in the RDC lakes. Bivalves can accumulate heavy metals to concentrations several orders of magnitude greater than the surrounding water because they efficiently filter feed in the sediment porewaters, and are exposed to MeHg from both sediment and phytoplankton (see Naimo, 1995). There were no significant regional differences in [MeHg] in Chironomidae or Tanypodinae, which is perhaps not surprising as both of these taxa can live and feed in either sediment porewaters (higher MeHg in ATQ) or biofilm (higher in MeHg in RDC; Merrit and Cummins,1996), and we collected individuals in a variety of habitats with a combination of dip-netting and sediment dredging from both of these environments.

I suspect that, for both zooplankton and benthic macroinvertebrates, more paired-taxa comparisons between regions would have revealed more significant results. I would expect Cladoceran taxa (especially Daphnia) to have higher [MeHg] in the ATQ lakes than in the RDC lakes, due to higher sediment MeHg concentrations and phytoplankton abundance. Additionally, I would expect benthic macroinvertebrates that feed exclusively in and on the biofilm to have higher MeHg concentrations in the RDC lakes than in the ATQ lakes. Unfortunately, since the biomass of several invertebrate and zooplankton taxa were so low, a considerably higher sampling effort would be required for more taxa-specific comparisons.

Following the examination of primary consumers, I investigated regional differences and drivers of [MeHg] in Ninespine stickleback. Contrary to my predictions, I did not see higher [MeHg] in stickleback in the RDC lakes. Although the stickleback from the ATQ lakes were typically lower in [MeHg] than the RDC lakes, there was one ATQ lake (ATQ 201) with fish

that had relatively high [MeHg], and one RDC lakes (RDC 309) with fish that had relatively low [MeHg]. I identified SO_4 as a significant abiotic driver of among-lake variability in stickleback MeHg concentrations, and SO_4 was higher in the more allochthonous RDC lakes than in the more autochthonous ATQ lakes; however, this relationship was mediated by the significant biotic driver, growth (age-at-size), which did not differ between regions.

The significant positive relationship between age-at-size and length-adjusted mean [MeHg] in Ninespine stickleback indicates that the faster-growing fish have lower MeHg concentrations, which is a commonly observed phenomenon, termed somatic growth dilution (Karimi et al. 2007). Essentially, faster growing organisms gain more biomass per unit food intake, and therefore dilute the MeHg burden from the food they consume. Ninespine stickleback from the three lakes with the highest length-adjusted mean [MeHg] (RDC 311, RDC 308, and ATQ 201), were all older at the standardized length of 50 mm. Similar results of fish mercury concentrations being best predicted by age-at-size, have been found in several other Arctic studies including two on Arctic char (*Salvelinus alpinus*; Swanson et al. 2010; Swanson et al. 2011) and one on Lake trout (*Salvelinus namaycush*; Swanson et al. 2011).

I initially expected that DOC or Chl-*a* would be related to [MeHg] in Ninespine stickleback, because previous studies have shown that type and amount of organic matter can influence methylation, and consequently the pool of methylmercury, which is one of the main controls on fish MeHg concentration. This prediction was predicated on the assumption that the primary transport routes for Hg were the same among lakes, and that methylation was

primarily occurring in the sediment porewaters in both regions. Results indicate, however, that methylation locations and routes of MeHg entering the food web are different between the two regions studied. I have demonstrated that methylation is higher in the sediments of the ATQ lakes and in the periphyton of the RDC lakes, and I infer from water chemistry and stable isotope results that ATQ lakes support a grazing food web whereas RDC lakes support a biofilm-based food web.

The significant positive relationship between lake water SO_4 and length-adjusted mean MeHg concentration in stickleback suggests that the rate of mercury methylation is likely a major control of fish MeHg concentration in lakes across the ACP. We know that sulphate can stimulate methylation, but how that translates into differences in the fish is complex, as MeHg must first be taken up by primary consumers, and we did not see differences between regions in primary consumer [MeHg]. There were also no relationships between [MeHg] in primary consumers and lake water SO_4 (analysis not shown). Literature reports of empirical relationships between lake water SO_4 and fish MeHg concentration are scarce, which is not surprising given the many complex and indirect mechanisms that may affect the relationship. A study completed on fish from across the Florida everglades (Gabriel et al. 2014) found that although the relationship between fish MeHg and SO_4 was non-linear, concentrations of fish Hg were highest in waters with SO_4 concentrations ranging from 1-12 mg/L, a range that only the highest-sulphate lake in this study (RDC 308) falls within.

We can begin to form an inferred conceptual understanding of the link between lake water SO_4 and fish [MeHg] in these lakes if we examine differences in the food webs and the diet

of Ninespine stickleback between lakes and regions. The $\delta^{13}C$ ratios of fish, invertebrates and zooplankton in the ATQ lakes all have $\delta^{13}C$ values that are indicative of a classic pelagic signal (France et al. 1995), while each of these taxa is more ^{13}C -depleted in the RDC lakes. Lower $\delta^{13}C$ values can be indicative of a more bacterial-based food web (Bunn and Boon, 1993). This suggests that the ATQ lakes support a grazing food web, while the RDC allochthonous lakes support a biofilm-based food web, although research that included fatty acid signatures would be helpful in further testing this assertion. The extent to which a food web is phytoplankton or bacterial-based can have implications for mercury uptake and accumulation (de Wit et al. 2012).

Differences in primary consumer [MeHg] based on food web structure have been previously documented. Chételat et al. (2011) found that pelagic zooplankton had higher [MeHg] than littoral macroinvertebrates in Canadian mid-latitude lakes. The authors of this work attribute this difference to the pelagic zooplankton community efficiently taking up MeHg from bacteria and algae in the water column and potentially gaining access to MeHg-rich areas of the hypolimnion through vertical migration, whereas littoral invertebrates in the studied lakes primarily feed on detrital organic matter with low [MeHg] (Chételat et al. 2011). The results that Chételat and colleagues report (2011) are analogous to the regional fish [MeHg] concentrations presented here, albeit via a different mechanism due to major morphometric and ecological differences in the lakes investigated. The zooplankton in Chételat et al. (2011) were exposed to higher concentrations of MeHg via bacteria in the water column, whereas the invertebrates in this study were exposed to higher concentrations of MeHg via periphyton than the zooplankton via phytoplankton.

Information about availability of potential prey items further indicates differences at the base of the food web between ATQ and RDC lakes. Zooplankton abundance was generally higher in the ATQ lakes than in the RDC lakes, with the exception of RDC 309. Stickleback hunt by sight and are selective in their feeding, and local conditions (e.g., prey availability) can affect feeding preferences (Saunders, 1914; Delbeek and Williams, 1988; Laske et al. 2018). Crustacean zooplankton are often chief components of stickleback diet; however, stickleback can also eat insect larvae, worms, mollusks, and larger crustaceans (Hynes, 1950; Laske et al. 2018). It has been shown that when zooplankton are scarce (e.g., during winter months), fish are driven to eat other less desirable (more difficult to consume/catch) items (Hynes, 1950). In a recent study on fish feeding habits on the Arctic Coastal Plain of Alaska, Laske and others (2018) found that although stickleback had a great diversity of prey items in their diets, cladoceran zooplankton and dipteran larvae comprised the largest numeric proportion. In both RDC 308 and RDC 311, zooplankton abundance was quite low (1.1 and 4.3 individuals/L, respectively) compared to the other lakes, so it is logical that the fish in these lakes would rely more heavily on other macroinvertebrate prey items, which on average have higher MeHg concentrations than crustacean zooplankton across all lakes. Many benthic macroinvertebrates taxa collected in these lakes are classified as collector-gatherers (Merrit and Cummins,1996) and feed on a variety of detritus, algae, and bacteria; all of which are components of biofilm/periphyton. Conversely, zooplankton, which in these lakes were dominated by the Cladoceran species *Bosmina longirostris* (Guernon et al. 2019), predominantly feed on phytoplankton in the water column (DeMott, 1982). As such, it is logical that even though there were no significant differences in zooplankton or invertebrate

mean [MeHg], the among-lake differences in stickleback [MeHg] that were attributed to SO_4 in the statistical analysis could partially be explained by the proportion of diet comprised by higher MeHg prey, necessitated by the scarcity of zooplankton in the higher catchment influenced lakes. This could also help explain why stickleback in RDC 309 are comparatively lower in MeHg than the other RDC lakes, since zooplankton in this lake were abundant.

Summary and proposed mechanisms

I have reinforced the earlier work from Chapter 2 and shown that there are some lakes that are more influenced by their catchments than others, and that in this study the RDC lakes have higher catchment influence that the ATQ lakes. I provide evidence that the physico-chemistry and food web structure of lakes in the RDC and ATQ regions are very different. I proffer that higher sedimentation rates in the RDC lakes have led to the development/persistence of extensive macrophyte beds with associated biofilm (confirmed visually), which, combined with sulphate inputs from the catchment, become methylation "hot spots". Littoral macroinvertebrates feed directly on this biofilm (algae, OM, bacteria and MeHg), accumulate MeHg, and are subsequently consumed by stickleback, especially in lakes with low zooplankton abundance. The ATQ lakes are less impacted by catchment processes, and are phytoplankton- rather than macrophyte-dominated. Within the ATQ lakes, the chief location of methylation is in the sediment porewaters. MeHg subsequently diffuses into the water column, bio-concentrates in phytoplankton, and is consumed by and bioaccumulated within zooplankton. Ninespine stickleback rely on zooplankton more heavily in the ATQ lakes, as they are relatively more abundant. Since zooplankton are scarce

in the RDC lakes (save RDC 309, which has the lowest fish MeHg concentrations in the RDC region), macroinvertebrates comprise a larger proportion of stickleback diets in those lakes. So, not only is sulphate stimulating greater methylation in the biofilm of the RDC lakes, but it is also an overall tracer of catchment influence, and increased inputs from the catchment leading to a more biofilm-based food web could be causing a stickleback diet more reliant on invertebrates (due to lower phytoplankton production and thus lower zooplankton abundance). I propose that the combination of these direct and indirect mechanisms explain the observed relationship between SO_4 and stickleback [MeHg] concentration on the ACP. Further, the reason that there is not a significant regional difference in stickleback [MeHg] is because the effect of SO_4 on [MeHg] in fish is mediated by fish growth; fish growth was the overall best predictor of stickleback [MeHg] in these study lakes.

Implications for a changing climate

The Arctic Coastal Plain is a dynamic landscape that is likely to experience many climate-related changes that could impact mercury uptake and accumulation. Effects of climate-related change may differ between regions, however. The expected increases in primary production could have major implications for the "lower catchment influence" autochthonous lakes. Higher production could lead to greater scavenging of Hg from the water column (Outridge et al. 2007) and a subsequent increase in Hg methylation rates in sediment. However, higher algal density may also lead to a dilution of MeHg entering the food web (Pickhardt et al. 2002). More intense weather and increased permafrost degradation could lead to greater inputs of SO_4, OM, and THg from the catchment, which could further increase

mercury methylation rates in biofilms and periphyton. The lakes that are currently "lower-catchment influence" are not impervious to thermokarstic events, including retrogressive thaw slumps. A slump could lead to an inundation of ion-rich permafrost soil, which would lead to the absorption and flocculation of DOM, increased water clarity, increased macrophyte growth, and a shift away from phytoplankton dominance (Thompson et al. 2008). If a thaw slump or other major thermokarstic event were to occur in the ATQ lakes, it is possible that the controls and routes of MeHg would start to resemble those that I am currently inferring in the RDC lakes. Finally, a climate-related change that could impact fish MeHg concentrations in both regions is increases in summer water temperatures. Water temperature can affect fish growth (Reist et al. 2006b), which is currently the best predictor of fish [MeHg] in this study. Thus, it is possible that fish MeHg concentrations could decrease in both regions.

Future work will focus on investigating the drivers of fish growth in this region, and determining whether the patterns identified here are consistent in other thermokarst lakes, as these landscapes cover a significant portion of the northern permafrost region. The ability to tease apart and quantify the dominant drivers of mercury accumulation at the landscape-level is critical to enable predictions of how climate will impact mercury concentrations and accumulation in northern lakes.

3.6 Figures

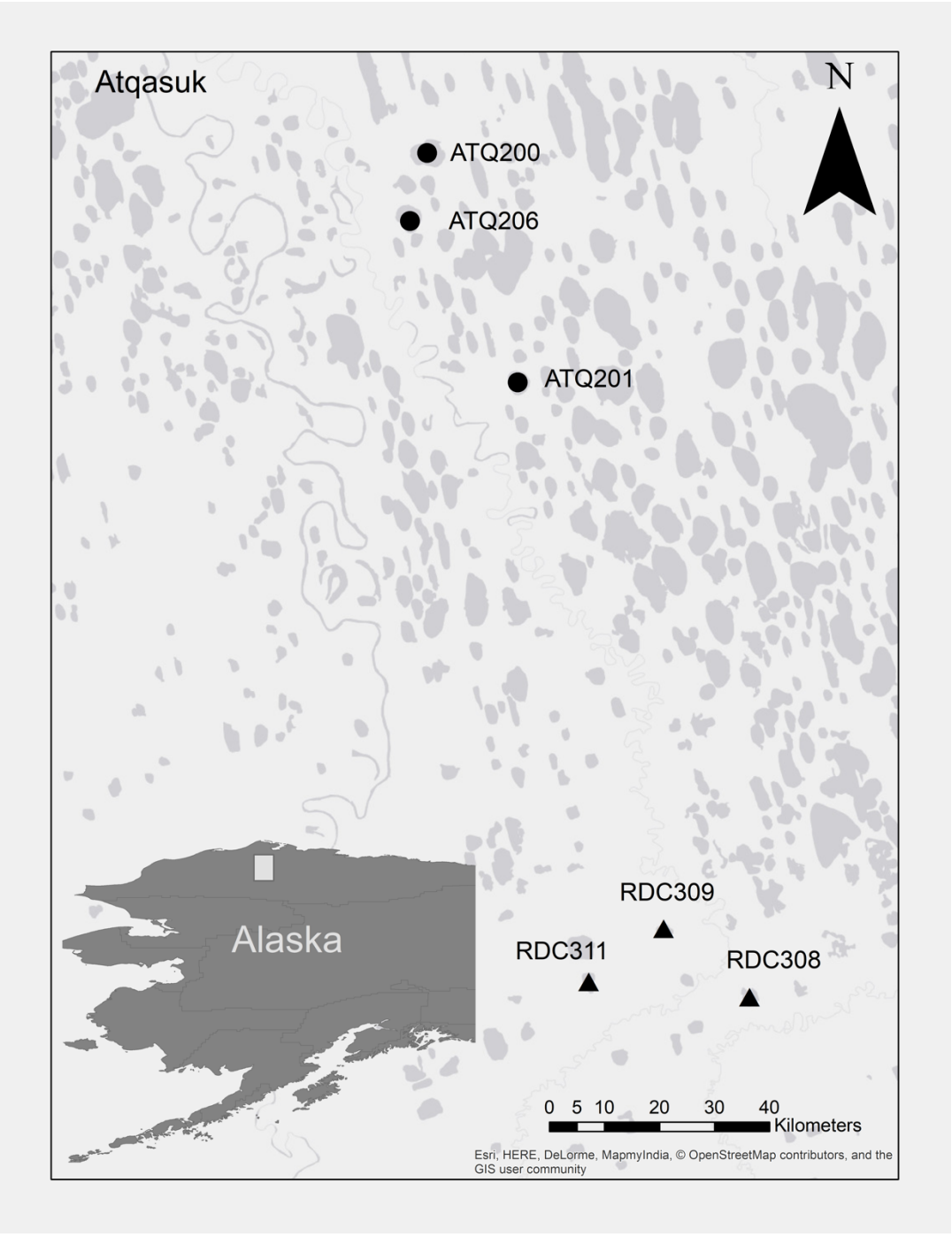

Figure 3.1. Study lakes on the Arctic Coastal Plain of Alaska (ATQ 200, ATQ 201, ATQ 206, RDC 308, RDC 309, RDC 311); black circles represent the ATQ lakes, black triangles represent the RDC lakes

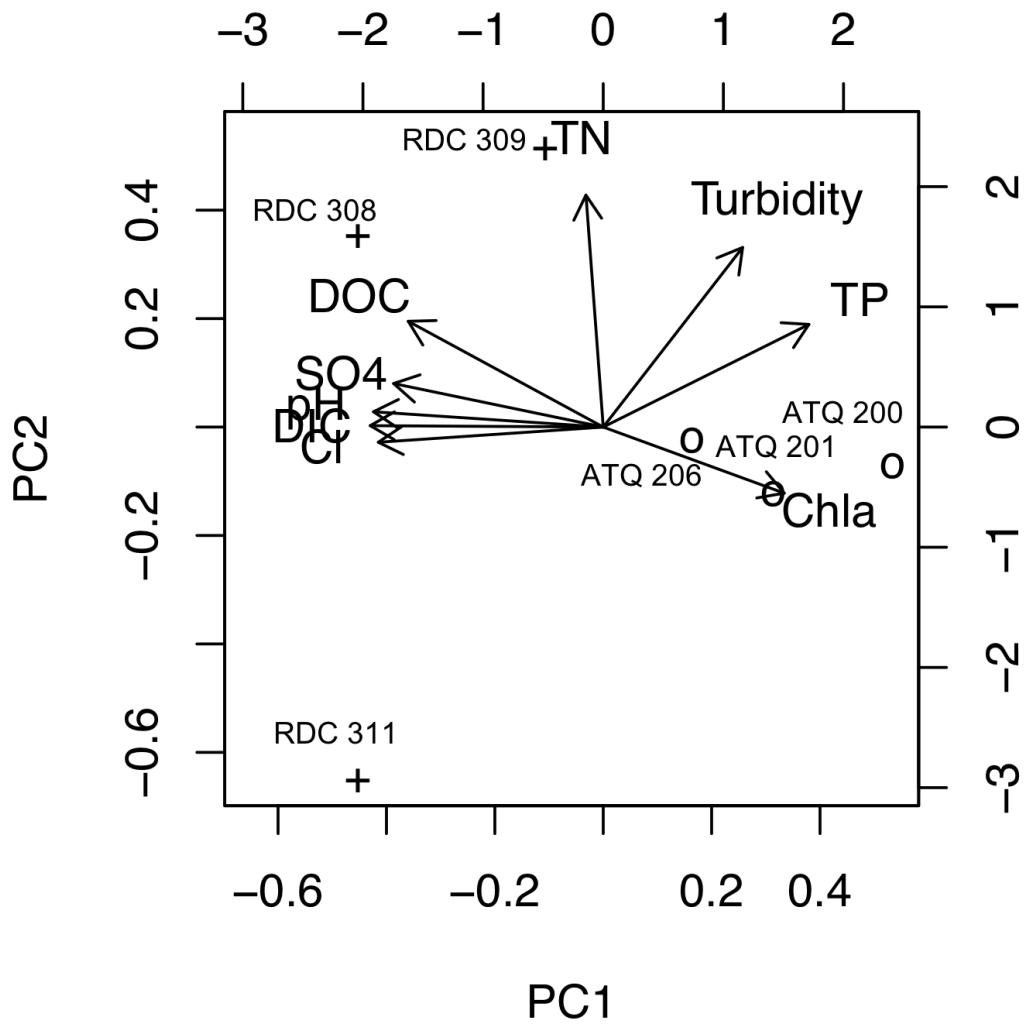

Figure 3.2. Biplot of a principal components analysis for water chemistry data on the six study lakes; ATQ lakes are represented with circles and RDC lakes are represented with crosses; ATQ lakes have more positive loadings on PC1, and are associated with indicators of higher autochthonous production whereas RDC lakes have more negative loadings, and are associated with indicators of catchment inputs.

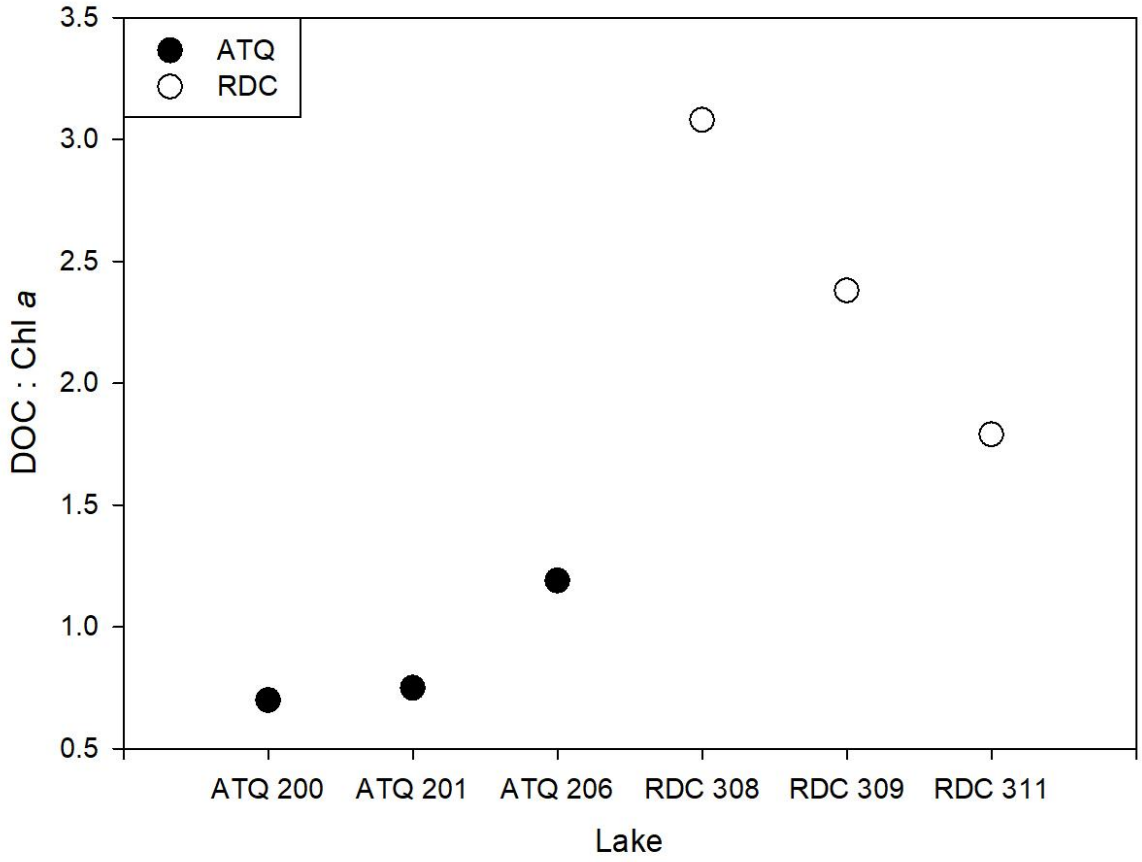

Figure 3.3. Ratios of DOC to Chl-*a* for each of the six study lakes on the Arctic Coastal Plain of Alaska (ATQ 200, ATQ 201, ATQ 206, RDC 308, RDC 309, RDC 311). Data were collected in summer 2016. Black circles represent ATQ lakes, and white circles represent RDC lakes. DOC: Chl-*a* ratios were significantly higher in RDC lakes than in ATQ lakes (T-test; t=3.83, p=0.04, df=2.68)

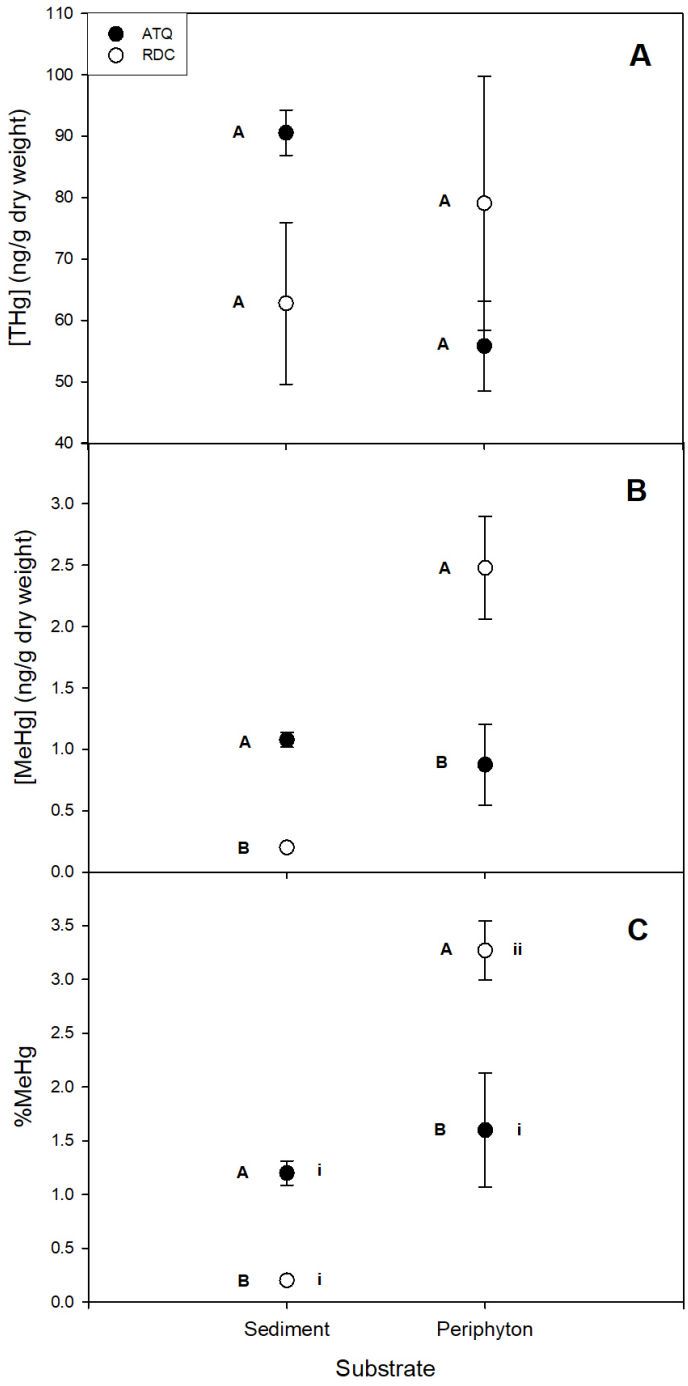

Figure 3.4. Mean ± SE of mean total mercury concentrations (A), methyl mercury concentrations (B), and %MeHg (C) in sediment and periphyton for each of the two regions. Black circles represent ATQ lakes, and white circles represent RDC lakes. Significant within substrate differences between regions are indicated by different letters, and significant within region differences between substrate types (i.e., sediment and periphyton) are indicated by different roman numerals.

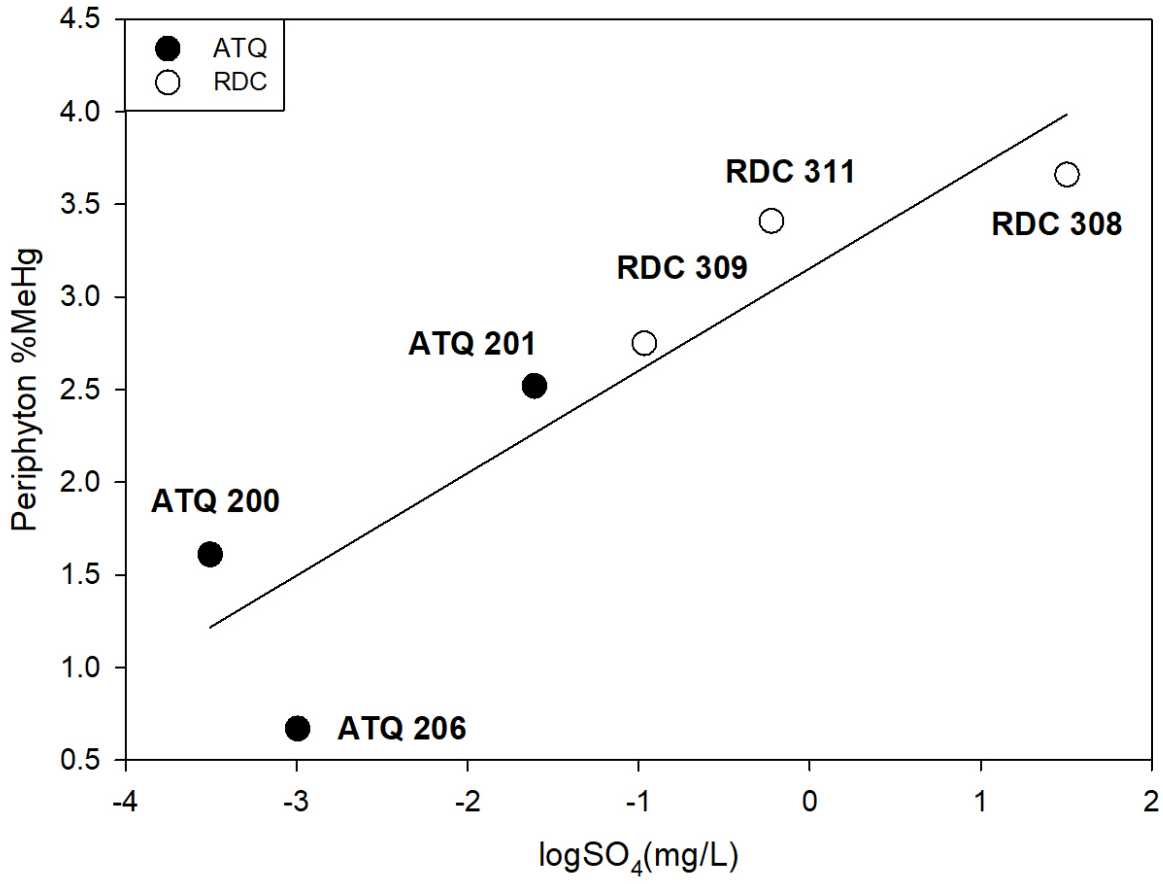

Figure 3.5. Percent MeHg in periphyton related to log[SO_4] for each study lake on the Arctic Coastal Plain of Alaska; black circles represent ATQ lakes, and white circles represent RDC lakes. There was a significant and positive relationship between %MeHg in periphyton and log[SO_4] (Linear regression, R^2=0.77, $F_{(1,4)}$=17.75, p=0.01.

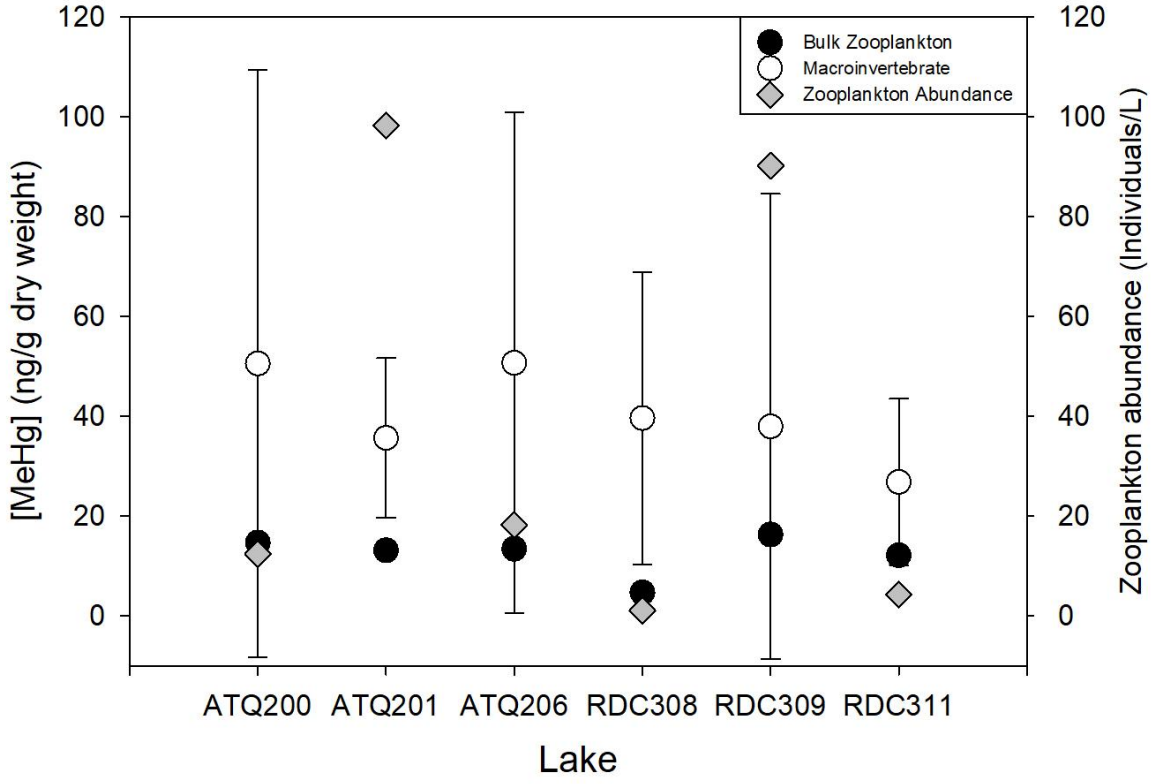

Figure 3.6 Mean ± SE MeHg concentrations in benthic macroinvertebrate and bulk zooplankton, as well as zooplankton abundance for the six study lakes. There were no significant differences in [MeHg] in zooplankton ($p=0.51$) or benthic macroinvertebrates ($p=0.17$) between regions. In each lake, benthic macroinvertebrates had higher [MeHg] than zooplankton.

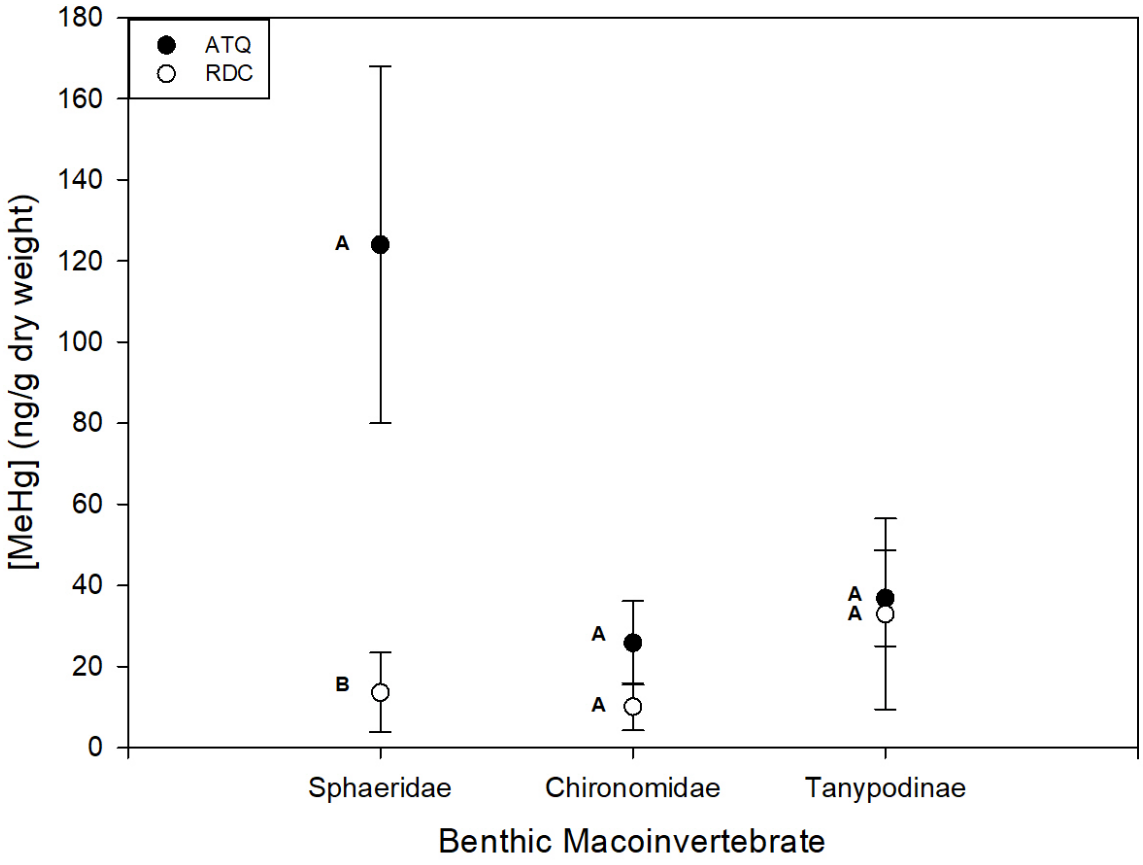

Figure 3.7. Mean ± SE MeHg concentrations in Sphaeridae, Chironomidae, and Tanypodinae. Significant differences (T-test, $p<0.05$) between regions (within taxa) are indicated by different letters. Filter-feeding Sphaeridae had significantly higher [MeHg] in the ATQ lakes than in RDC lakes ($p=0.04$). Black circles represent ATQ lake means, and white circles represent RDC lake means.

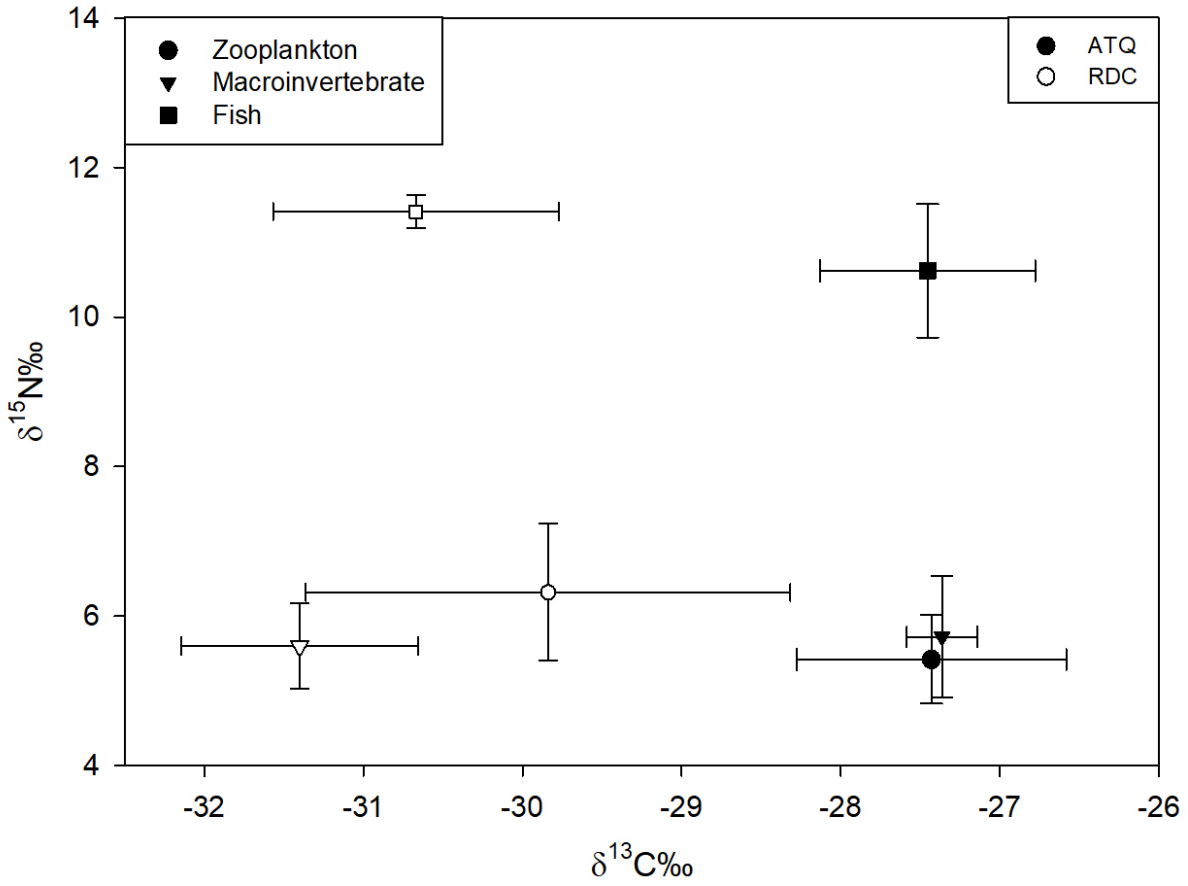

Figure 3.8. Mean ± SE $\delta^{15}N$ and $\delta^{13}C$ for bulk zooplankton (circles), benthic macroinvertebrates (triangles), and whole body Ninespine stickleback (squares). Stickleback ($p=0.05$) and invertebrates ($p=0.02$) from the RDC lakes (white symbols) were significantly more ^{13}C-depleted than those in the ATQ lakes (black symbols).

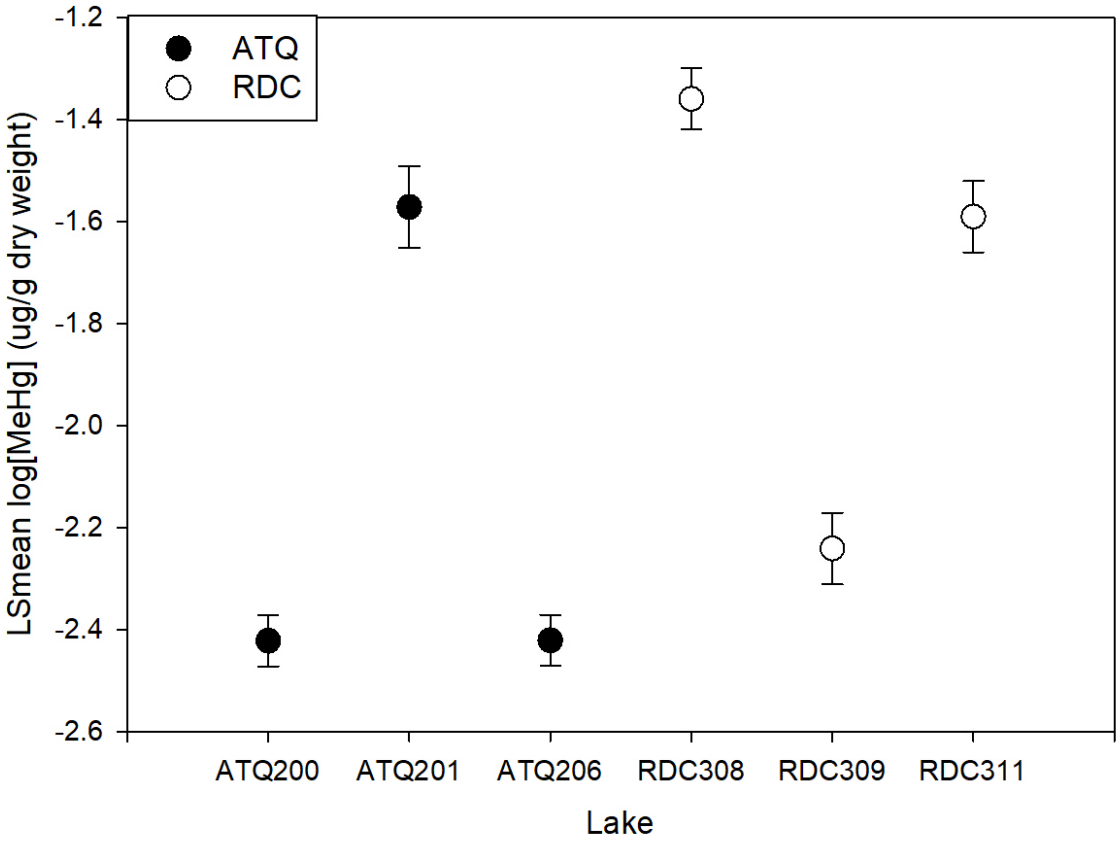

Figure 3.9. Least-squares mean log[MeHg] (µg/g) ± SE calculated at a mean size of 50 mm for each of the six study lakes. Black circles represent ATQ lakes, and white circles represent RDC lakes.

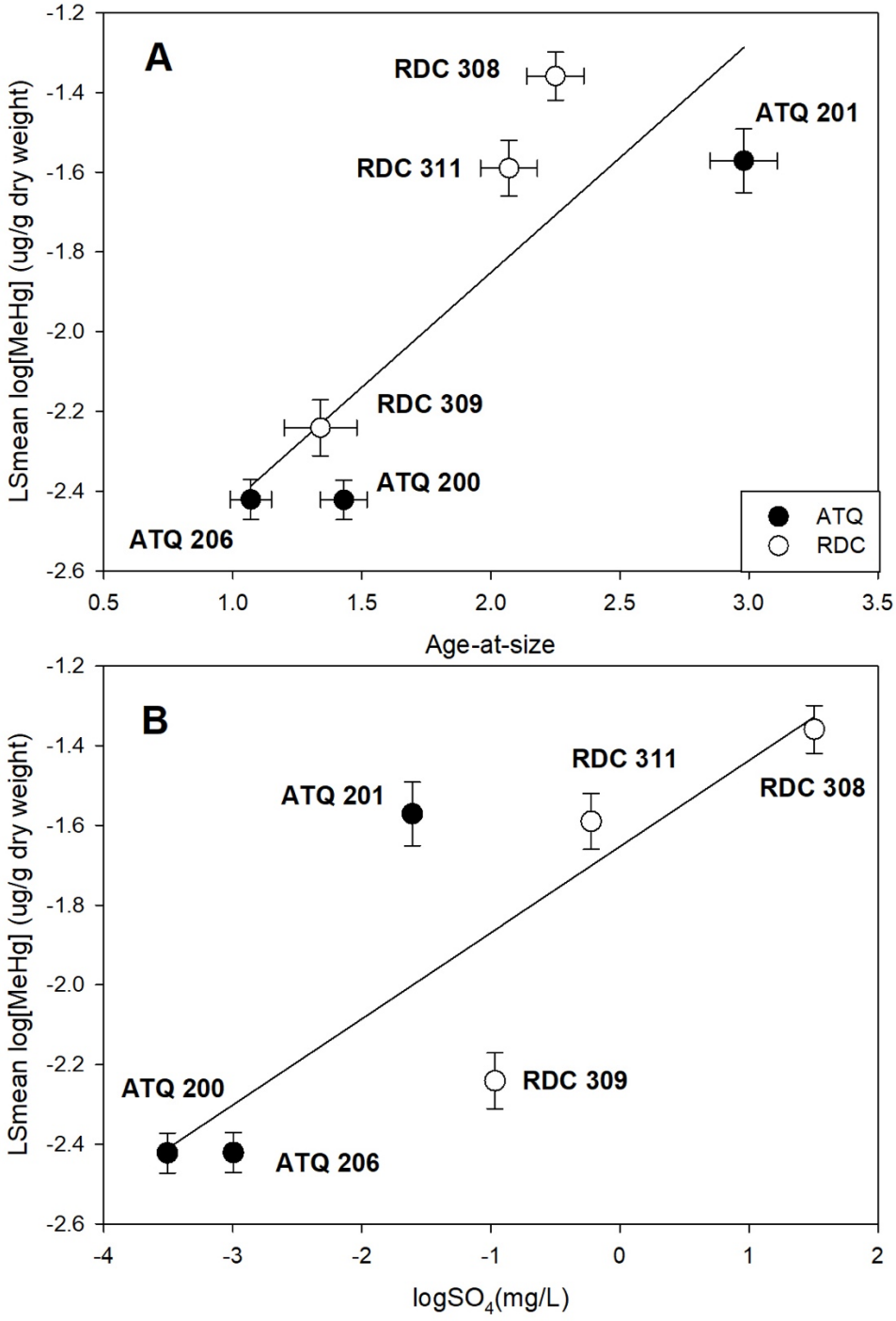

Figure 3.10. Least squares mean [MeHg] in stickleback ± SE (µg/g dry weight) related to (A) least squares mean age-at-size and (B) log[SO_4] for each study lake. Black circles represent ATQ lakes, and white circles represent RDC lakes.

3.7 Tables

Table 3.1. Select physical and chemical characteristics of the six study lakes (ATQ 200, ATQ 201, ATQ 206, RDC 308, RDC 309, RDC 311). Samples for all lakes were collected in summer 2016.

	ATQ 200	ATQ 201	ATQ 206	RDC 308	RDC 309	RDC 311
Latitude (decimal degrees)	70.453	70.327	70.416	69.987	70.025	69.995
Longitude (decimal degrees)	-156.953	-156.805	156.981	-156.427	-156.567	-156.689
Surface area (km)	2.49	1.37	1.79	0.73	0.50	0.67
Zmax (m)	2.56	3.0	2.96	4.08	2.07	3.05
THg (ng/L)	0.45	0.46	0.44	0.29	0.49	0.25
MeHg (ng/L)	0.026	0.022	0.012	0.015	0.015	0.015
pH	7.1	7.25	7.59	8.46	7.74	8.19
DOC (mg/L)	3.22	4.87	4.17	8.09	8.1	5.99
DIC (mg/L)	1.94	3.39	7.13	23.5	10.06	23.21
SO_4 (mg/L)	0.03	0.20	0.05	4.51	0.38	0.80
TN (µg/L)	367	367	378	407	440	331
TP (µg/L)	12	11	7	5	9	3
Chl-*a* (µg/L)	4.59	6.51	3.51	2.63	3.4	3.34
Turbidity (NTU)	0.73	0.51	0.62	0.58	0.62	0.18
SUVA	1.34	0.89	1.28	2.01	2.18	1.36

Table 3.2. Results from Pearson product-moment correlations between water chemistry variables and %MeHg in sediment and periphyton; asterisks represent a significant relationship.

	%MeHg in Sediment		%MeHg in Periphyton	
Variable	r	p	r	p
logSO4	-0.85	**0.03***	0.90	**0.01***
logDIC	-0.80	0.06	0.65	0.16
logCl	-0.93	**<0.01***	0.80	**0.05***
logDOC	-0.92	**0.01***	0.77	0.08
DOC:Chla	-0.83	**0.04***	0.68	0.14
logTN	-0.28	0.59	0.06	0.92
logTP	0.59	0.22	-0.53	0.28
pH	-0.78	0.07	0.69	0.12
logTurbidity	0.48	0.34	-0.49	0.31
logChl-*a*	0.56	0.25	-0.33	0.52

Table 3.3. Results from Pearson's product-moment correlations relating stickleback length-adjusted log[MeHg] (μg/g) to relevant environmental covariates; significant relationships are indicated with an asterisk.

Variable	r	$t_{(1,4)}$	p
logSO_4	0.83	2.99	**0.04***
logDOC	0.55	1.30	0.262
logDIC	0.54	1.34	0.25
logCl	0.62	1.59	0.19
logTN	-0.20	-0.40	0.71
logTP	-0.52	-1.23	0.29
pH	0.61	1.55	0.20
logTurbidity	-0.50	-1.16	0.31
logChl-*a*	-0.11	-0.21	0.84
logWater THg	-0.03	-0.06	0.96
logWater MeHg	-0.68	-1.87	0.14

4 Parasitism of Ninespine stickleback (*Pungitius pungitius*): impacts on growth and mercury accumulation in lakes on the Arctic Coastal Plain of Alaska

4.1 Introduction

Ninespine stickleback (*Pugitius pungitius*) is a freshwater fish species of the family Gasterosteidae that is widely distributed throughout northern, circumpolar aquatic ecosystems in North America, Iceland, Fennoscandia, and Russia (Keivany and Nelson, 2000). Stickleback are secondary consumers that primarily prey on zooplankton and benthic invertebrates (Hynes, 1950), and are ecologically important prey fish for higher trophic level taxa, including Arctic Char (*Salvelinus alpinus*; Hunter 1968; Karlsson and Bystrom, 2005; Gallagher and Dick, 2010), Lake trout (*Salvelinus namaycush*; Johnson, 1975), and migratory waterfowl (Kertell, 1996). There is a well-established parasitic relationship between fishes of the family Gasterosteidae and cestodes of the genus *Schistocephalus*.

Stickleback are the second intermediate host for *Schistocephalus* and become infected by consuming copepods that contain the procercoid larval phase of *Schistocephalus*. Upon consumption, the parasite penetrates the intestinal wall of the host stickleback, and develops into a plerocercoid within the peritoneal cavity. During this stage, the plerocercoids can grow large and cause visible distension of the abdominal cavity; the parasite(s) weight can be greater than that of the host tissue (Arme and Owen, 1967). The Ninespine stickleback is specifically parasitized by *Schistocephalus pungitii*, which is similar to the well-documented parasite of the Three-spined stickleback (*Gasterosteus aculeatus*), *Schistocephalus solidus*.

While research on the effects of *Schistocephalus pungitii* is limited, many studies have been completed on the congeneric *Schistocephalus solidus*. An infestation of *Schistocephalus* can lead to both physical and behavioral effects in stickleback hosts (e.g., Milinski et al. 1985; Tierney et al. 1996). The growth of *Scistocephalus* is fueled by nutrients from the alimentary canal of the host fish, including partially digested food and other breakdown products (Arme and Owen, 1967). Consequently, an infestation can limit the amount of energy available for host growth and sexual development (e.g., Shultz et al. 2006). Field studies have shown lower somatic body condition (Tierney et al. 1996), impaired female gonadogenesis (Heins and Baker, 2008), and underdeveloped male secondary sexual traits (Tierney et al. 1996) in parasitized Three-spined stickleback. There is also evidence for modification of foraging behaviour in parasitized fish, with effects including altered prey selection (Milinski, 1984) and increased risks taken to access food, which increases vulnerability to predators (Milinkski et al. 1985; Tierney et al. 1993).

Parasites have an important ecological role in aquatic food webs (Lafferty et al. 2008). They increase food chain length and the amount of omnivory, consequently altering food web structure and function (Lafferty et al. 2008; Thieltges et al. 2013). Before the routine use of stable isotope ratios in ecology, little was known about the trophic relationships between fish parasites and their hosts (Williams and Jones, 1994). Although it might be expected that parasites have higher $\delta^{15}N$ values than their hosts due to feeding on host tissues, cestode parasites can be significantly depleted in ^{15}N compared to host muscle tissue (e.g., Pinnegar et al. 2001; Power and Klein, 2004; Eloranta et al. 2015). It is currently unclear why cestodes are ^{15}N-depleted compared to their hosts; however, Pinnegar et al. (2001) suggests

that this could be due to their ability to utilize ammonia (^{15}N-depleted) excreted from the host to synthesize amino acids, or due to the differential selection of isotopically light amino acids. The trophic relationships between cestode hosts and fish parasites are complex. Because cestodes lack a digestive system they must absorb all of their nutrients from the contents of host's alimentary canal, and this may include food items, mucous, and the gut lining (Pappas, 1975). The lack of knowledge on the trophic ecology of *S. pungitii* precludes understanding how its presence and abundance in an ecosystem affect food web structure, and therefore, concentrations of biomagnifying contaminants (e.g., mercury).

Mercury is a neurotoxin that, in its methylated form (MeHg), can bioaccumulate and biomagnify through food webs, sometimes reaching high concentrations in upper trophic levels (e.g., Kidd et al. 1995). There are well-established links between mercury (Hg) concentration in fish and both trophic position (δ^{15}N; e.g., Kidd et al. 2012) and growth rate (e.g., Karimi et al. 2007); however, not much is known about the relationship between host and parasite mercury concentrations in fish. Results from previous research on the bioaccumulation of heavy metals in parasites compared to their fish hosts is mixed. In an experimental study on the effects of parasitic acanthocephalans (thorny-headed worms, which also feed in the host alimentary canal) on lead (Pb) accumulation in common chub (*Leuciscus cephalus*), the authors found that the parasites had higher concentrations of lead and cadmium than their fish hosts (Sures et al. 1999). In contrast, authors of another experimental study on the toxicity of cadmium to Three-spine stickleback found that cestode parasites had lower cadmium concentrations than their hosts (Pascoe and Cram, 1977). Little

research has been done on the bioaccumulation of Hg between host and parasite, which is critically important because unlike other heavy metals, mercury can biomagnify.

Because Hg biomagnifies, the trophic relationship between parasite and host will affect accumulation in each. For example, we might expect higher mercury concentrations in parasites relative to hosts when parasites feed directly on host tissue (e.g., blood, flesh), but we would not expect this if the parasite is feeding on host gut contents. In a study on an estuarine grass shrimp and its hematophagous (blood-feeding) isopod parasite, the authors found lower concentrations of MeHg in the parasite compared to the host (Bergey et al. 2002), whereas authors of a study on double-crested cormorants (*Phalacrocorax auritus*) and their nematode and trematode parasites found higher MeHg concentrations in parasites relative to hosts, and determined that these parasites were likely consuming host tissue (Robinson et al. 2010).

Regardless of their mode of feeding, parasites may influence concentrations of mercury in their hosts. There has been some work suggesting that parasites can act as a form of protection from high heavy metal concentrations, since they can absorb and sequester metals that otherwise could have been assimilated by the host (Turcekova and Hanzelova, 1999). In addition, parasites can indirectly affect concentrations of bioaccumulating metals, such as mercury, in host tissue through impacts on host growth. There is a well-documented negative relationship between fish growth rates and mercury concentrations that is caused by somatic growth dilution (e.g., Karimi et al. 2007), wherein a faster growing fish gains more biomass to dilute the burden of MeHg from the food they consume than slower growing

counterparts. Many factors can influence fish growth rates, including warming air temperatures (Reist et al. 2006b) and parasitization (e.g., Shultz et al. 2006). Finally, if a fish is viewed as the sum of its parts, then the concentration of mercury in a parasite (be it higher or lower than the host) could impact the overall mercury burden in a "fish meal" to predators. To my knowledge, this has yet to be studied or quantified.

Climate warming is amplified in polar regions (see Prowse et al. 2006). In addition to altering fish growth rates (Reist et al. 2006b), warming temperatures can affect host-parasite dynamics by increasing parasite growth, transmission rates, and life-cycle completion rates (Lv et al. 2006). Macnab and Barber (2012) investigated the effects of elevated temperatures on *S. solidus,* and found that plerocercoids of host stickleback reared at higher environmental temperatures had faster growth rates than those reared at lower temperatures, which resulted in much higher incidence of plerocercoids weighing >50 mg (the threshold mass at which the parasite has a significantly higher chance of successful lifecycle completion, termed infective mass; Macnab and Barber, 2012). Finally, there is evidence that upon reaching an infective mass, *S. solidus* can manipulate their hosts to seek out warmer water, which further increases the growth and fecundity of the parasite and transmission to the definitive host (Barber et al. 2008; Macnab and Barber, 2012).

Ninespine stickleback occur throughout the lake-rich region of the Arctic Coastal Plain (ACP) of Alaska. In recent work on fish mercury concentrations in ACP lakes, growth rate was found to be a significant driver of methylmercury (MeHg) concentration in Ninespine stickleback, with slower growing fish having higher mercury concentrations (Chapter 3).

Current research suggests that warming should result in increased fish growth rates (Reist et al. 2006b) and dilution of fish MeHg (e.g., Karimi et al. 2007). However, since parasitism can affect growth, and is more prevalent and intense at warmer temperatures (Marcogliese, 2001), the relationship between parasitism, growth, and MeHg concentration must be further explored. This is especially important in lakes on the ACP, where warming is occurring at an amplified rate (see Prowse et al. 2006) and where Ninespine stickleback are an important prey item for larger fishes and piscivorous birds (e.g., Gallagher and Dick, 2011; Laske et al. 2018).

The objectives of this study were to: 1) determine if there are differences in the magnitude and intensity of *Schistocephalus pungitii* infections among six lakes on the ACP; 2) determine if there are differences in trophic position ($\delta^{15}N$) and MeHg concentration between parasite and host, and if so, the nature of this difference; and, 3) determine if there are differences in MeHg concentration between infected and uninfected stickleback, and identify the drivers of differences (e.g., growth). Results were then used to elucidate how parasitism affects mercury transfer through food webs of shallow Arctic lakes.

4.2 Methods

Study Area

The lakes in this study are located on the Arctic Coastal Plain (ACP) of Alaska, which is an area of continuous permafrost that extends from the foothills of the Brooks Range (68°N) to the Beaufort and Chukchi Seas (71°N). The six lakes in this study (ATQ 200, ATQ 201, ATQ 206, RDC 308, RDC 309, RDC 311; Table 4.1) are from two regions on the ACP, Atqasuk (ATQ) and Reindeer Camp (RDC), and were previously included in a study on the drivers of fish mercury concentrations (Chapter 3). These lakes were selected from a larger set of lakes monitored by the Circum-Arctic Lakes Observation Network (http://arcticlakes.org). The lakes in this study are shallow (2-4 m), small (0.5-2.5 km^2), well-mixed, and do not strongly stratify. The food webs of ACP lakes are simple, and contain few fish species (e.g., Carey and Zimmerman, 2014; Laske et al. 2018). The most common fish species are Ninespine stickleback (*Pungitius pungitius*) and Alaska blackfish (*Dallia pectoralis*). The ACP is a heterogeneous landscape, and as such, there are hydrological and other physical differences between the ATQ and RDC regions; briefly, catchments in the ATQ region are small relative to lake areas, and are characterized by sandy, well-drained soils with high hydraulic conductivity (Chapter 2; Koch, unpublished data, 2015). Catchments in the RDC region are larger relative to lake area than catchments in the ATQ region (Chapter 2), and are located in the ACP foothills transition zone, which is an area where topography and ice-rich soils lead to bank erosion and shoreline subsidence (Hinkel et al. 2012). Catchment soils in the RDC region are silty with a thick organic-rich surface layer (Jorgensen and Grunblat, 2013), and have a lower hydraulic conductivity (Koch, unpublished data, 2015) than those in the ATQ.

Sample collection and preparation

In August 2016, Ninespine stickleback were collected from the six study lakes using a combination of fyke nets and minnow traps. Upon capture, stickleback were weighed and measured for fork length (to the nearest mm), and frozen whole for transport back to the laboratory at the University of Waterloo.

Laboratory Analysis

Fish were thawed at room temperature, and an incision was made on the ventral side of each fish so that the alimentary tract and other viscera could be removed. Both the alimentary tract and the peritoneal cavity were then examined. If cestodes were present, they were retained, enumerated, and individually weighed. Otoliths were then removed for age determination. Following this, whole dressed stickleback (minus viscera and parasites) were freeze-dried using a LabConco FreeZone operated at -54°C and 0.014 mBar for 48 hours. Freeze-dried samples were then ground to a uniform powder using scissors inside borosilicate scintillation vials. Parasites from the same individual were combined, freeze-dried, and also ground to a uniform powder using scissors inside borosilicate scintillation vials.

Total mercury analysis was completed on 260 fish (~44±12/lake) at the University of Waterloo, Ontario, Canada, using an Ohio Lumex PYRO-915+ (100-240V, 50/60Hz, 700W; Burger et al. 2004). Between 10-15 mg of dry tissue was analyzed per fish. The mean detection limit was 0.02 ± 0.01 μg /g (dry weight), relative percent difference between duplicates was 9.5±5.6% (n=28), and mean percent recovery of the certified reference

material (DORM-4, National Research Council of Canada 2012) was 95.9±7.4% (n=33). Method blanks were consistently below the detection limit (n=38). Following dissection and total mercury analysis, methylmercury analysis was completed on subsample of 34 (of 260) stickleback. To generate the subsample, three parasitized and three unparasitized fish were randomly selected from each lake (except for ATQ 201 where there was only one unparasitized fish). MeHg analysis was also completed on the corresponding parasites of the parasitized fish from the sub-sample (n=18), all at the Biotron Laboratory (Western University, London, Ontario, Canada). Briefly, a potassium hydroxide solution (KOH) was added to sample tissues prior to hot block digestion (Bloom and Fitzgerald, 1988), and the resulting extracts were speciated by gas chromatography and analyzed using cold vapor atomic fluorescence spectroscopy on a Tekran 2700 Automated MeHg Analysis System following U.S. EPA method 1630 (U.S. EPA, 1998). The method detection limit was 0.009 ng/g (dry weight), mean relative percent difference between duplicates was 9.6±9.5% (n=28), and mean percent recovery of certified reference material was 85.5±14.4% (n= 24; DORM-4, National Research Council of Canada 2012). Method blanks were consistently below the detection limit (n=27).

Carbon and nitrogen stable isotope analyses were completed on all of the fish (n=260), as well as the parasites from the 34 fish sub-sample (n=18) at the Environmental Isotope Laboratory at the University of Waterloo, Ontario. Stable isotope ratios are expressed as delta values ($\delta^{13}C$, $\delta^{15}N$) in parts permil (‰) relative to international standards (Pee-Dee Belemnite and N_2 gas, respectively). Analytical error for $\delta^{13}C$ and $\delta^{15}N$ never exceeded 0.3 and 0.2‰, respectively, based on measurements of standardized reference materials cross-

calibrated to the international standards, that comprised no less than 20% of samples. The mean relative percent difference between duplicate samples was 1.2±1.8% (n=104) for $\delta^{13}C$ and 6.4±8.3% (n=104) for $\delta^{15}N$.

Sagittal otoliths were used for fish aging. One otolith from each fish was submerged in water and photographed (Leica Application Suite version 4.0.0, Leica Microsystems [Switzerland] Limited) at 40x magnification under reflected light using a dissecting microscope (Leica M60) at the USGS Alaska Science Center, Anchorage, Alaska. Two independent readers estimated age by counting the number of visible annuli on photographs (Jones and Hynes 1950; DeFaveri et al. 2014). If estimated ages differed between the two readers, a third reader provided an estimate (< 7%).

Fish (n=34) and parasites (n=18) that were analyzed for stable isotope ratios and methyl mercury were also analyzed for caloric density at the University of Waterloo using a bomb calorimeter. A pellet was formed from the homogenized, dried samples and analyzed using a Parr™ Semi-micro Calorimeter 6725 (Parr™ Instrument Company, Moline, IL). A duplicate sample and commercial analytical standard (Parr™ benzoic acid pellet) were each run for every ten samples. The mean relative percent difference between duplicates was 3.3±1.0% (n=5), and mean percent recovery of analytical reference material was 100.6±0.41%

Data Analysis

Statistical analyses were completed in R Studio v 1.0.136 and R v 3.5.1 with core packages in addition to "lsmeans" (Lenth et al. 2016) and "vegan" (Oksanen et al. 2018). All figures

were generated in Sigmaplot v 11.0 (Systat, 2008) or Arcmap™ 10.2.2 (ESRI, 2016). All comparisons between hosts and parasites ($\delta^{15}N$, [MeHg], caloric density) were completed on the subsample of infected fish (n=18) and their corresponding parasites (n=18), that were each analyzed for [MeHg], $\delta^{15}N$, and caloric density. Since MeHg analyses were only completed on a subsample of fish (n=34), a mean ratio of MeHg to THg concentrations was completed on the subsample for each lake, and these ratios were used to estimate MeHg concentrations for fish that were not analyzed for MeHg but were analyzed for THg (Table S4.1, Appendix C). These estimated values (n=260) were used to determine differences in mercury concentrations between whole dressed parasitized and unparasitized fish. When data were not normally distributed, a $\log_e$ transformation was applied, and residuals were examined following analyses to ensure assumptions of each test (normal residuals, homogeneity of variance) were met. For all significance testing, alpha was set to 0.05.

Statistical analyses were completed on several variables. The following are explicit definitions of variables used throughout this chapter. "Parasitization index" refers to the proportion of fish body mass comprised of parasite tissue (i.e., total parasite mass divided by fish mass*100). "Whole dressed" refers to a fish (parasitized or unparasitized) that has had its viscera and parasites (in infected fish) removed. "Host" refers to whole dressed tissue of fish that were infected with *Schistoceophalus* parasites. "Parasite" refers to the homogenized parasite tissue from a given host; comparisons involving parasites are always made specifically between the parasite and its corresponding host (i.e., paired comparisons). "Fish meal" refers to the reconstructed combined package of fish plus parasites(s) in parasitized fish (detail provided below). "Fish age-at-size" is a proxy for fish growth. Least-squares

mean age were calculated at a fish length of 50 mm using an ANCOVA (length and lake as covariates).

To address objective one, an analysis of variance (ANOVA) was used to assess differences in parasitization indices among lakes, and a post-hoc Tukey's test was used to assess pairwise differences. For objective two, paired t-tests were used to assess differences in [MeHg] and $\delta^{15}N$ between whole dressed host fish and corresponding parasites in the study lakes. To determine if there were relationships between parasite and host $\delta^{15}N$, and between parasite and host [MeHg], analyses of covariance (ANCOVA) were used to model $\delta^{15}N$ and [MeHg] in parasites as a function of host $\delta^{15}N$ and [MeHg], respectively, and "lake" as a categorical variable. To assess differences in estimated MeHg concentration between parasitized and unparasitized fish (n=260), a general linear model with two categorical variables (parasite status and lake) and a covariate ($\log_e$ length) was used. To illustrate length-adjusted mean MeHg for parasitized versus unparasitized fish in each lake, least-squares means were calculated for each lake using parasite status as a categorical variable and length as a covariate.

To gain a better understanding of how parasitism may influence mercury exposure to predators of stickleback, I estimated [MeHg] and caloric density of a "fish meal" (whole dressed fish + parasite). This was completed by first calculating the proportion of the whole fish weight (weighed prior to dissection) comprised by the parasite (i.e., the parasitization index). Proportions of weight accounted for by whole dressed fish tissue and parasites were multiplied by their respective MeHg concentrations and then summed together to calculate

concentration of MeHg in a "fish meal." Calculated proportions were also multiplied by their respective caloric densities to calculate caloric density in a "fish meal". Differences in [MeHg] and caloric density between whole dressed fish and the "fish meal" (i.e., parasite incorporated) were compared using paired t-tests, and differences in [MeHg] between parasitized and unparasitized "fish meals" were assessed using a general linear model. Caloric density was also compared between parasites and hosts using paired t-tests applied to means for each study lake, and a general linear model with two categorical variables (parasite status and lake) was used to determine differences in caloric density between parasitized and unparasitized fish. Finally, to understand the relationship between parasitization and fish growth, an ANCOVA was used to generate LSmean age-at-size (50 mm; a proxy for fish growth) for each lake. Age-at-size was then related to percent of the population parasitized using a linear regression.

4.3 Results

There was a large range in the percentage of stickleback parasitized among the six study lakes. The lake with the smallest proportion of infected fish was ATQ 206, with 8% of fish parasitized. The lake with the greatest proportion of infected fish was ATQ 201; 98% of stickleback captured from this lake were parasitized by *S. pungitii* (Table 4.1).

The proportion of body mass comprised by parasites (parasitization index) ranged from 12-23% (lake means), and differed significantly among the study lakes (Fig 4.2; ANOVA, $F_{(5, 112)}= 6.24$, $p<0.0001$). A post-hoc Tukey's test indicated that the parasitization index in ATQ 201 was significantly higher than the parasitization indices in ATQ 200, ATQ 206, and RDC 311 (Fig 4.2, $p<0.01$).

A comparison of $\delta^{15}N$ between hosts and parasites revealed that, in all lakes, parasites were significantly depleted in ^{15}N (Fig 4.3a; paired t-test, $t=17.58$, $p<0.0001$, $df=5$) and had significantly lower MeHg concentrations (Fig 4.3b; paired t-test, $t=6.75$, $p=0.001$, $df=5$) than their hosts. While $\delta^{15}N$ in parasites was significantly and positively related to $\delta^{15}N$ in hosts, $\delta^{15}N$ in parasites did not differ among lakes (ANCOVA; $R^2_{adj}=0.92$, $F_{(6,9)}=28.54$, $p<0.0001$). MeHg concentrations in parasites were also significantly and positively related to [MeHg] in hosts, but in contrast with the results for $\delta^{15}N$, MeHg concentrations in parasites differed significantly among lakes, and the lake*host[MeHg] interaction term was significant (ANCOVA; $R^2_{adj}=0.87$, $F_{(11,6)}=11.51$, $p=0.004$). These analyses indicate that the $\delta^{15}N$ and [MeHg] of the host can explain a significant amount of variability in $\delta^{15}N$ and MeHg of the

parasite, respectively, and that factors other than host [MeHg] result in among-lake variability in parasite [MeHg].

To assess differences in MeHg concentration between parasitized and unparasitized whole dressed fish, a general linear model with two categorical variables (parasite status and lake) and a covariate ($\log_e$ length) was performed. All fixed terms and one interaction term (lake*length) were significant (General linear model; $R^2_{adj}=0.78$, $F_{(12,247)}=78.38$, $p<0.0001$). While the categorical variable, lake, and fish length explained more variability in fish [MeHg] than parasite status, parasitized whole dressed fish tissue had significantly higher [MeHg] than unparasitized whole dressed fish tissue (Fig 4.4).

Although MeHg concentrations in whole dressed fish tissue from parasitized fish were higher than those in unparasitized whole dressed fish tissue, the importance of parasitization in affecting Hg exposure to predators must be examined by considering the parasites as part of a "fish meal" in terms of mercury and energy. I did this by artificially reconstructing the fish and calculating an overall [MeHg] for the "fish meal." Comparisons of [MeHg] in parasitized whole dressed stickleback to [MeHg] in reconstructed "fish meals" revealed that [MeHg] in the "fish meal" was significantly lower than in whole dressed tissue (Fig 4.5; paired t-test, $t=4.73$, $p<0.01$, $df=5$), indicating that by accounting for the parasite in the overall MeHg concentration of a fish meal, a predator is exposed to significantly lower [MeHg] than the whole dressed tissue concentrations would suggest. A comparison between "fish meal" MeHg concentration in parasitized versus unparasitized fish can be made if we assume that the whole dressed MeHg concentration of unparasitized fish is representative of the "fish

meal". For this comparison, a general linear model with two categorical variables (parasite status and lake) and a covariate ($\log_e$ length) was performed on the sub-sample of fish (n=34). While lake ($p<0.0001$) and length ($p=0.01$), as well as their interaction term ($p=0.02$), were significant, parasite status ($p=0.16$) was not (General linear model, $R^2=0.72$, $F_{(12,21)}=1.24$, $P<0.0001$). These results indicate that although the whole dressed tissue of parasitized fish is higher than that of unparasitized fish, when considering the fish as "fish meals", the higher tissue mercury concentration is offset by the presence of the (relatively low [MeHg]) parasite.

Similar to $\delta^{15}N$ and [MeHg], there was a significant difference in mean caloric density between the hosts and parasites in all of the study lakes, such that hosts (whole dressed tissue) had a significantly higher caloric density than parasites (Fig 4.6; paired t-test, $t=2.5$, $p=0.05$, $df=5$). To determine if infection impacted the caloric density of whole dressed fish tissue, a general linear model with "parasite status" and "lake" as fixed terms was used, and neither variable could explain a significant amount of variability in caloric density (General linear model, $R^2=0.07$, $F_{(11,22)}=1.24$, $P=0.32$). This indicates that, unlike MeHg, caloric density of a fish is not affected by parasitism. To determine if the lower caloric density of the parasite compared to the whole dressed host tissue would result in the "fish meal" having a significantly lower caloric density than the whole dressed host (similar to what was found with [MeHg]), a paired t-test was performed. In contrast with the result for [MeHg], the caloric densities of the "fish meals" were not significantly different from the corresponding whole dressed host (Paired t-test, $t=1.93$, $p=0.11$, $df=5$). These results indicate that although the whole dressed tissue had a higher caloric density than the parasite tissue, the difference

was small enough to be negligible when considering overall caloric density of the "fish meal".

Finally, I examined the relationship between parasitization and fish growth. Stickleback age-at-size (a proxy for growth, such that fish older at size are slower growing) was previously calculated for each study lake in Chapter 3; briefly, least-squares means were generated from an ANCOVA that related fish age to $\log_e$length (mm), lake, and the interaction (R^2=0.77, $F_{(6,268)}$=158.2, p<0.0001). There was a significant and positive relationship between least squares mean age-at-size (at 50 mm) and percent of Ninespine stickleback parasitized in each lake (Fig 4.7; R^2_{adj}=0.62, $F_{(1,4)}$=9.29, p=0.04). This indicates that parasitization of Ninespine stickleback by cestodes negatively affects fish growth.

4.4 Discussion

Parasite Infectivity

Schistocephalus infection rates were variable across the six different populations of Ninespine stickleback that were studied, ranging from 8-98%. Rates vary among other populations in the literature as well, with some being as high as 85-95% (Arme and Owen, 1967; Godin and Sproul 1988), and others as low as <1% (Jakobsen et al. 1988). Since the *Schistocephalus* lifecycle is complex and because *Schisotocephalus* is trophically transmitted, there are several factors that impact infection rates, including the presence of intermediate and definitive hosts (see Heins and Baker, 2008). A concurrent in-depth study on the zooplankton community composition was completed on the same study lakes by Guernon (2019), that reported copepod concentrations that ranged from <1 -11 individuals/L among lakes. Since copepods are the first intermediate host of *S. pungitii*, I expected that among-lake differences in zooplankton community composition would be reflected in differences in infection rates, such that lakes with high infection rates would have higher copepod concentrations; however, this was not the case (see Guernon, 2019). It is likely that the among-lake differences in infection rates I observed are a product of ecological differences that were not quantified, such as the presence and abundance of piscivorous birds, which are the definitive hosts of *Schistocephalus* cestodes.

In addition to assessing infection rates, I also assessed infection intensities. *Schistocephalus* plerocercoids can grow to enormous sizes, often approaching or exceeding 50% of the total host mass (Arme at Owen, 1967; Macnab and Barber, 2012). There was a significant difference in the mean parasitization index among lakes (ranging between 12-23%);

however, in no lakes did the parasite load comprise 50% of the host, which has been found in other systems. Plerocercoids achieve an infective mass at 50 mg, at which point they have a significantly higher chance of successfully completing their lifecycle (Tierney and Crompton, 1992). The fact that the parasitization indices in this study are lower than those reported in other studies could be because the fish with the highest parasitization indices were eaten. Once parasites reach an infective mass they can manipulate their host into becoming more conspicuous to predators by reducing mobility, decreasing predator avoidance, increasing buoyancy, and changing coloration (LoBue and Bell, 1993), making them more likely to be predated upon. As plerocercoids increase in size, the likelihood of lifecycle completion increases, and greater effects are also observed on host growth and development (Tierney et al. 1996; Barber et al. 2008).

There are possible implications of *Schistocephalus* infections on energy flow and contaminant bioaccumulation in the study lakes, particularly as infection rates were as high as 98% and a substantial amount of fish biomass (up to 23%) was comprised of parasite tissue. Ninespine stickleback are important prey fish on the Arctic Coastal Plain (Laske et al. 2018), and the definitive hosts for *Schistocephalus* are piscivorous birds (40 species; Heins and Baker, 2008); however, to the many organisms that consume infected stickleback, the parasite is merely nutrition. To assess the potential implications of parasitism on mercury bioaccumulation in the study lakes, I investigated the trophic relationship between parasite and hosts, and tested for differences in mercury concentrations and caloric density between hosts and parasites.

Host-parasite trophic relationships and mercury

Considering parasites in food web studies is relatively new (Lafferty et al. 2006), even though parasitism is the most common feeding strategy on Earth (DeMeeus and Renaud, 2002), and parasites comprise the greatest proportion of biomass in several aquatic ecosystems (Kuris et al. 2008). Traditionally, when parasites are included in food webs, one or two parasite taxa are listed as "top carnivores", which, based on the diversity of feeding strategies, is too simplistic (Marcogliese, 2003). I found that the parasites in this study (*S. pungitii*) did not occupy a higher trophic position than their stickleback hosts, as they had consistently lower $\delta^{15}N$ and mercury concentrations.

The lower $\delta^{15}N$ in cestode parasites relative to their stickleback hosts indicates that the parasites are primarily feeding on the gut contents of the fish, and not on the fish tissue itself. This is consistent with previous literature on cestode parasites (Pinnegar et al. 2001; Power and Klein, 2004; Eloranta et al. 2015). The fact that the parasites are ^{15}N-depleted compared to their hosts, even though they are exposed to the same food supply, indicates that the parasites and hosts likely have different isotopic discrimination factors. Although isotopic discrimination factors are often assumed to be 3.4‰, this represents an average across different taxa that span a range of several permil (Minagawa and Wada, 1984). McCutchan et al. (2003) found that isotopic discrimination factors differed based on feeding strategy, such that higher protein diets resulted in higher $\delta^{15}N$ discrimination factors. They also found that fluid-feeders (e.g., internal parasites) had lower $\delta^{15}N$ discrimination factors than non-fluid-feeders, and attributed this to the fluids being isotopically different than the bulk food item (McCutchan et al. 2003). The consistently lower parasite MeHg concentration is

unsurprising when considering their $\delta^{15}N$ values (e.g., Kidd et al. 1995); however, since the host and parasite have the same dietary supply this is slightly curious, and can likely be explained by a combination of different physiological characteristics including metabolism and age, as these also affect Hg concentration (Sandheinrich and Weiner, 2011), or by differences in trophic shift and concomitant biomagnification.

Cestodes do not have a functional digestive tract and, as such, acquire all of their nutritional needs through their outer membrane, which is called a tegument (Pappas, 1975). This is typically achieved through the processes of facilitated diffusion or active transport (Pappas, 1975), and is also how MeHg enters the organism. In fish, MeHg accumulates in the gut following exposure, where it is then taken up across the intestinal epithelial cells, sometimes taking several days to be transferred into the bloodstream (see Bradley et al. 2017). It was a previously held belief that nearly all of the MeHg a fish is exposed to was assimilated into their bloodstream; however, multiple studies have shown that this is false, and that assimilation efficiencies of MeHg in fish are highly variable, ranging from 10-100% (Bradley et al. 2017). Currently we do not have a full understanding of the drivers of MeHg assimilation efficiency in fish, but it may be influenced by the concentration and time of exposure to MeHg (see Bradley et al. 2017). The parasitized stickleback in this study provide an example where not all MeHg is assimilated by the fish as, an albeit depleted amount compared to the fish, accumulates in the parasite tissue. I propose that higher MeHg concentrations in whole dressed host tissue compared to corresponding parasite tissue could indicate that host fish have a higher assimilation efficiency than their parasites. This could be a product of the biochemical processes related to assimilation (diffusion, active transport), or

may be because parasites are physically located in an area of the gut where the MeHg is less readily available for uptake.

Another explanation for the elevated concentrations of MeHg in hosts compared to parasites is organism age. Once MeHg has been taken up into a fish, it can take several months to years to be eliminated (Trudel and Rasmussen, 1997), which explains why older fish often have higher mercury concentrations than younger conspecifics (Sandheinrich and Weiner, 2011). Naturally, hosts are older than their parasites, and in this study, none of the fish under one year of age were parasitized (Table S4.2, Appendix C). As such, age could contribute to the higher MeHg concentrations in hosts compared to parasites.

Effects of parasitism on stickleback mercury

In addition to the differences between host and parasite MeHg concentrations, there were also significant differences in [MeHg] between parasitized and unparasitized fish, such that when variability due to fish length and among-lake differences was accounted for, [MeHg] in whole dressed tissue from parasitized fish was significantly higher than [MeHg] in whole dressed tissue from unparasitized fish. One explanation for the difference in MeHg concentration between parasitized and unparasitized fish is that parasitized fish grow more slowly, as nutrients are diverted to the growth of cestodes in parasitized fish. Growth (age-at-size) was found to be a significant driver of among-lake variability in stickleback MeHg concentration in the study lakes (Chapter 3), and here I found a significant positive relationship between the percentage of the stickleback population that was infected with cestodes and age-at-size. This indicates that growth was slower in lakes where a larger

proportion of the stickleback population was infected. This result is consistent with the literature. In an experiment conducted by Barber and Svensson (2003), it was found that artificially infected Three-spined stickleback had significantly lower growth rates than uninfected individuals. Slower growth rates in cestode-infected fish have been found in other species as well, including Atlantic Salmon (Saksvik et al. 2001). Another potential contributing factor to the higher MeHg concentrations in parasitized versus unparasitized fish is compensatory feeding, as parasitized fish must consume more food to offset the nutrients lost to their parasites (Barber et al. 2005). This elevated food intake could lead to greater MeHg bioaccumulation, because not only are the fish consuming more food, but they are also allocating more resources to metabolic costs instead of growth, and thus have lower growth efficiency (Trudel and Rasmussen, 2006).

Ostensibly, parasitized fish could lead to an overall increase in Hg bioaccumulation in the food web, since tissue from parasitized fish generally has higher mercury concentrations than tissue from unparasitized fish; however, a different conclusion is drawn when the MeHg concentration of the stickleback tissue and the parasite are considered together as a "fish meal" for predators. Although I found that whole dressed tissue from parasitized fish had higher [MeHg] than whole dressed tissue from unparasitized fish, a substantial portion of the mass of parasitized fish (12-23%) was comprised of parasite tissue. This parasite tissue had lower [MeHg], and would also be digested and assimilated by a consumer. When I accounted for the proportion of fish and parasite mass and their respective MeHg concentrations, results indicate that the overall MeHg concentration of the "fish meal" (incorporating the parasite) was significantly lower than the corresponding whole dressed host tissue. Further, there was

no significant difference in parasitized vs unparasitized "fish meal" [MeHg]. Essentially, the presence of a parasite dilutes the overall mercury concentration of the "fish meal", and offsets the higher mercury in the whole dressed fish tissue of parasitized fish. This could result in lower MeHg exposure to predators if the energy density of the "fish meal" is similar to the corresponding whole dressed host.

To gain a more complete understanding of how presence of *Schistocephalus* parasites impacts mercury bioaccumulation in the food web, the relative food quality of parasitized and unparasitized stickleback must also be considered. Although the host fish did have higher caloric density than their corresponding parasites, this difference became negligible when the proportional masses of the host and parasite were considered (outlined in methods); results indicate no significant differences in caloric density between parasitized and unparasitized stickleback. In theory, therefore, predators would not have to compensate for an energy deficit imposed by the parasite to the overall "fish meal". Consequently, it is unlikely that predators feeding on parasitized fish would be exposed to greater concentrations of MeHg overall, and with a high enough parasitization index, the parasites could even act as a form of mercury dilution. However, in order to definitively test this, I would need to analyze parasitized and unparasitized whole-body stickleback (including viscera), as the current analysis does not account for these components due to how the fish were processed.

Parasites have historically been neglected in food web studies, as they were thought to comprise negligible amounts of biomass in a system (Polis and Strong, 1996; Poulin, 1999). Kuris et al. (2008) quantified the biomass of both free-living and parasitic taxa in three

different estuaries and found that the biomass of the parasites exceeded that of top predators. In many shallow lakes on the Arctic Coastal plain of Alaska, Ninespine stickleback are the only fish species present, which was true for two of the lakes in this study (Chapter 3). Although I have not quantified it, I posit that *Schistocephalus* parasites comprise a substantial amount of overall biomass in these simple ecosystems, especially in the lakes with high infection rates and parasitization indices. Since stickleback are an important component of these simple Arctic lake food webs, and the parasites have depleted mercury concentrations and make up nearly 25% of the body mass in some of these fish (and likely a greater proportion in fish consumed by definitive hosts), it is critical to consider them in food web studies. The ACP is home to many breeding waterfowl populations that feed on fish, including the rare Yellow-billed loon (*Gavia adamsii*). Elevated concentrations of MeHg have been observed in Yellow-billed loons captured on the ACP, and there is concern that these birds are at risk for lowered production due to high exposure to mercury (Evers et al. 2014). Thus, understanding how *Schistocephalus* parasites impact the flow of mercury in these lakes is critical. Moreover, with rising air temperatures it is possible that we could see ever-increasing infection rates, as warming waters can lead to enhanced parasite metabolism, higher fecundity, and more rapid spreading (see Lõhmus and Björklund, 2015), which further underscores the importance of considering them.

Summary and Conclusions

I found varying *S. pungitii* infection rates and parasitization indices in lakes across the Arctic Coastal Plain of Alaska. The cestodes were depleted in both ^{15}N and MeHg compared to their hosts, likely due to their mode of feeding and indicating a difference in assimilation

efficiency. Tissue from parasitized stickleback had higher MeHg concentrations than tissue from unparasitized conspecifics in the study lakes, which was likely a product of slower growth rates and/or compensatory feeding. However, when stickleback are considered as a "fish meal" that includes both fish tissue and parasite tissue (comparatively depleted in MeHg), results indicate that since there was no significant difference in overall caloric density, consuming a parasitized fish might not result in increased MeHg uptake, as would be suggested by the higher [MeHg] of whole dressed parasitized tissue compared to whole dressed unparasitized tissue. Because parasitization indices can be much greater than what we observed here (>50%), it is possible that parasites could act to dilute mercury transfer to higher trophic levels; however, further work wherein the MeHg body burden (including viscera) of infected and uninfected fish is quantified would be required to test this hypothesis. The findings I have presented here show that it is important to consider *S. pungitii* in food web and contaminant studies in the Arctic, especially as we may see increased infection rates with anthropogenic warming.

4.6 Figures

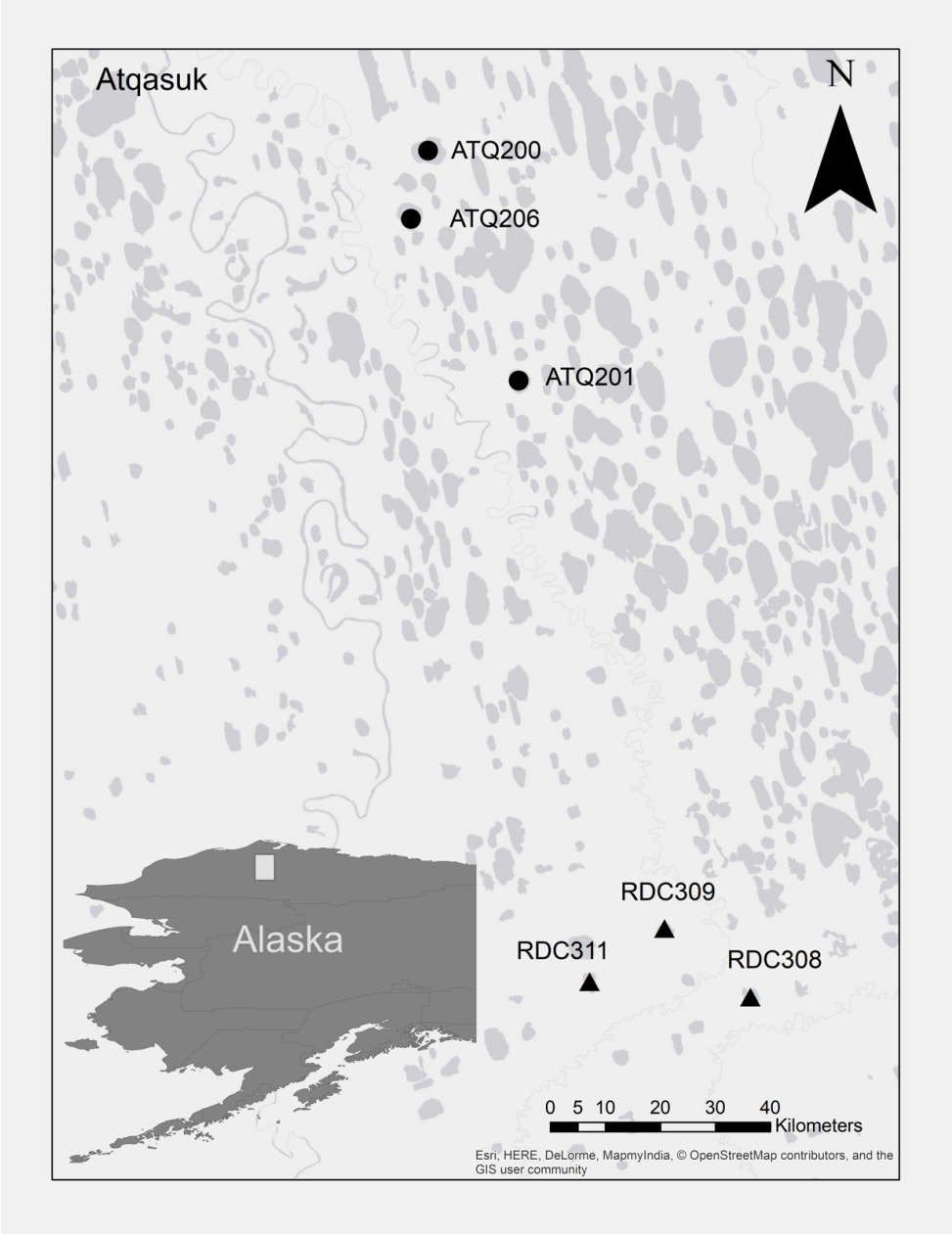

Figure 4.1. Study lakes on the Arctic Coastal Plain of Alaska (ATQ 200, ATQ 201, ATQ 206, RDC 308, RDC 309, RDC 311); black circles represent the ATQ lakes, black triangles represent the RDC lakes.

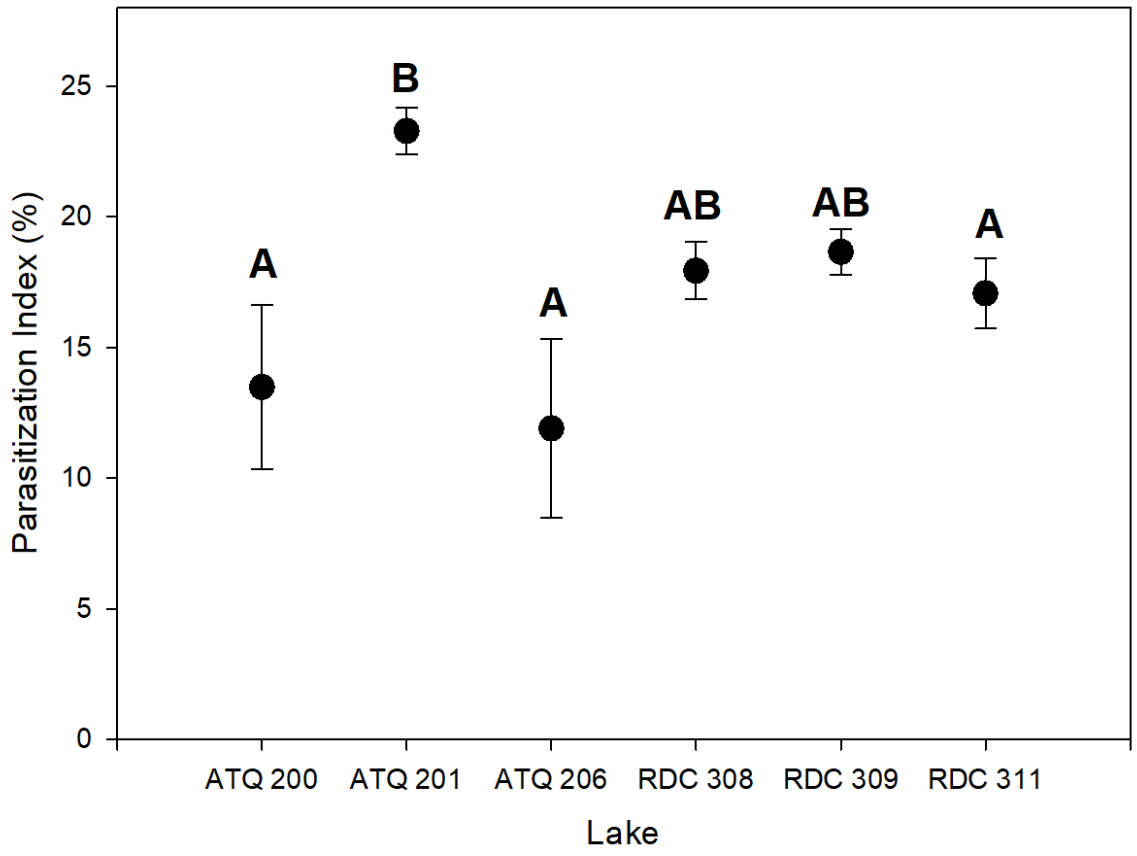

Figure 4.2. Mean ± (SE) parasitization index (proportional mass of parasite within host) for parasitized fish in each of the six study lakes. The parasitization index was significantly higher in ATQ 201 than in ATQ 200, ATQ 206, or RDC 311. Letters represent significant pairwise differences (Tukey's test).

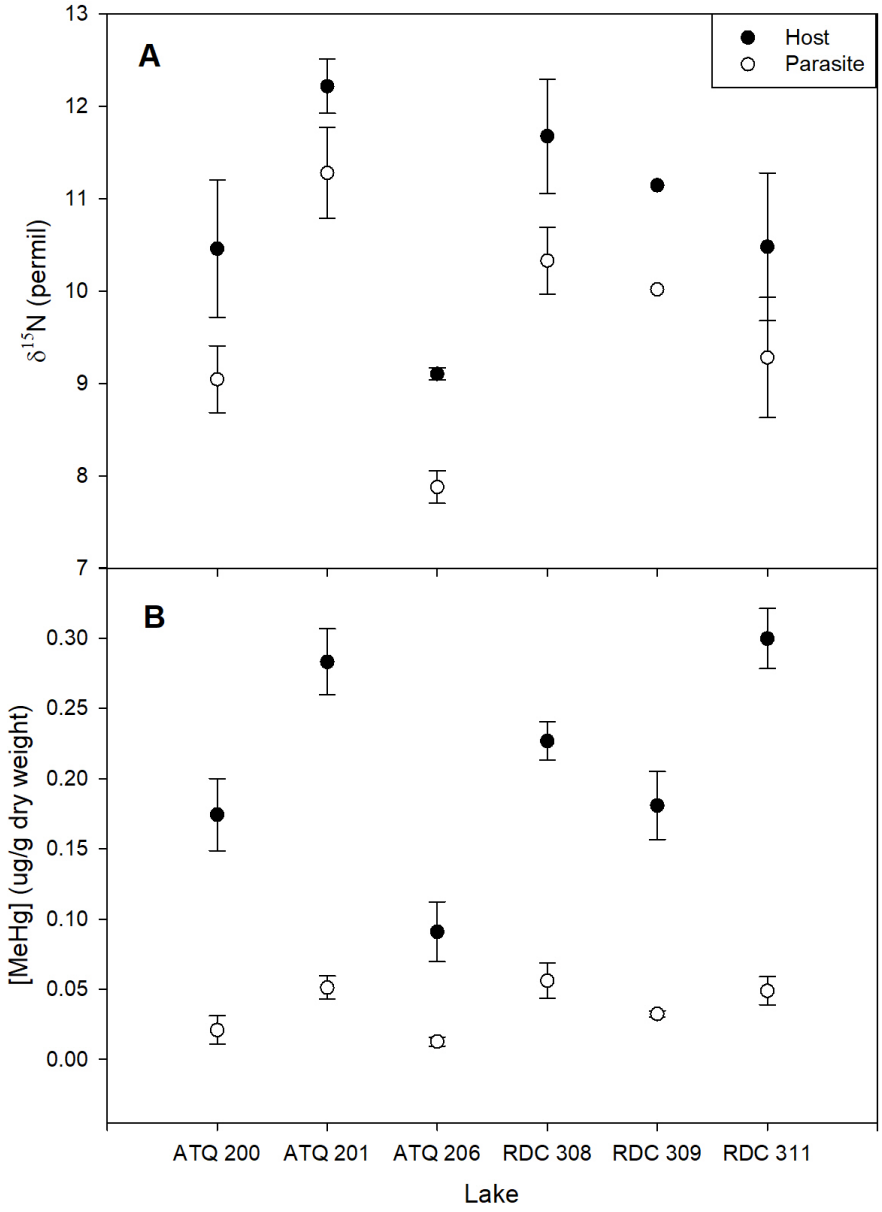

Figure 4.3. Mean ± SE (A) $\delta^{15}N$ (permil) and (B) MeHg concentrations (µg /g dry weight) for stickleback hosts and their respective parasites from the six study lakes. Black circles represent stickleback hosts, whereas white circles represent cestode parasites. In all lakes, mean $\delta^{15}N$ and mean [MeHg] were significantly lower in parasites than in hosts.

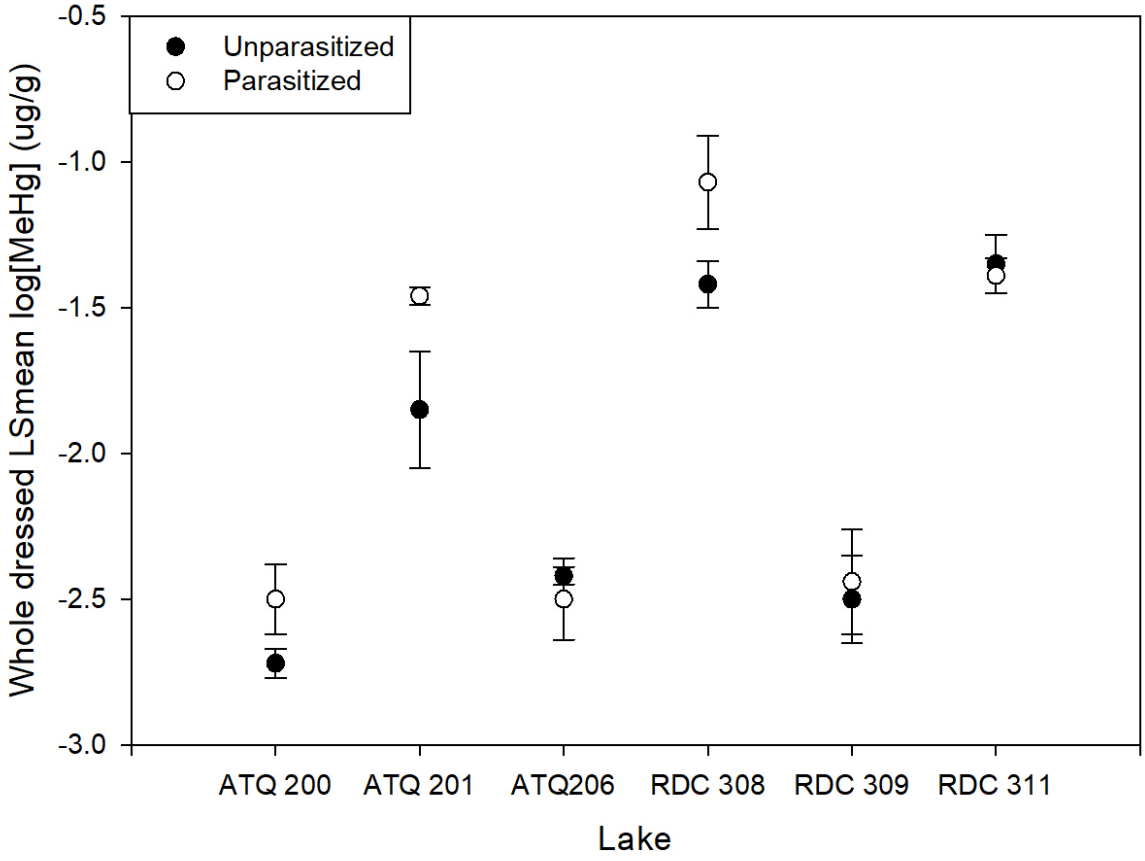

Figure 4.4. LSmean log[MeHg] ± SE (µg /g) for Ninespine stickleback (at fork length 50 mm) in the six study lakes on the Arctic Coastal Plain of Alaska sampled in the summer of 2016. Black circles represent whole dressed fish tissue from unparasitized fish, and white circles represent whole dressed fish tissue from parasitized fish. Whole dressed tissue from parasitized fish had higher log[MeHg] then whole dressed tissue from unparasitized fish at the standardized length of 50 mm.

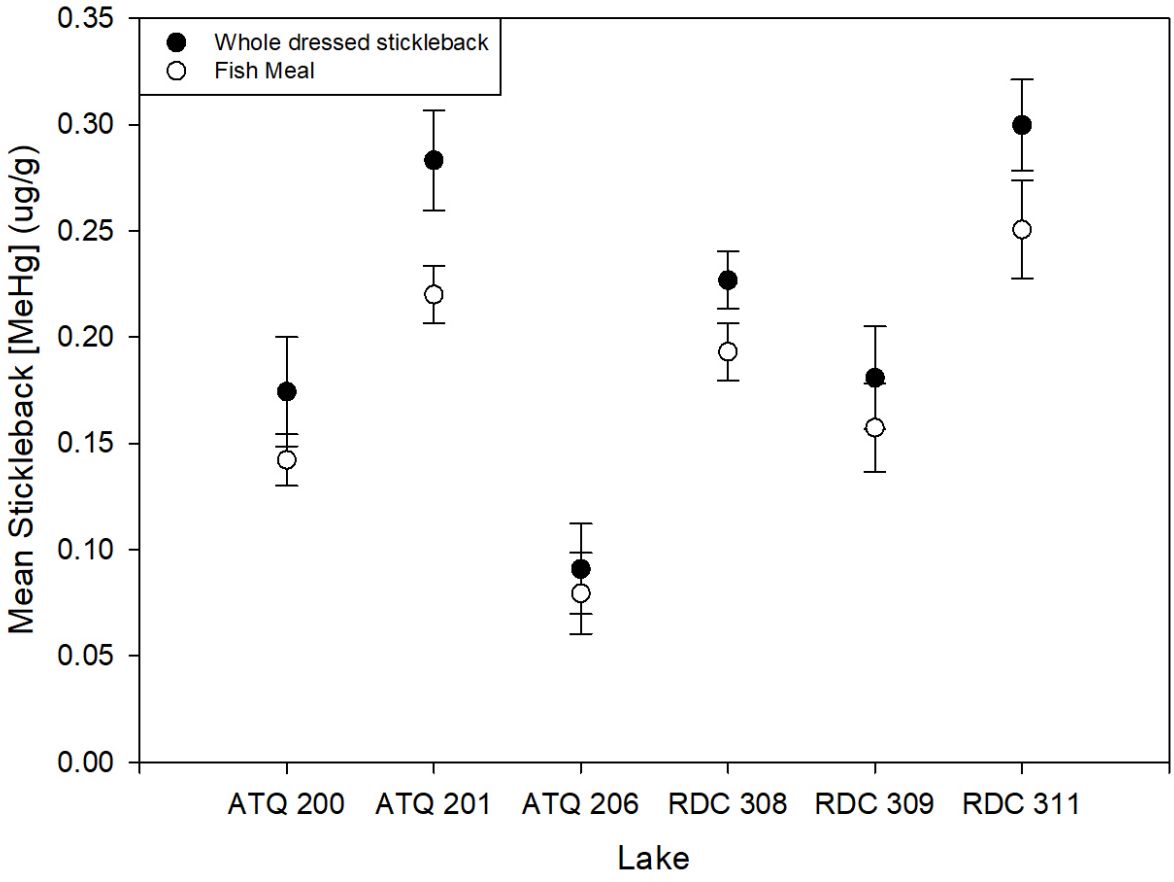

Figure 4.5. Mean [MeHg] in stickleback [MeHg]± SE (µg g) from the six study lakes on the Arctic Coastal Plain of Alaska sampled in the summer of 2016. Black circles represent [MeHg] in whole dressed host fish, and white circles represent [MeHg] in the reconstructed "fish meal" Whole dressed fish had significantly higher [MeHg] than reconstructed fish meals (Paired t-test, $t=4.73$, $p<0.01$, $df=5$).

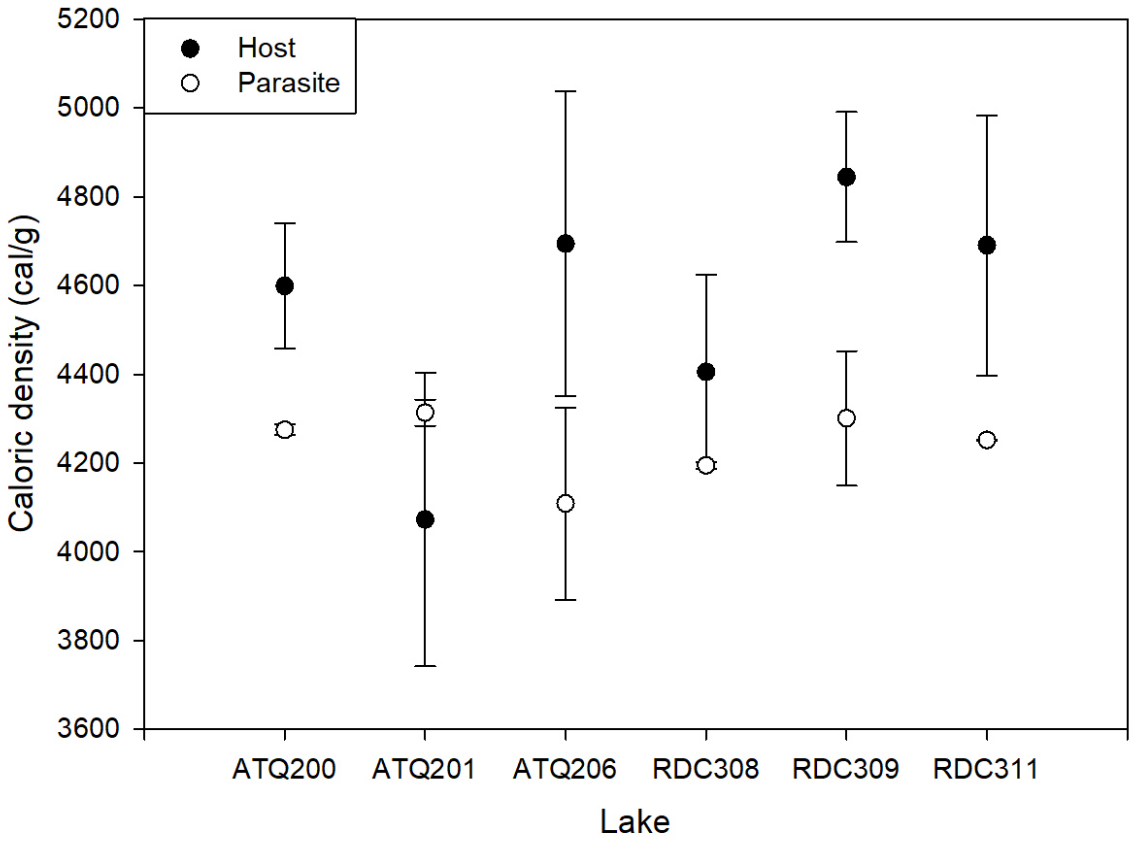

Figure 4.6. Mean caloric density ± SE (cal/g) in hosts and parasites for each of the six study lakes on the Arctic Coastal Plain of Alaska. Black circles represent the host, whereas white circles represent the parasite. Whole dressed host fish had significantly higher caloric density than their corresponding parasites (Paired t-test, t=2.5, p=0.05, df=5).

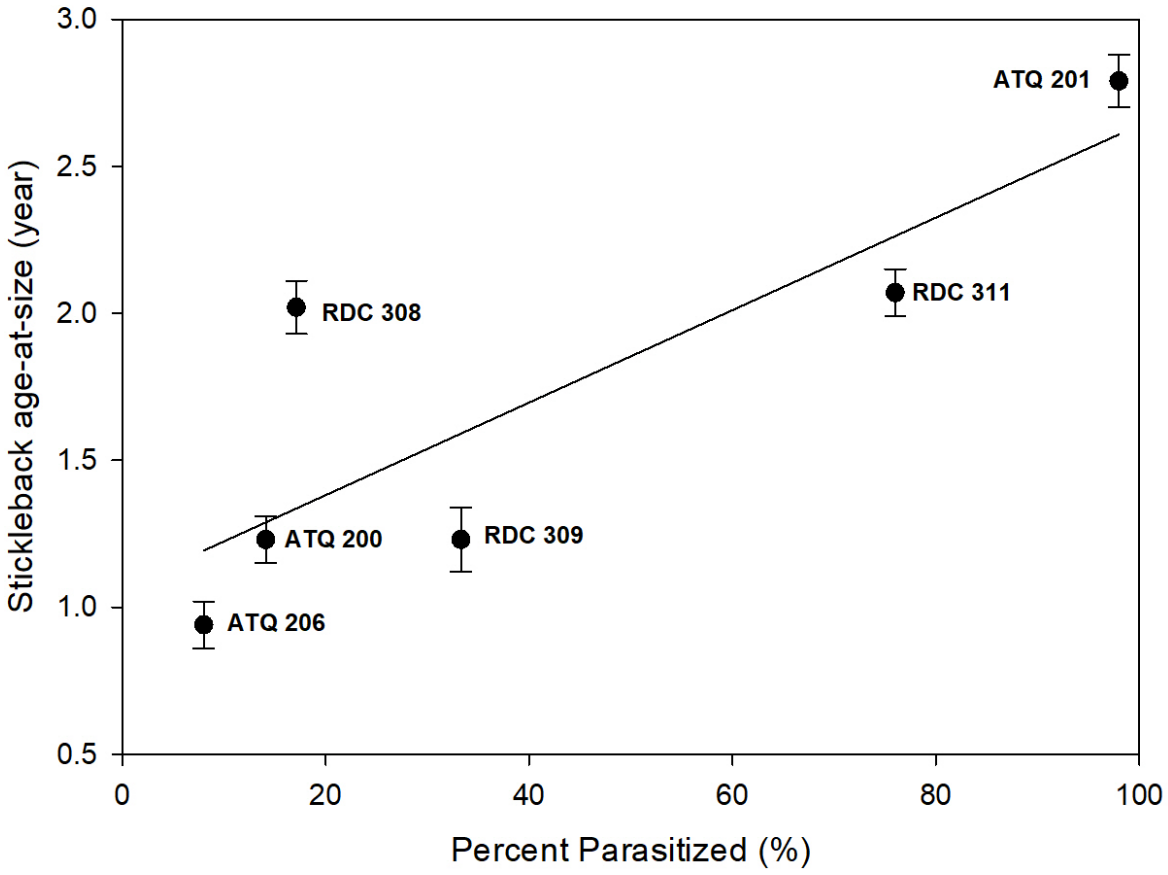

Figure 4.7. Least-squares mean stickleback age-at-size (50mm) + SE related to the percentage of stickleback parasitized from six study lakes on the Arctic Coastal Plain of Alaska. There was a significant and positive relationship between percent parasitized and age-at-size (R^2_{adj}=0.62, $F_{(1,4)}$=9.29, p=0.04)

4.7 Tables

Table 4.1. Location, basic morphometry, and sample sizes for each of six study lakes on the Arctic Coastal Plain of Alaska. Sampling occurred in summer 2016.

	ATQ 200	ATQ 201	ATQ 206	RDC 308	RDC 309	RDC 311
Latitude (decimal degrees)	70.453	70.327	70.416	69.987	70.025	69.995
Longitude (decimal degrees)	-156.953	-156.805	-156.774	-156.427	-156.567	-156.689
Surface area (km)	2.49	1.37	1.79	0.73	0.50	0.67
Z_{max} (m)	2.56	3.0	2.96	4.08	2.07	3.05
Number of fish sampled	64	50	50	41	33	50
Percent of stickleback parasitized	14.1	98	8	17.1	33.3	76

5 General Discussion and Conclusion

5.1 Synthesis of novel contributions

Results from the body of research included in this thesis indicate that effects of environmental change on mercury accumulation in lakes on the Arctic Coastal Plain (ACP) of Alaska will vary spatially and be mediated by several interacting biotic and abiotic variables. I found that patterns of mercury accumulation in sediments and food webs reflected variability in several proximate factors, many of which are ultimately related to catchment influence.

Paleolimnological analyses conducted on cores from three lakes that represented the Barrow (BRW), Atqasuk (ATQ), and Reindeer Camp (RDC) regions on the ACP indicated that Hg accumulation in thermokarst lake sediments was highest and most variable in lakes that had relatively high catchment influence (Chapter 2). Mercury accumulation rates in the two lakes with higher catchment influence (BRW 100 and RDC 312) were driven by high and variable sedimentation rates, which were inferred to reflect higher relative catchment size, lower hydraulic conductivity, and higher thermokarst activity (e.g., thermal erosion; Chapter 2). There were no significant temporal trends in mercury accumulation in either of these high catchment influence lakes. Mercury accumulation rates were lowest and least variable in the lake with lower inferred catchment influence (ATQ 206). In this lake, Hg accumulation rates were most closely related to mercury concentration rather than sedimentation rates, and a temporal increase in mercury accumulation over the last ~100 years was best explained by an increase in sediment Hg concentration, which was driven by changes in lake primary production (Chl-*a*). These results suggest that climate change will alter Hg accumulation in

the sediments of these lakes differently, and that climate-driven increases in primary production could lead to increases in sediment Hg concentration in other 'low catchment influence' lakes across the ACP, while increased incidence of sedimentation events could lead to higher and more variable mercury accumulation in 'high catchment influence' lake sediments.

Because I found that catchment influence varied spatially on the ACP, and that it appeared to affect the amount of, and pathways by which, mercury accumulated in lake sediments (Chapter 2), I hypothesized that catchment influence may also affect how mercury enters and accumulates in lake food webs on the ACP. Expanding the investigation of mercury accumulation from sediments to include water chemistry, periphyton, benthic invertebrates, zooplankton, and fish revealed differences between the two regions - Atqasuk and Reindeer Camp - that were studied more intensively (Chapters 3 and 4). Synthesized results from the three data chapters indicate a complex interaction of biotic (e.g., fish growth) and abiotic (e.g., sulphate) drivers that affect mercury delivery, uptake, and accumulation in food webs and fish. These synthesized results are summarized in a conceptual figure (Figure 5.1).

Results from analyses of water chemistry revealed that lakes in the Reindeer Camp region, which have larger relative catchment areas and lower hydraulic conductivity (Chapter 2), appeared to be driven more by allochthonous production than lakes in the Atqasuk region, which were driven more by autochthonous production. Lakes in the RDC region had higher concentrations of DOC, DIC, and ions, lower concentrations of total phosphorus, total nitrogen, and chlorophyll-*a*, and higher coverage of macrophytes (personal observation). Methylation rates, inferred from results of %MeHg (of total) were higher in sediments in the

autochthonous, phytoplankton-dominated lakes (ATQ region), but higher in periphyton in the allochthonous, macrophyte-dominated lakes (RDC region). I postulate that higher SO_4 concentrations observed in the allochthonous lakes stimulate mercury methylation in biofilms associated with periphyton, as there was a positive and significant predictive relationship between sulphate concentration in the water column and %MeHg in periphyton (Chapter 3). I further inferred from stable isotope results that food webs in the allochthonous lakes are likely more bacterial-based than those in the autochthonous lakes, as they had more negative $\delta^{13}C$, which is an indicator of increased bacterial activity (Bunn and Boon, 1993).

I initially hypothesized that fish in the more allochthonous RDC lakes would have higher concentrations of MeHg than fish in the more autochthonous ATQ lakes, due to elevated catchment inputs of Hg and OM in the more allochthonous RDC lakes. Although the fish MeHg concentrations were generally higher in the RDC lakes, there was one ATQ lake (ATQ 201) with relatively high fish mercury concentrations, in fact higher than in one of the RDC lakes (RDC 309) that had relatively low fish MeHg concentrations. While there was a positive relationship between SO_4 (a catchment indicator) and MeHg concentrations in fish, and although SO_4 concentrations were higher in the more allochthonous RDC lakes, there was no significant difference in MeHg in fish between the two regions. SO_4 was not the only significant predictor variable of MeHg in fish, however, MeHg concentrations in fish were also significantly and positively related to age-at-size (slower growing fish had higher MeHg), and age-at-size did not differ significantly between the RDC and ATQ regions.

Possible effects of water column SO_4 on fish MeHg concentrations are indirect and, as such, are difficult to elucidate. As mentioned above, SO_4 can stimulate methylation (Gilmour et al. 1992), which could affect MeHg concentrations in fish. Concentrations of SO_4 in water may also trace catchment-derived inputs of mercury. I found a significant, positive relationship between sulphate concentration in water and %MeHg (a proxy for methylation) in periphyton, but there was no relationship between sulphate concentration in water and THg concentration in periphyton. This indicates that higher MeHg in periphyton in the RDC lakes was due to higher methylation rates, and not higher catchment-derived inputs of inorganic mercury. Further, the lakes with higher MeHg concentration in periphyton also had more biofilm/bacterial based food webs (inferred by more negative $\delta^{13}C$ values) and lower primary production. Although the abundance of benthic invertebrates was not quantified, fish in the more allochthonous RDC lakes likely consumed more benthic invertebrates than zooplankton (due to less autochthonous production and zooplankton abundance in the RDC lakes), and benthic invertebrates invariably had higher MeHg concentrations than zooplankton. These findings are consistent with the expectation that fish would have higher MeHg in the RDC lakes, and if fish growth did not differ among the study lakes, it is indeed likely that fish in the RDC lakes would have had higher MeHg. However, growth rates in fish varied among lakes in a pattern that was independent of region.

Fish growth, which was quantified and analyzed as age-at-size, differed significantly among lakes. Although there are several factors that can influence fish growth, including primary production, one factor that affects stickleback growth in this region was identified while in the field. During sample collection, it became apparent that infections by *Schistocephalus*

pungitii were common, and that the prevalence of infection likely varied among lakes. Through the diversion of nutrients from their hosts, cestode parasites can slow host growth (e.g., Shultz et al. 2006). I found that the tissue of parasitized fish had higher mercury concentrations than un-parasitized conspecifics. I also found a significant positive relationship between *S. pungitii* infection rate and age-at-size among lakes. Together with the finding that MeHg concentrations in stickleback were significantly and positively related to stickleback age-at-size, there results indicate that among-lake differences in prevalence of infection likely affects LSmean MeHg concentrations in stickleback.

Although analyzing and comparing whole dressed tissue of parasitized and un-parasitized Ninespine stickleback helped elucidate linkages among parasitism, fish growth, and mercury accumulation, inferences of effects on higher-level predators, such as fish-eating wildlife, required analyses of whole bodies (fish + parasite), termed a 'fish meal'. I found that: i) the cestode parasites are depleted in MeHg compared to stickleback hosts; and, ii) that the 'fish meals' have similar energy densities as whole dressed fish tissue. It is thus unlikely that infection of stickleback by cestodes would lead to higher Hg exposure in predators of stickleback. This is important because infections of stickleback by *S. pungitii* are predicted to increase with warming water temperatures. While warming temperatures will likely increase infection prevalence and intensity, my results indicate that this may actually result in reduced Hg exposure to predators of stickleback.

5.2 Implications of a changing climate on Hg accumulation in the study lakes

Climate warming is amplified in the Arctic (IPCC, 2007), and there are several factors that affect the accumulation of mercury in lakes that are subject to climate-induced change. Two such factors are primary production and ground ice degradation. To predict effects of climate change on Hg accumulation, we first have to understand drivers of current variability, and we then have to understand and predict effects of climate change on those drivers.

The two main limiters of primary production are light (Huisman et al. 1994) and nutrients (Schindler et al. 1978), both of which are expected to be impacted by climate change. Warmer air temperatures will lead to earlier ice-off in northern lakes, and consequently more light availability and higher primary production (Prowse et al. 2006). Warmer temperatures are also expected to lead to increases in precipitation in the Arctic (Trenberth et al. 2011), resulting in greater nutrient deposition and higher primary production (Paerl and Huisman, 2008). In addition to a general increase in lake primary production, there is an expected shift from benthic production to pelagic/planktonic production in Arctic lakes (Sierszen et al. 2003; Wrona et al. 2006).

Another primary effect of climate change on Arctic lakes and lake catchments is the thawing of permafrost/degradation of ground ice. Rising air temperatures are leading to enhanced thermokarstic activity, including thermal erosion, retrogressive thaw slumps, and a deepening of the active layer (see Grosse et al. 2013). Degrading permafrost can result in the release of

previously unavailable Hg, organic matter, and soluble ions (e.g., SO_4). Thermokarstic activity can have an antagonistic effect on lake primary production compared to climate change, as the solutes released from the active layer can lead to the complexation and scavenging of phytoplankton from the water column, and a subsequent shift from pelagic to benthic production (Thompson et al. 2008). Climate-induced changes to primary production and permafrost degradation could have profound effects on accumulation of mercury in ACP lake sediments, accumulation of mercury in ACP food webs, and increases in prevalence and intensity of *Schistocephalus pungitii* infections in stickleback on the ACP. Accurately predicting the net effect of these changes on fish mercury concentrations requires an understanding of the catchment properties of each region.

I found that the drivers of mercury accumulation in lake sediments varied with catchment properties on the ACP. In lakes with well-drained soils and small relative catchment sizes (low catchment influence; the ATQ lakes in this study), one could expect mercury accumulation to steadily increase with increases in primary production, consistent with the algal scavenging hypothesis (Outridge et al. 2007). Climate-related changes in sediment mercury accumulation rates in lakes with larger relative catchment sizes and poorly-drained soils (high catchment influence; the RDC lakes in this study) are more difficult to predict, because they are more influenced by unpredictable sedimentation events (e.g., extreme weather events, thaw slumping). However, the frequency and intensity of thermokarstic activity (Prowse et al. 2006) and precipitation (Trenberth et al. 2011) are both predicted to increase, so it is probable that the frequency and severity of sedimentation events will also increase, which will lead to large increases in Hg accumulation in these lakes. In a meta-

analysis (Chapter 2), I found that sediment Hg accumulation rates were more variable in lakes from thermokarst landscapes than in lakes from non-thermokarst landscapes, and because all of the study lakes are located on thermokarst landscapes, they are susceptible to thermokarstic activity. As such, there is a possibility that lakes with historically low catchment influence on sediment mercury accumulation could experience a sedimentation event, such as a retrogressive thaw slump, which could cause higher and more variable Hg accumulation rates.

There are several potential implications of climate change on the uptake and accumulation of MeHg into lake food webs on the Arctic Coastal Plain of Alaska. Sulphate (via a methylation mechanism or as a tracer of catchment influence) is currently the best abiotic predictor of fish MeHg concentration in the study lakes. With enhanced thermokarst activity (Grosse et al. 2013), solutes, like SO_4, that were once stored in the permafrost will become mobilized. Due to the relationship between SO_4 and %MeHg in periphyton, it is likely that SO_4 affected methylation via the stimulation of methylating bacteria, and not by simply tracing the amount of inorganic mercury available. Thus, although there are obvious direct effects from the release of stored legacy Hg from catchments, there are also potential indirect effects from the release of other ions from permafrost. In fact, recent work conducted on a lake in the high Arctic by Roberts et al. (2017) demonstrated a 500% increase (3-15 mg/L) in SO_4 concentration over 10 years as a result of multiple slumping events. It is difficult to predict how fish mercury concentrations in the study lakes on the ACP of Alaska would respond to dramatic increases in sulphate loads, since the lakes currently span a relatively small gradient in sulphate concentration (0.03-4.51 mg/L), and previous research has

indicated that the relationship between SO_4 and fish Hg is non-linear (e.g., Gabriel et al. 2014). At high concentrations, SO_4 can have an inhibitory effect on mercury methylation. A by-product of sulphate reduction is sulfide, which is a strong ligand for Hg, and the binding of Hg to sulfide can make it biologically unavailable (Gilmour et al. 1992). Some studies suggest that fish Hg concentrations peak at SO_4 concentrations from 1-12 mg/L (Gabriel et al. 2014), so it is possible that thermokarst-related increases in SO_4 could decrease methylation rates, and possibly fish MeHg concentrations in the future. It is especially difficult to predict the effects of increased sulphate loads, as they occur concomitantly with loading of other material, like organic matter and inorganic mercury from the catchment, both of which can influence methylation rates as well.

Results from stable isotope analysis (i.e., RDC lakes had more negative $\delta^{13}C$ suggesting more bacterial based food webs), differences in autochthony vs. allochthony, and variability in zooplankton abundance indicated that mercury is entering food webs through different routes in lakes from each region, and I infer that this affects Hg concentrations in fish. Results from water chemistry and chlorophyll-*a* analyses indicate that phytoplankton form the base of the food web in the low catchment influence (ATQ) lakes, and that pelagic primary production is higher in the ATQ lakes than in the RDC lakes. In lakes where pelagic phytoplankton underpin most of the food web, it is likely that rising temperatures will lead to a continued increase in lake primary production (Brylinsky and Mann, 1973; Rouse et al. 1997), and this could affect MeHg concentrations in higher trophic levels, including fish. Based on the fact that MeHg concentrations were higher in the sediments of the more autochthonous lakes, likely through a combination of algal scavenging (Outridge et al. 2007)

and enhanced methylation (Bravo et al. 2017), it is probable that increased pelagic production could further stimulate methylation in lake sediments, and result in higher concentrations of methylmercury in the water column (Bravo et al. 2017). However, higher phytoplankton densities may also decrease the amount of mercury that accumulates and magnifies through the food web through bloom dilution, because higher concentrations of algal cells can lead to a decrease in the amount of MeHg entering the food web (Pickhardt et al. 2002). In summary, increases in pelagic production are more likely to affect fish Hg concentrations in the study lakes that were less influenced by their catchment (i.e., the ATQ lakes), but it is not yet clear where the threshold is between enhanced methylation and bloom dilution.

Lakes in the Reindeer Camp region have larger relative catchments, and water chemistry data indicate that these lakes are more heavily influenced by allochthonous inputs than lakes in the Atqasuk region. The RDC lakes are located in the ACP foothills transition zone, an area where the topography and ice-rich soil composition makes them especially vulnerable to bank erosion and shoreline subsidence (Hinkel et al. 2012). As such, lakes in the RDC region will likely be more susceptible to degrading permafrost and increases in thermokarst activity than the ATQ lakes. Additionally, with changes to precipitation and weather patterns, it is likely that increased runoff, in addition to enhanced thermokarst, could lead not only to increased deposition of SO_4, but also organic matter, minerogenic matter, and total and methylmercury, all of which can impact the methylation and uptake of mercury into the food web (see Lehnerr et al. 2014). Thus, the climate-related effects on fish Hg concentrations in the lakes that were more influenced by their catchment (i.e., the RDC lakes) are likely a

product of increased inputs from the catchment (e.g., SO_4, Hg, OM) through increased runoff or thermokarsting, in contrast to the ATQ lakes, where fish Hg concentrations will likely be more influenced by changes in primary production.

The best biotic predictor of among-lake variability in MeHg concentrations in fish was growth, and fish growth will be affected by climate change in several ways. It is often thought that fish growth will increase in response to warming temperatures in the Arctic; however, growth rates in fish may also decrease if thermal optima are exceeded as a result of increased intensity of inter- or intra-specific competition (Reist el al. 2006b), or as a result of increased parasitism (e.g., Shultz et al. 2006). An in-depth analysis of fish bioenergetics was not within the scope of this thesis; however, a factor currently impacting the growth rate of Ninespine stickleback in lakes on the ACP is the prevalence of *Schistocephalus pungitii* infection (Chapter 4). Parasites often decrease growth rates in hosts through diversion of nutrients, and parasite infection rate is influenced by climate (see Lõhmus and Björklund, 2015). There is evidence that *Schistocephalus solidus* (hosted by Three-spined stickleback) experience higher plerocercoid growth rates at elevated temperatures and can manipulate hosts to seek out warmer environments, which collectively can lead to a higher infection rate (Macnab and Barber, 2012). It is difficult to predict the impact of climate change on fish growth rates on the ACP since longer growing seasons and higher nutrient loads could increase growth rates, while increased parasite infections could decrease growth rates. Although the lower growth rates induced by parasitism could lead to higher concentrations of fish MeHg, when considering an infected stickleback as a meal to upper trophic levels, it could actually dilute the amount of MeHg entering the food web. The life-cycle of an

endoparasite is complex, so there are other factors outside of the scope of this thesis to consider, such as how climate change will impact the distribution of the definitive hosts of *Schistocephalus*, piscivorous birds.

Results of this research indicate that climate-induced changes in primary production, sulphate, and fish growth may affect delivery of Hg to lakes and accumulation in food webs on the ACP, and that effects may differ depending on sources of primary production and degree of catchment influence. It is also possible, however, that climate change may induce a shift in lake state that changes how MeHg enters food webs. As outlined by Scheffer et al. (1993), shallow lakes have two alternate stable states (i.e., turbid and clearwater), and although these are stable equilibria, a major event can induce a shift from one state to the other. In this study, the ATQ lakes would be classified as "turbid" whereas the RDC lakes would be classified as "clearwater". Studies have found that thermokarstic activity, such as retrogressive thaw slumps, can lead to a shift from a turbid to clearwater state, as the inundation of ion-rich permafrost soil can lead to the absorption and flocculation of DOM, which increases water clarity, increases macrophyte growth, and results in a decrease in phytoplankton dominance (Thompson et al. 2008). If a thaw slump or other major thermokarstic event were to occur in the ATQ lakes, it is possible that the food webs and routes of MeHg could begin to resemble those in the RDC lakes.

5.3 Relevance

The research in this thesis elucidated patterns and controls of mercury accumulation in the sediments and simple food webs of lakes on the Arctic Coastal Plain of Alaska; however, it is highly relevant to lake ecosystems across the circum-Arctic. In Chapter 2 and Chapter 3, I presented evidence suggesting that catchment properties may impact mercury accumulation in sediments and food webs. The mercury dynamics in some lakes are highly influenced by external processes (e.g., sedimentation events) while others are not, and with enhanced permafrost degradation, lakes historically not impacted by their catchments could experience a sedimentation event, potentially altering their structure and function. The Arctic is rich in small, shallow lakes (Grosse, 2013) like the ones in this study, and thermokarst landscapes cover >20% of the northern permafrost region (Olefeldt et al. 2016). Based on this, and the fact that Hg accumulation is higher and more variable in lakes from thermokarst landscapes, it is clear that the prevalence of thermokarst landscapes could have implications for Arctic biological and human communities.

The main exposure of humans to mercury is through the consumption of fish, which can be a significant component of Indigenous diets in the Arctic (VanOostdam et al. 2005). On the Arctic Coastal Plain, subsistence fishing remains an important food source (e.g., George et al. 2004). The fish species in this study, the Ninespine stickleback, is not a food fish; however, it is an important prey item for other food fishes in this region (Laske et al. 2018). I have demonstrated that stickleback in shallow lakes on the ACP can have significantly different MeHg concentrations, and that among-lake differences are driven by a combination of

several proximate abiotic and biotic factors, some of which are governed by ultimate control exerted by catchments. We can only predict the future effects of climate change on fish MeHg concentrations if we identify and understand the current drivers of spatial variability.

5.4 Future Directions

The deposition, methylation, uptake, and bioaccumulation of mercury are complex processes, as has been demonstrated throughout this research and by many previous investigators (e.g., Gilmour et al. 1992; Branfireun et al. 1999; Pickhardt et al. 2002; Outridge et al. 2007; Swanson et al. 2011; Kidd et al. 2012). Since there are both synergistic and antagonistic drivers of mercury transport and accumulation, and because effects of drivers appear to differ spatially, it is difficult to predict the net effect of climate change on mercury dynamics in Arctic lakes. Based on my research results, I predict that permafrost degradation will exert a dominant effect on future accumulation of Hg in Arctic lakes, particularly in lakes with relatively large catchment sizes.

Numerous studies describe how the secondary effects of climate change (e.g., increased primary production) will impact fish mercury; however, far less is known about how the degradation of permafrost will influence fish mercury, either directly or indirectly. The amount of available total mercury in lake sediments is increasing with degradation of permafrost, and mercury stored in thawing permafrost (Deison et al. 2012) can be mobilized and deposited to downstream lakes (Grosse et al. 2013). Recently it was shown that a globally significant amount of mercury is stored in permafrost soils (Schuster et al. 2018). However, it is unclear how this will impact fish mercury concentrations, as mercury must be methylated before being taken up into the food web, and there are several interrelated mechanisms that affect methylation, which have been outlined throughout the thesis. Recently, a seminal paper was published that described how differences in sources of organic matter (OM; either terrestrial or phytoplankton-derived) can affect mercury methylation

(Bravo et al. 2017). The authors found that catchments have profound effects on the dominant form of OM and on mercury methylation rates. Results from this study (conducted on a small geographic scale), were consistent with some of my findings from Arctic Alaska, which show that the level of catchment influence drives mercury accumulation in lake sediments and affects the dominant form of primary production (terrestrial versus phytoplankton) and methylation dynamics.

We do not yet fully understand how catchment size and composition, active layer depth and composition, lake chemistry, and lake trophic state interact to govern variability in mercury methylation and uptake into aquatic food webs at large spatial scales in the North American Arctic. Future research should focus on filling this knowledge gap. Specific questions that should be addressed include: i) Can physical lake and catchment properties predict the dominant form of primary production in a lake?; ii) Does the dominant form of primary production (phytoplankton vs macrophytes/biofilm) dictate the primary methylation location within a lake?; and, iii) Does the dominant form of primary production influence how methyl mercury enters the food web?

5.5 Concluding remarks

The findings of this thesis represent the first in-depth analysis of mercury accumulation in lake sediments and mercury concentrations in food webs of lakes on the Arctic Coastal Plain of Alaska. Results of this research provide further evidence that mercury dynamics in lakes are complex, and can be directly or indirectly influenced by both biotic and abiotic factors. It is clear that catchment characteristics play a significant, albeit not fully understood, role in the deposition and accumulation of mercury in lake sediments, and that catchment characteristics also affect methylation and uptake of mercury into the food webs. Findings are relevant across the circumpolar Arctic, and future research should focus on identifying mechanisms that underpin relationships among different variables that affect fish mercury concentrations. Results from this and future research will ultimately help inform predictions of how fish mercury concentrations may respond to climate change.

5.6 Figures

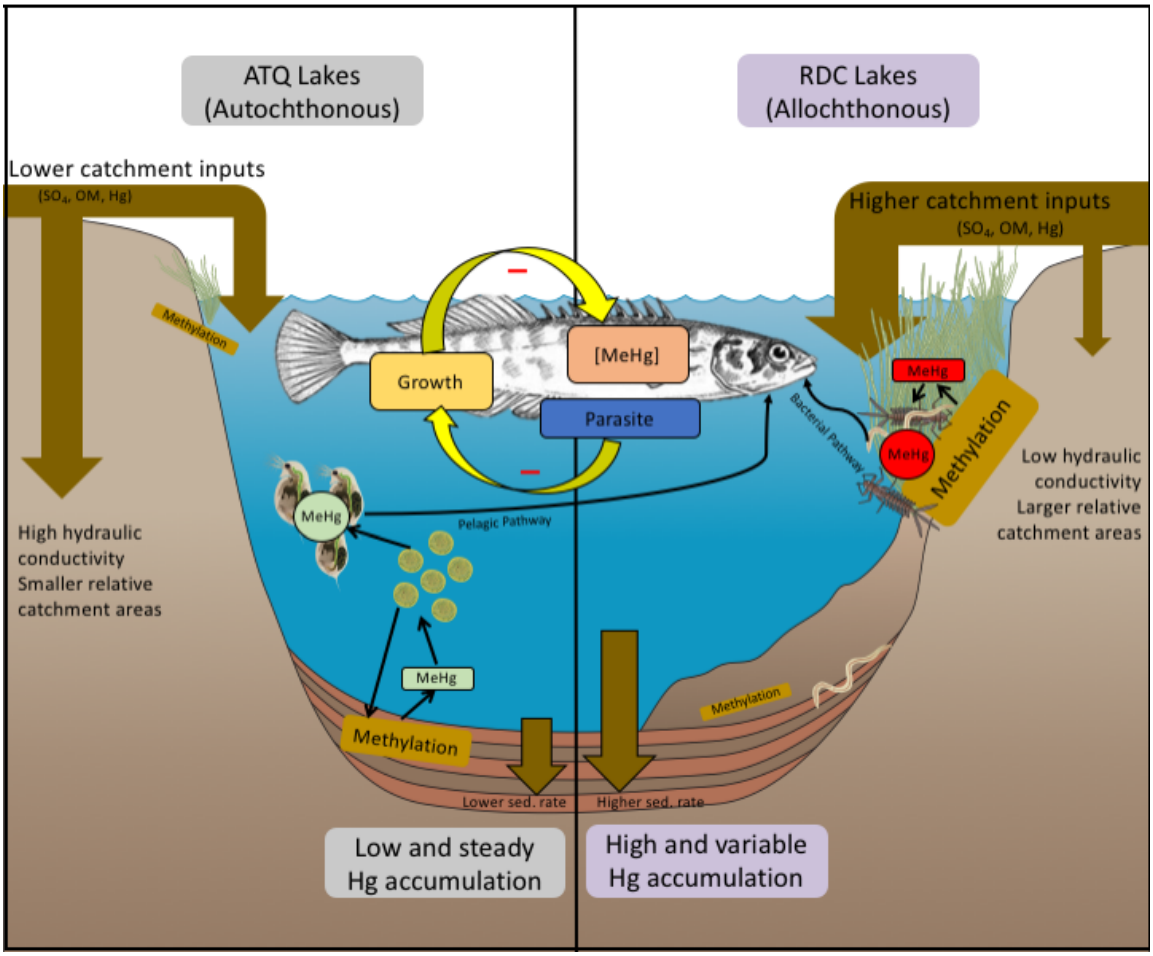

Figure 5.1. Conceptual diagram of factors influencing mercury accumulation in the sediments and food webs of study lakes on the Arctic Coastal Plain of Alaska. Lakes in the ATQ region experience lower catchment inputs and are primarily autochthonous, while the RDC lakes experience higher catchment inputs and are more allochthonous. Lower sedimentation rates in the ATQ lakes lead to lower and more uniform Hg accumulation rates in sediments, whereas the higher sedimentation rate in RDC lakes leads to high and variable Hg accumulation rates in sediments. Low catchment inputs in the ATQ lakes lead to phytoplankton dominance and higher methylation rates in sediments, whereas higher catchment inputs in the RDC lakes lead to macrophyte dominance and higher methylation in biofilms associated with periphyton. The energy pathways in the ATQ lakes are more pelagic, and zooplankton (with relatively lower MeHg) are relied upon heavily as a food source, whereas the energy pathways in the RDC lakes are more bacterial, and invertebrates (with relatively higher MeHg) are relied upon more heavily as a food source. All of these factors, along with fish growth, which is influenced by parasitism in a pattern that is independent of region, interact to affect MeHg concentrations in fish.

References

Allen-Gil, S. M., Gubala, C. P., Landers, D. H., Lasorsa, B. K., Crecelius, E. A., & Curtis, L. R. (1997). Heavy metal accumulation in sediment and freshwater fish in US Arctic lakes. *Environmental Toxicology and Chemistry*, *16*(4), 733-741.

Appleby, P. G., & Oldfield, F. (1978). The calculation of lead-210 dates assuming a constant rate of supply of unsupported 210Pb to the sediment. *Catena*, *5*(1), 1-8.

Arctic Monitoring and Assessment Programme (2011) Mercury in the Arctic. Arctic Monitoring and Assessment Programme (AMAP), Oslo, Norway. xiv. 191 pp.

Arctic Monitoring and Assessment Programme (AMAP)/United Nations Environment Programme (UNEP). (2019) Global Mercury Assessment 2018. Oslo, Norway/UNEP Chemicals Branch, Geneva, Switzerland.

Arme, C., & Owen, R. W. (1967). Infections of the three-spined stickleback, Gasterosteus aculeatus L., with the plerocercoid larvae of Schistocephalus solidus (Müller, 1776), with special reference to pathological effects. *Parasitology*, *57*(2), 301-314.

Arp, C. D., Jones, B. M., Urban, F. E., & Grosse, G. (2011). Hydrogeomorphic processes of thermokarst lakes with grounded-ice and floating-ice regimes on the Arctic Coastal Plain, Alaska. *Hydrological Processes*, *25*(15), 2422-2438.

Arp, C. D., Jones, B. M., Lu, Z., & Whitman, M. S. (2012). Shifting balance of thermokarst lake ice regimes across the Arctic Coastal Plain of Northern Alaska. *Geophysical Research Letters*, *39*(16), doi:10.1029/2012GL052518

Atwell, L., Hobson, K. A., & Welch, H. E. (1998). Biomagnification and bioaccumulation of mercury in an arctic marine food web: insights from stable nitrogen isotope analysis. *Canadian Journal of Fisheries and Aquatic Sciences*, *55*(5), 1114-1121.

Barber, I. (2005). Parasites grow larger in faster growing fish hosts. *International Journal for Parasitology*, *35*(2), 137-143.

Barber, I., Wright, H. A., Arnott, S. A., & Wootton, R. J. (2008). Growth and energetics in the stickleback–Schistocephalus host–parasite system: a review of experimental infection studies. *Behaviour*, *145*(4), 647-668.

Barber, I., & Svensson, P. A. (2003). Effects of experimental Schistocephalus solidus infections on growth, morphology and sexual development of female three-spined sticklebacks, Gasterosteus aculeatus. *Parasitology*, *126*(4), 359-367.

Barnett, T. P., Adam, J. C., & Lettenmaier, D. P. (2005). Potential impacts of a warming climate on water availability in snow-dominated regions. *Nature*, *438*(7066), 303-309.

Bergey, L., Weis, J. S., & Weis, P. (2002). Mercury uptake by the estuarine species Palaemonetes pugio and Fundulus heteroclitus compared with their parasites, Probopyrus pandalicola and Eustrongylides sp. *Marine Pollution Bulletin*, *44*(10), 1046-1050.

Biester, H., Bindler, R., Martinez-Cortizas, A., & Engstrom, D. R. (2007). Modeling the past atmospheric deposition of mercury using natural archives. *Environmental Science & Technology*, *41*(14), 4851-4860.

Bindler, R., Olofsson, C., Renberg, I., & Frech, W. (2001). Temporal trends in mercury accumulation in lake sediments in Sweden. *Water, Air and Soil Pollution: Focus*, *1*(3-4), 343-355.

Bisogni Jr, J. J., & Lawrence, A. W. (1975). Kinetics of mercury methylation in aerobic and anaerobic aquatic environments. *Journal (Water Pollution Control Federation)*, 1(47), 135-152.

Bloom, N., & Fitzgerald, W. F. (1988). Determination of volatile mercury species at the picogram level by low-temperature gas chromatography with cold-vapour atomic fluorescence detection. *Analytica Chimica Acta*, *208*, 151-161.

Bodaly, R. A., Rudd, J. W. M., Fudge, R. J. P., & Kelly, C. A. (1993). Mercury concentrations in fish related to size of remote Canadian Shield lakes. *Canadian Journal of Fisheries and Aquatic Sciences*, *50*(5), 980-987.

Bookman, R., Driscoll, C. T., Engstrom, D. R., & Effler, S. W. (2008). Local to regional emission sources affecting mercury fluxes to New York lakes. *Atmospheric Environment*, *42*(24), 6088-6097.

Boudou, A., & Ribeyre, F. (1997). Mercury in the food web: accumulation and transfer mechanisms. *Metal Ions in Biological Systems*, *34*, 289-320.

Bradley, M. A., Barst, B. D., & Basu, N. (2017). A review of mercury bioavailability in humans and fish. *International Journal of Environmental Research and Public Health*, *14*(2), 169-189.

Branfireun, B. A., Roulet, N. T., Kelly, C., & Rudd, J. W. (1999). In situ sulphate stimulation of mercury methylation in a boreal peatland: Toward a link

between acid rain and methylmercury contamination in remote environments. *Global Biogeochemical Cycles*, *13*(3), 743-750.

Bravo, A. G., Bouchet, S., Tolu, J., Björn, E., Mateos-Rivera, A., & Bertilsson, S. (2017). Molecular composition of organic matter controls methylmercury formation in boreal lakes. *Nature Communications*, 8, 14255, doi:10.1038/ncomms14255

Brylinsky, M., & Mann, K. (1973). An Analysis of Factors Governing Productivity in Lakes and Reservoirs. *Limnology & Oceanography*, *18*(1), 1-14.

Bunn, S. E., & Boon, P. I. (1993). What sources of organic carbon drive food webs in billabongs? A study based on stable isotope analysis. *Oecologia*, *96*(1), 85-94.

Burger, J., Stern, A. H., & Gochfeld, M. (2004). Mercury in commercial fish: optimizing individual choices to reduce risk. *Environmental Health Perspectives*, *113*(3), 266-271.

Cabana, G., & Rasmussen, J. B. (1996). Comparison of aquatic food chains using nitrogen isotopes. *Proceedings of the National Academy of Sciences*, *93*(20), 10844-10847.

Capone, D. G., & Kiene, R. P. (1988). Comparison of microbial dynamics in marine and freshwater sediments: Contrasts in anaerobic carbon catabolism. *Limnology & Oceanography*, *33*(4part2), 725-749.

Carey, M. P., & Zimmerman, C. E. (2014). Physiological and ecological effects of increasing temperature on fish production in lakes of Arctic Alaska. *Ecology and Evolution*, *4*(10), 1981-1993.

Chetelat, J., & Amyot, M. (2009). Elevated methylmercury in High Arctic Daphnia and the role of productivity in controlling their distribution. *Global Change Biology*, *15*(3), 706-718.

Chételat, J., Amyot, M., & Garcia, E. (2011). Habitat-specific bioaccumulation of methylmercury in invertebrates of small mid-latitude lakes in North America. *Environmental Pollution*, *159*(1), 10-17.

Clilverd, H., White, D., & Lilly, M. (2009). Chemical and Physical Controls on the Oxygen Regime of Ice-Covered Arctic Lakes and Reservoirs. *Journal of the American Water Resources Association*, *45*(2), 500-511.

Corbitt, E. S., Jacob, D. J., Holmes, C. D., Streets, D. G., & Sunderland, E. M. (2011). Global source–receptor relationships for mercury deposition under present-day and 2050 emissions scenarios. *Environmental Science & Technology*, *45*(24), 10477-10484.

Clow, G. D., & Urban, F. E. (2002). Large permafrost warming in northern Alaska during the 1990's determined from GTN-P borehole temperature measurements. In *AGU Fall Meeting Abstracts*.

Compeau, G. C., & Bartha, R. (1985). Sulfate-reducing bacteria: principal methylators of mercury in anoxic estuarine sediment. *Applied and Environmental Microbiology*, *50*(2), 498-502.

Crawford, R. H. (1974). Structure of an air-breathing organ and the swim bladder in the Alaska blackfish, Dallia pectoralis Bean. *Canadian Journal of Zoology*, *52*(10), 1221-1225.

Cummins, K. W., & Wuycheck, J. C. (1971). Caloric Equivalents for Investigations in Ecological Energetics: With 2 figures and 3 tables in the text. *Internationale Vereinigung für Theoretische und Angewandte Limnologie: Mitteilungen*, *18*(1), 1-158.

DeFaveri, J., T. Shikano, and J. Merilä. 2014. Geographic variation in age structure and longevity in the nine-spined stickleback (*Pungitius pungitius*). PLoS ONE 9:e102660

Dean, W. E. (1974). Determination of carbonate and organic matter in calcareous sediments and sedimentary rocks by loss on ignition; comparison with other methods. *Journal of Sedimentary Research*, *44*(1), 242-248.

De Meeûs, T., & Renaud, F. (2002). Parasites within the new phylogeny of eukaryotes. *Trends in Parasitology*, *18*(6), 247-251.

de Wit, H. A., Kainz, M. J., & Lindholm, M. (2012). Methylmercury bioaccumulation in invertebrates of boreal streams in Norway: Effects of aqueous methylmercury and diet retention. *Environmental Pollution*, *164*, 235-241.

Deison, R., Smol, J. P., Kokelj, S. V., Pisaric, M. F., Kimpe, L. E., Poulain, A. J., ... & Blais, J. M. (2012). Spatial and temporal assessment of mercury and organic matter in thermokarst affected lakes of the Mackenzie Delta Uplands, NT, Canada. *Environmental Science & Technology*, *46*(16), 8748-8755.

Delbeek, J. C., & Williams, D. D. (1988). Feeding selectivity of four species of sympatric stickleback in brackish-water habitats in eastern Canada. *Journal of Fish Biology*, *32*(1), 41-62.

DeMott, W. R. (1982). Feeding selectivities and relative ingestion rates of Daphnia and Bosmina. *Limnology and Oceanography*, *27*(3), 518-527.

Dibike, Y, Prowse, T. Saloranta, T, Ahmed, R. (2011) Response of Northern Hemisphere lake-ice cover and lake-water thermal structure patterns to a

changing climate. *Hydrological Processes,* 25, 2942-2953.

Drevnick, P. E., Yang, H., Lamborg, C. H., & Rose, N. L. (2012). Net atmospheric mercury deposition to Svalbard: Estimates from lacustrine sediments. *Atmospheric Environment*, *59*, 509-513.

Drevnick, P. E., Cooke, C. A., Barraza, D., Blais, J. M., Coale, K. H., Cumming, B. F., ... & Engstrom, D. R. (2016). Spatiotemporal patterns of mercury accumulation in lake sediments of western North America. *Science of the Total Environment*, *568*, 1157-1170.

Driscoll, C. T., Mason, R. P., Chan, H. M., Jacob, D. J., & Pirrone, N. (2013). Mercury as a global pollutant: sources, pathways, and effects. *Environmental Science & Technology*, *47*(10), 4967-4983.

Drott, A., Lambertsson, L., Björn, E., & Skyllberg, U. (2007). Do potential methylation rates reflect accumulated methyl mercury in contaminated sediments? *Environmental Science & Technology*, *42*(1), 153-158.

Eloranta, A. P., Knudsen, R., Amundsen, P. A., & Merilä, J. (2015). Consistent isotopic differences between Schistocephalus spp. parasites and their stickleback hosts. *Diseases of Aquatic Organisms*, *115*(2), 121-128.

Engstrom, D. R., & Swain, E. B. (1997). Recent declines in atmospheric mercury deposition in the upper Midwest. *Environmental Science & Technology*, *31*(4), 960-967.

Engstrom, D. R., Balogh, S. J., & Swain, E. B. (2007). History of mercury inputs to Minnesota lakes: influences of watershed disturbance and localized atmospheric deposition. *Limnology and Oceanography*, *52*(6), 2467-2483.

Environmental Systems Research Institute (ESRI) (2016) ArcGIS Desktop: release 10 Redlands, CA: Environmental Systems Software

Eure, H. (1976). Seasonal abundance of Neoechinorhynchus cylindratus taken from largemouth bass (Micropterus salmoides) in a heated reservoir. *Parasitology*, *73*(3), 355-370.

Evers, D. C., Schmutz, J. A., Basu, N., DeSorbo, C. R., Fair, J., Gray, C. E., ... & Wright, K. G. (2014). Historic and contemporary mercury exposure and potential risk to Yellow-billed Loons (Gavia adamsii) breeding in Alaska and Canada. *Waterbirds*, *37*(1), 147-160.

Fitzgerald, W. F., Engstrom, D. R., Lamborg, C. H., Tseng, C. M., Balcom, P. H., & Hammerschmidt, C. R. (2005). Modern and historic atmospheric mercury fluxes in northern Alaska: Global sources and Arctic depletion. *Environmental Science & Technology*, *39*(2), 557-568.

France, R. L. (1995). Differentiation between littoral and pelagic food webs in lakes using stable carbon isotopes. *Limnology and Oceanography*, *40*(7), 1310-1313.

Gabriel, M. C., Howard, N., & Osborne, T. Z. (2014). Fish mercury and surface water sulfate relationships in the Everglades Protection Area. *Environmental Management*, *53*(3), 583-593.

Gallagher, C. P., & Dick, T. A. (2010). Trophic structure of a landlocked Arctic char Salvelinus alpinus population from southern Baffin Island, Canada. *Ecology of Freshwater Fish*, *19*(1), 39-50.

Gallagher, C. P., & Dick, T. A. (2011). Ecological characteristics of ninespine stickleback Pungitius pungitius from southern Baffin Island, Canada. *Ecology of Freshwater Fish*, *20*(4), 646-655.

Gaye-Siessegger, J., Focken, U., Muetzel, S., Abel, H., & Becker, K. (2004). Feeding level and individual metabolic rate affect δ 13 C and δ 15 N values in carp: implications for food web studies. *Oecologia*, *138*(2), 175-183.

George, J. C., Zeh, J., Suydam, R., & Clark, C. (2004). Abundance and population trend (1978-2001) of western arctic bowhead whales surveyed near Barrow, Alaska. *Marine Mammal Science*, *20*(4), 755-773.

Gilmour, C. C., Henry, E. A., & Mitchell, R. (1992). Sulfate stimulation of mercury methylation in freshwater sediments. *Environmental Science & Technology*, *26*(11), 2281-2287.

Gilmour, C. C., & Henry, E. A. (1991). Mercury methylation in aquatic systems affected by acid deposition. *Environmental pollution*, *71*(2-4), 131-169.

Godin, J. G. J., & Sproul, C. D. (1988). Risk taking in parasitized sticklebacks under threat of predation: effects of energetic need and food availability. *Canadian Journal of Zoology*, *66*(11), 2360-2367.

Golding, G. R., Kelly, C. A., Sparling, R., Loewen, P. C., & Barkay, T. (2007). Evaluation of mercury toxicity as a predictor of mercury bioavailability. *Environmental Science & Technology*, *41*(16), 5685-5692

Graham, A. M., Aiken, G. R., & Gilmour, C. C. (2013). Effect of dissolved organic

matter source and character on microbial Hg methylation in Hg–S–DOM solutions. *Environmental Science & Technology*, *47*(11), 5746-5754.

Graham, A. M., Aiken, G. R., & Gilmour, C. C. (2012). Dissolved organic matter enhances microbial mercury methylation under sulfidic conditions. *Environmental Science & Technology*, *46*(5), 2715-2723.

Grigal, D. F. (2002). Inputs and outputs of mercury from terrestrial watersheds: a review. *Environmental Reviews*, *10*(1), 1-39.

Grosse, G, Jones B, Arp C (2013) Thermokarst lakes, drainage, and drained basins. In: Schroder J (ed) Treatise on geomorphology, vol 8, glacial and periglacial geomorphology. Academic Press, San Diego, pp 325-353

Guzzo, M. M., & Blanchfield, P. J. (2016). Climate change alters the quantity and phenology of habitat for lake trout (Salvelinus namaycush) in small Boreal Shield lakes. *Canadian Journal of Fisheries and Aquatic Sciences*, *74*(6), 871-884.

Hall, B. D., Bodaly, R. A., Fudge, R. J. P., Rudd, J. W. M., & Rosenberg, D. M. (1997). Food as the dominant pathway of methylmercury uptake by fish. *Water, Air, and Soil Pollution*, *100*(1-2), 13-24.

Harris, H. H., Pickering, I. J., & George, G. N. (2003). The chemical form of mercury in fish. *Science*, *301*(5637), 1203-1203.

Harris, R. C., Rudd, J. W., Amyot, M., Babiarz, C. L., Beaty, K. G., Blanchfield, P. J., ... & Heyes, A. (2007). Whole-ecosystem study shows rapid fish-mercury response to changes in mercury deposition. *Proceedings of the National Academy of Sciences*, *104*(42), 16586-16591.

Hartman, K. J., & Brandt, S. B. (1995). Estimating energy density of fish. *Transactions of the American Fisheries Society*, *124*(3), 347-355.

Haynes, T. B., Rosenberger, A. E., Lindberg, M. S., Whitman, M., & Schmutz, J. A. (2014). Patterns of lake occupancy by fish indicate different adaptations to life in a harsh Arctic environment. *Freshwater Biology*, *59*(9), 1884-1896.

Heins, D. C., & Baker, J. A. (2008). The stickleback–Schistocephalus host–parasite system as a model for understanding the effect of a macroparasite on host reproduction. *Behaviour*, *145*(4), 625-645.

Hermanson, M. H. (1998). Anthropogenic mercury deposition to Arctic lake sediments. *Water, Air, and Soil Pollution*, *101*(1-4), 309-321.

Höglund, J., & Thulin, J. (1990). The epidemiology of the metacercariae of Diplostomum baeri and D. spathaceum in perch (Perca fluviatilis) from the

warm water effluent of a nuclear power station. *Journal of Helminthology*, *64*(2), 139-150.

Hill, D. K., & Magnuson, J. J. (1990). Potential effects of global climate warming on the growth and prey consumption of Great Lakes fish. *Transactions of the American Fisheries Society*, *119*(2), 265-275.

Hinkel, K. M., Lenters, J. D., Sheng, Y., Lyons, E. A., Beck, R. A., Eisner, W. R., ... & Potter, B. L. (2012). Thermokarst lakes on the Arctic Coastal Plain of Alaska: Spatial and temporal variability in summer water temperature. *Permafrost and Periglacial Processes*, *23*(3), 207-217.

Hinkel, K. M., Sheng, Y., Lenters, J. D., Lyons, E. A., Beck, R. A., Eisner, W. R., & Wang, J. (2012). Thermokarst lakes on the Arctic Coastal Plain of Alaska: Geomorphic controls on bathymetry. *Permafrost and Periglacial Processes*, *23*(3), 218-230.

Hinzman, L. D., Bettez, N. D., Bolton, W. R., Chapin, F. S., Dyurgerov, M. B., Fastie, C. L., ... & Jensen, A. M. (2005). Evidence and implications of recent climate change in northern Alaska and other arctic regions. *Climatic Change*, *72*(3), 251-298.

Huisman, J., & Weissing, F. J. (1994). Light-limited growth and competition for light in well-mixed aquatic environments: an elementary model. *Ecology*, *75*(2), 507-520.

Hunter, J. G. (1968). *Production of Arctic char (Salvelinus alpinus Linnaeus) in a small arctic lake* (Doctoral dissertation, McGill University).

Hynes, H. B. N. (1950). The food of fresh-water sticklebacks (Gasterosteus aculeatus and Pygosteus pungitius), with a review of methods used in studies of the food of fishes. *The Journal of Animal Ecology*, 19(1), 36-58.

IPCC (2007) Climate Change 2007: The physical science basis. Contribution from Working Group 1 to the fourth assessment report of the Inter-Governmental Panel on Climate Change, in *IPCC Fourth Assessment Report* edited by Solomon,S., Quin, D., Manning, M., Marquis, M., Averyt, M., Tignor, M., Miller, H.L. Cambridge University Press, Cambridge, U.K.

Jakobsen, P. J., Johnsen, G. H., & Larsson, P. (1988). Effects of predation risk and parasitism on the feeding ecology, habitat use, and abundance of lacustrine threespine stickleback (Gasterosteus aculeatus). *Canadian Journal of Fisheries and Aquatic Sciences*, *45*(3), 426-431.

Johnson, L. (1975). Distribution of fish species in Great Bear Lake, Northwest Territories, with reference to zooplankton, benthic invertebrates, and environmental conditions. *Journal of the Fisheries Board of Canada*, *32*(11), 1989-2004.

Jones, J. W., and H. B. N. Hynes. 1950. The age and growth of Gasterosteus aculeatus, Pygosteus pungitius and Spinachia vulgaris, as shown by their otoliths. *Journal of Animal Ecology,* 19:59–73.

Jorgenson, M. T., & Shur, Y. (2007). Evolution of lakes and basins in northern Alaska and discussion of the thaw lake cycle. *Journal of Geophysical Research: Earth Surface*, *112*(F2).

Jorgenson MT, Grunblatt J (2013). Landscape-level ecological mapping of northern Alaska and field site photography. Report prepared for the Arctic Landscape Conservation Cooperative.[Available at http://arcticlcc.org/assets/products/ALCC2011-06/reports/NorthernAK_Landscape Mappping_Field_Photos_Final_RPT. pdf]

Kalff J. (2001) Limnology: Inland Water Ecosystems. Prentice- Hall New Jersey.

Kamman, N. C., & Engstrom, D. R. (2002). Historical and present fluxes of mercury to Vermont and New Hampshire lakes inferred from 210Pb dated sediment cores. *Atmospheric Environment*, *36*(10), 1599-1609.

Karlsson, J., & Byström, P. (2005). Littoral energy mobilization dominates energy supply for top consumers in subarctic lakes. *Limnology and Oceanography*, *50*(2), 538-543.

Keivany, Y., & Nelson, J. S. (2000). Taxonomic review of the genus Pungitius, ninespine sticklebacks (Gasterosteidae). *Cybium*, *24*(2), 107-122.

Kertell, K. (1996). Response of Pacific loons (Gavia pacifica) to impoundments at Prudhoe Bay, Alaska. *Arctic*, 49(4), 356-366.

Karimi, R., Chen, C. Y., Pickhardt, P. C., Fisher, N. S., & Folt, C. L. (2007). Stoichiometric controls of mercury dilution by growth. *Proceedings of the National Academy of Sciences*, *104*(18), 7477-7482.

Kidd, K. A., Hesslein, R. H., Fudge, R. J. P., & Hallard, K. A. (1995). The influence of trophic level as measured by δ 15 N on mercury concentrations in freshwater organisms. In *Mercury as a Global Pollutant* (pp. 1011-1015). Springer, Dordrecht.

Kidd, K., Clayden, M., & Jardine, T. (2012). Bioaccumulation and biomagnification of mercury through food webs. *Environmental Chemistry and Toxicology of Mercury. Wiley, Hoboken*, 455-499.

Kidd, K. A., Muir, D. C., Evans, M. S., Wang, X., Whittle, M., Swanson, H. K., ... & Guildford, S. (2012). Biomagnification of mercury through lake trout (Salvelinus namaycush) food webs of lakes with different physical, chemical and biological characteristics. *Science of the Total Environment*, *438*, 135-143.

King, J. K., Kostka, J. E., Frischer, M. E., & Saunders, F. M. (2000). Sulfate-reducing bacteria methylate mercury at variable rates in pure culture and in marine sediments. *Applied and Environmental Microbiology*, *66*(6), 2430-2437.

Kirk, J. L., Muir, D. C., Antoniades, D., Douglas, M. S., Evans, M. S., Jackson, T. A., ... & Smol, J. P. (2011). Climate change and mercury accumulation in Canadian high and subarctic lakes. *Environmental Science & Technology*, *45*(3), 964-970.

Kokelj, S. V., & Burn, C. R. (2003). Ground ice and soluble cations in near-surface permafrost, Inuvik, Northwest Territories, Canada. *Permafrost and Periglacial Processes*, *14*(3), 275-289.

Kokelj, S. V., Zajdlik, B., & Thompson, M. S. (2009). The impacts of thawing permafrost on the chemistry of lakes across the subarctic boreal-tundra transition, Mackenzie Delta region, Canada. *Permafrost and Periglacial Processes*, *20*(2), 185-199.

Korthals, E. T., & Winfrey, M. R. (1987). Seasonal and spatial variations in mercury methylation and demethylation in an oligotrophic lake. *Applied and Environmental Microbiology*, *53*(10), 2397-2404.

Kuris, A. M., Hechinger, R. F., Shaw, J. C., Whitney, K. L., Aguirre-Macedo, L., Boch, C. A., ... & Lorda, J. (2008). Ecosystem energetic implications of parasite and free-living biomass in three estuaries. *Nature*, *454*(7203), 515.

Lagler, K.F., Bardach, J.E. & Miller, R.R. (1962) Icthyology. John Wiley and Sons, New York, New York, USA.

Lafferty, K. D., Allesina, S., Arim, M., Briggs, C. J., De Leo, G., Dobson, A. P., ... & Martinez, N. D. (2008). Parasites in food webs: the ultimate missing links. *Ecology Letters*, *11*(6), 533-546.

Landers, D. H., Gubala, C., Verta, M., Lucotte, M., Johansson, K., Vlasova, T., & Lockhart, W. L. (1998). Using lake sediment mercury flux ratios to evaluate the regional and continental dimensions of mercury deposition in arctic and boreal ecosystems. *Atmospheric Environment*, *32*(5), 919-928.

Laske, S. M., Rosenberger, A. E., Wipfli, M. S., & Zimmerman, C. E. (2018). Generalist feeding strategies in Arctic freshwater fish: A mechanism for dealing with extreme environments. *Ecology of Freshwater Fish*.

Lehnherr, I. (2014). Methylmercury biogeochemistry: a review with special reference to Arctic aquatic ecosystems. *Environmental Reviews*, *22*(3), 229-243.

Lenth, R.V. (2016). Least-Squares Means: The R Package lsmeans. Journal of Statistical Software, 69(1), 1-33.<doi:10.18637/jss.v069.i01>

Lewis, D. B., Walkey, M., & Dartnall, H. J. G. (1972). Some effects of low oxygen tensions on the distribution of the three-spined stickleback Gasterosteus aculeatus L. and the nine-spined stickleback Pungitius pungitius (L.). *Journal of Fish Biology*, *4*(1), 103-108.

Lindberg, S., Bullock, R., Ebinghaus, R., Engstrom, D., Feng, X., Fitzgerald, W., ... & Seigneur, C. (2007). A synthesis of progress and uncertainties in attributing the sources of mercury in deposition. *AMBIO: a Journal of the Human Environment*, *36*(1), 19-34.

Lindqvist, O., Johansson, K., Bringmark, L., Timm, B., Aastrup, M., Andersson, A., ... & Meili, M. (1991). Mercury in the Swedish environment—recent research on causes, consequences and corrective methods. *Water, Air, and Soil Pollution*, *55*(1-2), xi-261.

Lockhart, W. L., Stern, G. A., Wagemann, R., Hunt, R. V., Metner, D. A., DeLaronde, J., ... & Mount, K. (2005). Concentrations of mercury in tissues of beluga whales (Delphinapterus leucas) from several communities in the Canadian Arctic from 1981 to 2002. *Science of the Total Environment*, *351*, 391-412.

LoBue, C. P., & Bell, M. A. (1993). Phenotypic manipulation by the cestode parasite Schistocephalus solidus of its intermediate host, Gasterosteus aculeatus, the threespine stickleback. *The American Naturalist*, *142*(4), 725-735.

Lõhmus, M., & Björklund, M. (2015). Climate change: what will it do to fish—parasite interactions? Biological Journal of the Linnean Society, 116(2), 397-411

Lougheed, V. L., Butler, M. G., McEwen, D. C., & Hobbie, J. E. (2011). Changes in tundra pond limnology: Re-sampling Alaskan ponds after 40 years. *Ambio*, *40*(6), 589- 599

Lorey, P., & Driscoll, C. T. (1999). Historical trends of mercury deposition in Adirondack lakes. *Environmental Science & Technology*, *33*(5), 718-722.

Lv, S., Zhou, X. N., Zhang, Y. I., Liu, H. X., Zhu, D., Yin, W. G., ... & Jia, T. W. (2006). The effect of temperature on the development of Angiostrongylus cantonensis (Chen 1935) in Pomaceacanaliculata (Lamarck 1822). *Parasitology Research*, *99*(5), 583.

MacIntyre, S., Flynn, K. M., Jellison, R., & Romero, J. R. (1999). Boundary mixing and

nutrient fluxes in Mono Lake, California. *Limnology and Oceanography*, *44*(3), 512-529.

Macnab, V., & Barber, I. (2012). Some (worms) like it hot: fish parasites grow faster in warmer water, and alter host thermal preferences. *Global Change Biology*, *18*(5), 1540-1548.

Marcogliese, D. J. (2001). Implications of climate change for parasitism of animals in the aquatic environment. *Canadian Journal of Zoology*, *79*(8), 1331-1352.

Marcogliese, D. J. (2003). Food webs and biodiversity: are parasites the missing link. *Journal of Parasitology*, *89*(6), 106-113.

Mauro, J. B., Guimarães, J. R., & Melamed, R. (2001). Mercury methylation in macrophyte roots of a tropical lake. *Water, Air, and Soil Pollution*, *127*(1-4), 271-280.

Mauro, J., Guimaraes, J., Hintelmann, H., Watras, C., Haack, E., & Coelho-Souza, S. (2002). Mercury methylation in macrophytes, periphyton, and water–comparative studies with stable and radio-mercury additions. *Analytical and Bioanalytical Chemistry*, *374*(6), 983-989.

McCauley, E., & Kalff, J. (1981). Empirical relationships between phytoplankton and zooplankton biomass in lakes. *Canadian Journal of Fisheries and Aquatic Sciences*, *38*(4), 458-463.

McCutchan Jr, J. H., Lewis Jr, W. M., Kendall, C., & McGrath, C. C. (2003). Variation in trophic shift for stable isotope ratios of carbon, nitrogen, and sulfur. *Oikos*, *102*(2), 378-390.

McLeod, A.I. (2011) Kendall: Kendall rank correlation and Mann-Kendall trend test. R package version 2.2. https://CRAN.R-project.org/package=Kendall

Merritt, R. W., & Cummins, K. W. (Eds.). (1996). *An introduction to the aquatic insects of North America*. Kendall Hunt.

Mesquita, P. S., Wrona, F. J., & Prowse, T. D. (2010). Effects of retrogressive permafrost thaw slumping on sediment chemistry and submerged macrophytes in Arctic tundra lakes. *Freshwater Biology*, *55*(11), 2347-2358.

Michelutti, N., Wolfe, A. P., Vinebrooke, R. D., Rivard, B., & Briner, J. P. (2005). Recent primary production increases in arctic lakes. *Geophysical Research Letters*, doi:10.1029/2005GL023693

Michelutti, N., Blais, J. M., Cumming, B. F., Paterson, A. M., Rühland, K., Wolfe, A.

P., & Smol, J. P. (2010). Do spectrally inferred determinations of chlorophyll a reflect trends in lake trophic status? *Journal of Paleolimnology*, *43*(2), 205-217.

Milinski, M. (1984). Parasites determine a predator's optimal feeding strategy. *Behavioral Ecology and Sociobiology*, *15*(1), 35-37.

Milinski, M. (1985). Risk of predation of parasitized sticklebacks (Gasterosteus aculeatus L.) under competition for food. *Behaviour*, *93*(1), 203-216.

Miller, J. F. (1963). Probable maximum precipitation and rainfall-frequency data for Alaska.

Minagawa, M., & Wada, E. (1984). Stepwise enrichment of 15N along food chains: further evidence and the relation between δ15N and animal age. *Geochimica et Cosmochimica Acta*, *48*(5), 1135-1140.

Morel, F. M., Kraepiel, A. M., & Amyot, M. (1998). The chemical cycle and bioaccumulation of mercury. *Annual Review of Ecology and Systematics*, *29*(1), 543-566.

Muir, D. C. G., Wang, X., Yang, F., Nguyen, N., Jackson, T. A., Evans, M. S., ... & Smol, J. P. (2009). Spatial trends and historical deposition of mercury in eastern and northern Canada inferred from lake sediment cores. *Environmental Science & Technology*, *43*(13), 4802-4809.

Naimo, T. J. (1995). A review of the effects of heavy metals on freshwater mussels. *Ecotoxicology*, *4*(6), 341-362.

Nelson, J. S. (1968). Salinity tolerance of brook sticklebacks, Culaea inconstans, freshwater ninespine sticklebacks, Pungitius pungitius, and freshwater fourspine sticklebacks, Apeltes quadracus. *Canadian Journal of Zoology*, *46*(4), 663-667.

Obrist, D., Agnan, Y., Jiskra, M., Olson, C. L., Colegrove, D. P., Hueber, J., ... & Helmig, D. (2017). Tundra uptake of atmospheric elemental mercury drives Arctic mercury pollution. *Nature*, *547*(7662), https://doi.org/10.1038/nature22997

Oksanen, J., Blanchet, F. G., Kindt, R., Legendre, P., Minchin, P. R., O'hara, R. B., ... & Oksanen, M. J. (2013). Package 'vegan'. *Community ecology package, version*, *2*(9).

Olefeldt, D., Goswami, S., Grosse, G., Hayes, D., Hugelius, G., Kuhry, P., ... & Turetsky, M. R. (2016). Circumpolar distribution and carbon storage of thermokarst landscapes. *Nature Communications*, *7*, doi:10.1038/13043.

Olson, B. H., & Cooper, R. C. (1974). In situ methylation of mercury in estuarine

sediment. *Nature*, *252*(5485), 682.

Ostdiek, J. L., & Nardone, R. M. (1959). Studies on the Alaskan Blackfish Dallia pectoralis I. Habitat, size and stomach analyses. *American Midland Naturalist*, 61(1), 218-229.

Oswald, C. J., Heyes, A., & Branfireun, B. A. (2014). Fate and transport of ambient mercury and applied mercury isotope in terrestrial upland soils: insights from the METAALICUS watershed. *Environmental Science & Technology*, *48*(2), 1023-1031.

Outridge, P. M., Sanei, H., Stern, G. A., Hamilton, P. B., & Goodarzi, F. (2007). Evidence for control of mercury accumulation rates in Canadian High Arctic lake sediments by variations of aquatic primary productivity. *Environmental Science & Technology*, *41*(15), 5259-5265.

Paerl, H.W. & Huisman, J (2008) Blooms like it hot. *Science* 320, 57-58.

Pappas, P. W., & Read, C. P. (1975). Membrane transport in helminth parasites: a review. *Experimental Parasitology*, *37*(3), 469-530.

Paranjape, A. R., & Hall, B. D. (2017). Recent advances in the study of mercury methylation in aquatic systems. *Facets*, *2*(1), 85-119.

Pascoe, D., & Cram, P. (1977). The effect of parasitism on the toxicity of cadmium to the three-spined stickleback, Gasterosteus aculeatus L. *Journal of Fish Biology*, *10*(5), 467-472.

Peterson, B. J., & Fry, B. (1987). Stable isotopes in ecosystem studies. *Annual Review of Ecology and Systematics*, *18*(1), 293-320.

Pickhardt, P. C., & Fisher, N. S. (2007). Accumulation of inorganic and methylmercury by freshwater phytoplankton in two contrasting water bodies. *Environmental Science & Technology*, *41*(1), 125-131.

Pickhardt, P. C., Folt, C. L., Chen, C. Y., Klaue, B., & Blum, J. D. (2002). Algal blooms reduce the uptake of toxic methylmercury in freshwater food webs. *Proceedings of the National Academy of Sciences*, *99*(7), 4419-4423.

Pinnegar, J. K., Campbell, N., & Polunin, N. V. C. (2001). Unusual stable isotope fractionation patterns observed for fish host—parasite trophic relationships. *Journal of Fish Biology*, *59*(3), 494-503.

Plug, L. J., & West, J. J. (2009). Thaw lake expansion in a two-dimensional coupled model of heat transfer, thaw subsidence, and mass movement. *Journal of Geophysical Research: Earth Surface*, *114*(F1), doi:10.1029/2006JF000740

Polis, G. A., & Strong, D. R. (1996). Food web complexity and community dynamics. *The American Naturalist*, *147*(5), 813-846.

Poulin, R., & Morand, S. (1999). Geographical distances and the similarity among parasite communities of conspecific host populations. *Parasitology*, *119*(4), 369-374.

Power, M., Klein, G. M., Guiguer, K. R. R. A., & Kwan, M. K. H. (2002). Mercury accumulation in the fish community of a sub-Arctic lake in relation to trophic position and carbon sources. *Journal of Applied Ecology*, *39*(5), 819-830.

Power, M., & Klein, G. M. (2004). Fish host–cestode parasite stable isotope enrichment patterns in marine, estuarine and freshwater fishes from northern Canada. *Isotopes in Environmental and Health Studies*, *40*(4), 257-266.

Prowse, T. D., Wrona, F. J., Reist, J. D., Gibson, J. J., Hobbie, J. E., Lévesque, L. M., & Vincent, W. F. (2006). Climate change effects on hydroecology of Arctic freshwater ecosystems. *AMBIO: A Journal of the Human Environment*, *35*(7), 347-359.

Przybylak, R. (2007). Recent air-temperature changes in the Arctic. *Annals of Glaciology*, *46*, 316-324.

Quinlan, R., Douglas, M. S., & Smol, J. P. (2005). Food web changes in arctic ecosystems related to climate warming. *Global Change Biology*, *11*(8), 1381-1386.

R Core Team (2017) R: A language and environment for statistical computing. R Foundation to Statistical Computing, Vienna http://www.R-project.org/

Ravichandran, M. (2004). Interactions between mercury and dissolved organic matter—a review. *Chemosphere*, *55*(3), 319-331.

Regnell, O. (1990). Conversion and partitioning of radio-labelled mercury chloride in aquatic model systems. *Canadian Journal of Fisheries and Aquatic Sciences*, *47*(3), 548-553.

Reist, J. D., Wrona, F. J., Prowse, T. D., Power, M., Dempson, J. B., King, J. R., & Beamish, R. J. (2006). An overview of effects of climate change on selected Arctic freshwater and anadromous fishes. *AMBIO: A Journal of the Human Environment*, *35*(7), 381-387.

Rice, K. M., Walker Jr, E. M., Wu, M., Gillette, C., & Blough, E. R. (2014). Environmental mercury and its toxic effects. *Journal of Preventive Medicine and Public Health*, *47*(2), 74-83

Roberts, K. E., Lamoureux, S. F., Kyser, T. K., Muir, D. C. G., Lafrenière, M. J., Iqaluk, D., ... & Normandeau, A. (2017). Climate and permafrost effects on the chemistry and ecosystems of High Arctic Lakes. *Scientific Reports*, *7*(1), 13292.

Robinson, S. A., Forbes, M. R., & Hebert, C. E. (2010). Mercury in parasitic nematodes and trematodes and their double-crested cormorant hosts: Bioaccumulation in the face of sequestration by nematodes. *Science of the Total Environment*, *408*(22), 5439-5444.

Rohatgi, A. (2016). Web Plot Digitizer. Austin, TX (software)

Rose, K. C., Williamson, C. E., Kissman, C. E., & Saros, J. E. (2015). Does allochthony in lakes change across an elevation gradient? *Ecology*, *96*(12), 3281-3291.

Rounick, J. S., & Winterbourn, M. J. (1986). Stable carbon isotopes and carbon flow in ecosystems. *BioScience*, *36*(3), 171-177.

Rouse, W. R., Douglas, M. S., Hecky, R. E., Hershey, A. E., Kling, G. W., Lesack, L., ... & Smol, J. P. (1997). Effects of climate change on the freshwaters of arctic and subarctic North America. *Hydrological Processes*, *11*(8), 873-902.

Rydberg, J., Klaminder, J., Rosén, P., & Bindler, R. (2010). Climate driven release of carbon and mercury from permafrost mires increases mercury loading to sub-arctic lakes. *Science of the Total Environment*, *408*(20), 4778-4783.

Saksvik, M., Nilsen, F., Nylund, A., & Berland, B. (2001). Effect of marine Eubothrium sp.(Cestoda: Pseudophyllidea) on the growth of Atlantic salmon, Salmo salar L. *Journal of Fish Diseases*, 24(2), 111-119.

Sandheinrich, M. B., & Wiener, J. G. (2011). Methylmercury in freshwater fish: recent advances in assessing toxicity of environmentally relevant exposures. *Environmental Contaminants in Biota: Interpreting Tissue Concentrations*, *2*, 169-190.

Saunders, J. T. (1914). A note on the food of freshwater fish. In *Proceedings of the Cambridge Philosophical Soc*iety, 17, 236-239.

Scheffer, M., Hosper, S. H., Meijer, M. L., Moss, B., & Jeppesen, E. (1993). Alternative equilibria in shallow lakes. *Trends in Ecology & Evolution*, *8*(8), 275-279.

Scheuhammer, A. M., Basu, N., Burgess, N. M., Elliott, J. E., Campbell, G. D., Wayland, M., ... & Rodrigue, J. (2008). Relationships among mercury, selenium, and neurochemical parameters in common loons (Gavia immer) and bald eagles (Haliaeetus leucocephalus). *Ecotoxicology*, *17*(2), 93-101.

Schindler, D.W. (1978) Factors regulating phytoplankton production and standing crop in the world's freshwaters. *Limnology and Oceanography 23*, 478-486.

Schultz, T. E., Topper, M., & C. Heins, D. (2006). Decreased reproductive investment of female threespine stickleback Gasterosteus aculeatus infected with the cestode Schistocephalus solidus: parasite adaptation, host adaptation, or side effect? *Oikos*, *114*(2), 303-310.

Schuster, P. F., Schaefer, K. M., Aiken, G. R., Antweiler, R. C., Dewild, J. F., Gryziec, J. D., ... & Liu, L. (2018). Permafrost stores a globally significant amount of mercury. *Geophysical Research Letters*, *45*(3), 1463-1471.

Scott, D. P., & Armstrong, F. A. J. (1972). Mercury concentration in relation to size in several species of freshwater fishes from Manitoba and northwestern Ontario. *Journal of the Fisheries Board of Canada*, *29*(12), 1685-1690.

Shuter, B. J., & Post, J. R. (1990). Climate, population viability, and the zoogeography of temperate fishes. *Transactions of the American Fisheries Society*, *119*(2), 314-336.

Sierszen, M. E., McDonald, M. E., & Jensen, D. A. (2003). Benthos as the basis for arctic lake food webs. *Aquatic Ecology*, *37*(4), 437-445.

Slemr, F., Schuster, G., & Seiler, W. (1985). Distribution, speciation, and budget of atmospheric mercury. *Journal of Atmospheric Chemistry*, *3*(4), 407-434.

Slemr, F., Brunke, E. G., Ebinghaus, R., Temme, C., Munthe, J., Wängberg, I., ... & Berg, T. (2003). Worldwide trend of atmospheric mercury since 1977. *Geophysical Research Letters*, *30*(10).

Smol, J. P., Wolfe, A. P., Birks, H. J. B., Douglas, M. S., Jones, V. J., Korhola, A., ... & Brooks, S. J. (2005). Climate-driven regime shifts in the biological communities of arctic lakes. *Proceedings of the National Academy of Sciences*, *102*(12), 4397-4402.

Smol, J. P. (2009). *Pollution of Lakes and Rivers: a Paleoenvironmental Perspective*. John Wiley & Sons.

St. Louis, V. L., Rudd, J. W., Kelly, C. A., Beaty, K. G., Bloom, N. S., & Flett, R. J. (1994). Importance of wetlands as sources of methyl mercury to boreal forest ecosystems. *Canadian Journal of Fisheries and Aquatic Sciences*, *51*(5), 1065-1076.

St. Pierre, K. A., Zolkos, S., Shakil, S., Tank, S. E., St. Louis, V. L., & Kokelj, S. V. (2018). Unprecedented increases in total and methyl mercury concentrations downstream of retrogressive thaw slumps in the western Canadian Arctic. *Environmental Science &*

Technology, *52*(24), 14099-14109.

Stabel, H. H. (1986). Calcite precipitation in Lake Constance: Chemical equilibrium, sedimentation, and nucleation by algae 1. *Limnology and Oceanography*, *31*(5), 1081-1094.

Stern, G. A., Sanei, H., Roach, P., Delaronde, J., & Outridge, P. M. (2009). Historical interrelated variations of mercury and aquatic organic matter in lake sediment cores from a subarctic lake in Yukon, Canada: further evidence toward the algal-mercury scavenging hypothesis. *Environmental Science & Technology*, *43*(20), 7684-7690.

Sures, B., Siddall, R., & Taraschewski, H. (1999). Parasites as accumulation indicators of heavy metal pollution. *Parasitology Today*, *15*(1), 16-21.

Swanson, H. K., & Kidd, K. A. (2010). Mercury concentrations in Arctic food fishes reflect the presence of anadromous Arctic charr (Salvelinus alpinus), species, and life history. *Environmental Science & Technology*, *44*(9), 3286-3292.

Swanson, H., Gantner, N., Kidd, K. A., Muir, D. C. G., & Reist, J. D. (2011). Comparison of mercury concentrations in landlocked, resident, and sea-run fish (Salvelinus spp.) from Nunavut, Canada. *Environmental Toxicology and Chemistry*, *30*(6), 1459-1467.

Systat Software. (2008). SigmaPlot for Windows, version 11.0.

Tchounwou, P. B., Ayensu, W. K., Ninashvili, N., & Sutton, D. (2003). Environmental exposure to mercury and its toxicopathologic implications for public health. *Environmental Toxicology: An International Journal*, *18*(3), 149-175.

Thieltges, D. W., Amundsen, P. A., Hechinger, R. F., Johnson, P. T., Lafferty, K. D., Mouritsen, K. N., ... & Poulin, R. (2013). Parasites as prey in aquatic food webs: implications for predator infection and parasite transmission. *Oikos*, *122*(10), 1473-1482.

Thienpont, J. R., Rühland, K. M., Pisaric, M. F., Kokelj, S. V., Kimpe, L. E., Blais, J. M., & Smol, J. P. (2013). Biological responses to permafrost thaw slumping in Canadian Arctic lakes. *Freshwater Biology*, *58*(2), 337-353.

Thompson, M. S., Kokelj, S. V., Prowse, T. D., & Wrona, F. J. (2008). The impact of sediments derived from thawing permafrost on tundra lake water chemistry: An experimental approach. In *Proceedings of the 9th International Conference on Permafrost, edited by: Kane, DL and Hinkel, KM* (Vol. 2, pp. 1763-1768).

Tierney, J. F., & Crompton, D. W. T. (1992). Infectivity of plerocercoids of Schistocephalus solidus (Cestoda: Ligulidae) and fecundity of the adults in an experimental definitive host, Gallus gallus. *The Journal of Parasitology*, *78*(6), 1049-1054.

Tierney, J. F., Huntingford, F. A., & Crompton, D. W. T. (1996). Body condition and reproductive status in sticklebacks exposed to a single wave of Schistocephalus solidus infection. *Journal of fish Biology*, *49*(3), 483-493.

Tierney, J. F., Huntingford, F. A., & Crompton, D. W. (1993). The relationship between infectivity of Schistocephalus solidus (Cestoda) and anti-predator behaviour of its intermediate host, the three-spined stickleback, Gasterosteus aculeatus. *Animal Behaviour 46,* 603-605.

Trenberth, K. E. (2011). Changes in precipitation with climate change. *Climate Research*, *47*(1-2), 123-138.

Trudel, M., & Rasmussen, J. B. (1997). Modeling the elimination of mercury by fish. *Environmental Science & Technology*, *31*(6), 1716-1722.

Trudel, M., & Rasmussen, J. B. (2006). Bioenergetics and mercury dynamics in fish: a modelling perspective. *Canadian Journal of Fisheries and Aquatic Sciences*, *63*(8), 1890-1902.

Tundra Times (1966) Sen to ask for $350 000 for road. Tundra Times, Barrow, AK.

Turcekova, L., Hanzelova, V., 1999. Concentrations of heavy metals from bottom sediments in fish and their endoparasites. 5th Int. Symp. Fish Parasites. Book of Abstracts, 153

Ullrich, S. M., Tanton, T. W., & Abdrashitova, S. A. (2001). Mercury in the aquatic environment: a review of factors affecting methylation. *Critical Reviews in Environmental Science and Technology*, *31*(3), 241-293.

U.S. Environmental Protection Agency (EPA) (1998) Method 1630 Methyl Mercury in Water by Distillation, Aqueous Ethylation, Purge and Trap, and Cold Vapor Atomic Fluorescence Spectrometry https://www.epa.gov/sites/production/files/2015-08/documents/method_1630_1998.pdf

U.S. Environmental Protection Agency (EPA) (1996) Method 1669 Sampling ambient water for trace metals at EPA water quality criteria levels https://www.epa.gov/sites/production/files/201510/documents/method_1669_1996.pdf

U.S. Environmental Protection Agency (EPA) (2007) Method 7473 e Mercury in Solids and Solutions by Thermal Decomposition, Amalgamation, and Atomic Absorption Spectroscopy, Revision 0. http://www.epa.gov/osw/hazard/testmethods/sw846/pdfs/7473.pdf

U.S Geological Survey (USGS) (2016) Earth Explorer. Earth Resources Observation and Science (EROS) Center, Sioux Falls, SD (software)

Vadeboncoeur, Y., Jeppesen, E., Zanden, M. J. V., Schierup, H. H., Christoffersen, K., & Lodge, D. M. (2003). From Greenland to green lakes: cultural eutrophication and the loss of benthic pathways in lakes. *Limnology and Oceanography*, *48*(4), 1408-1418.

Van Oostdam, J., Donaldson, S. G., Feeley, M., Arnold, D., Ayotte, P., Bondy, G., & Kalhok, S. (2005). Human health implications of environmental contaminants in Arctic Canada: a review. *Science of the Total Environment*, 351, 165-246.

Verburg, P., & Hecky, R. E. (2009). The physics of the warming of Lake Tanganyika by climate change. *Limnology and Oceanography*, *54*(6part2), 2418-2430.

Wagner, C. Adrian, R. (2009). Cyanobacteria dominance: quantifying the effects of climate change. *Limnology and Oceanography. 54*, 2460-2468.

Ward, D. M., Nislow, K. H., Chen, C. Y., & Folt, C. L. (2010). Rapid, efficient growth reduces mercury concentrations in stream-dwelling Atlantic salmon. *Transactions of the American Fisheries Society*, *139*(1), 1-10.

Watras, C. J., & Bloom, N. S. (1992). Mercury and methylmercury, in individual zooplankton: Implications for bioaccumulation. *Limnology and Oceanography*, *37*(6), 1313-1318.

Watras, C. J., Morrison, K. A., Host, J. S., & Bloom, N. S. (1995). Concentration of mercury species in relationship to other site-specific factors in the surface waters of northern Wisconsin lakes. *Limnology and Oceanography*, *40*(3), 556 565.

Weishaar, J. L., Aiken, G. R., Bergamaschi, B. A., Fram, M. S., Fujii, R., & Mopper, K. (2003). Evaluation of specific ultraviolet absorbance as an indicator of the chemical composition and reactivity of dissolved organic carbon. *Environmental Science & Technology*, *37*(20), 4702-4708.

Williams, H. H., Jones, A., & Crompton, D. W. T. (1994). *Parasitic worms of fish* (No. 04; SH175, W5.). London: Taylor & Francis.

Winch, S., Praharaj, T., Fortin, D., & Lean, D. R. S. (2008). Factors affecting methylmercury

distribution in surficial, acidic, base-metal mine tailings. *Science of the Total Environment*, *392*(2-3), 242-251.

Wolfe, A. P. (2002). Climate modulates the acidity of Arctic lakes on millennial time scales. *Geology*, *30*(3), 215-218.

Wolfe, A. P., Vinebrooke, R. D., Michelutti, N., Rivard, B., & Das, B. (2006). Experimental calibration of lake-sediment spectral reflectance to chlorophyll a concentrations: methodology and paleolimnological validation. *Journal of Paleolimnology*, *36*(1), 91-100.

Wrona, F. J., Prowse, T. D., Reist, J. D., Hobbie, J. E., Lévesque, L. M., & Vincent, W. F. (2006). Climate change effects on aquatic biota, ecosystem structure and function. *AMBIO: A Journal of the Human Environment*, *35*(7), 359-370.

Yang, H., & Rose, N. L. (2003). Distribution of mercury in six lake sediment cores across the UK. *Science of the Total Environment*, *304*(1-3), 391-404.

Appendix A- Chapter 2

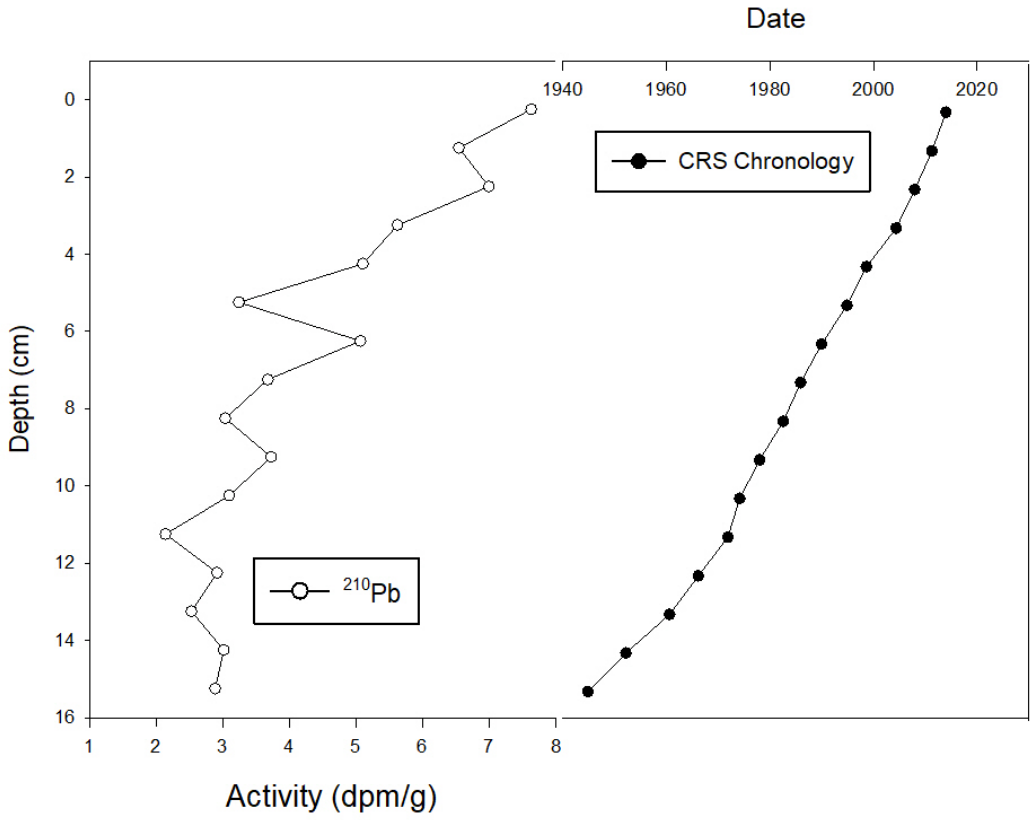

Figure S2.1. ^{210}Pb activity and depth-age profiles utilizing the constant rate of supply model for BRW 100 sediment core.

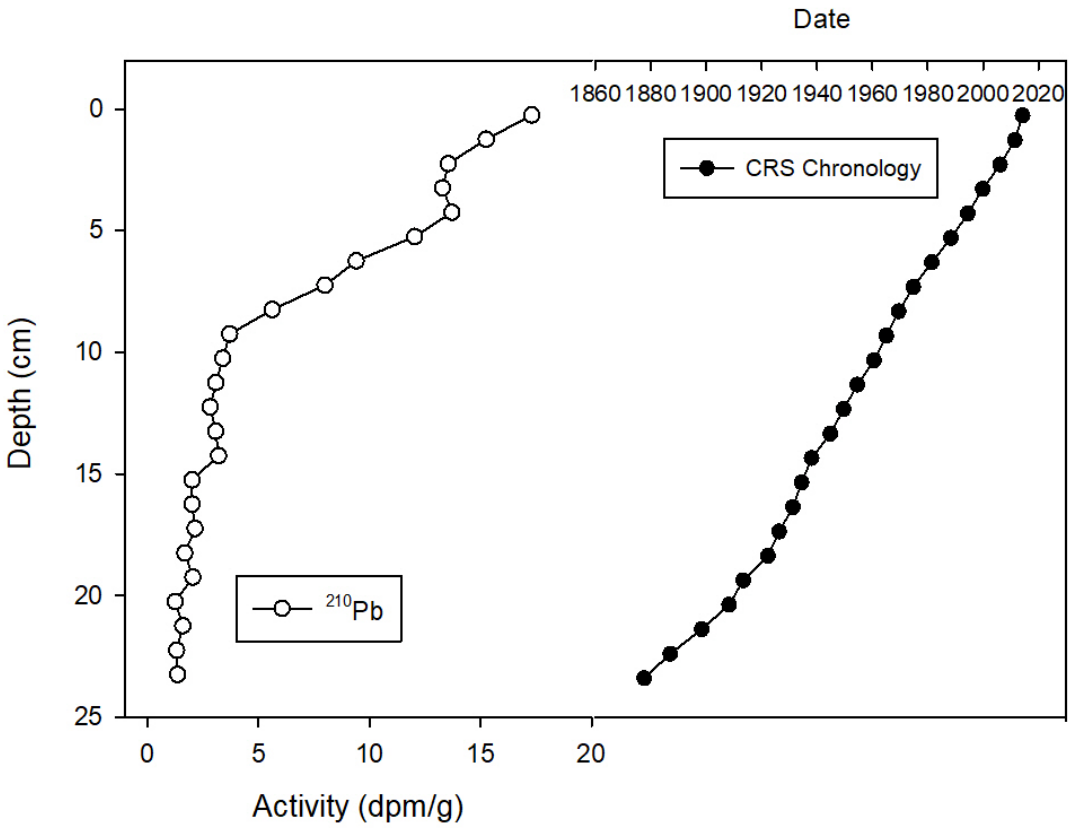

Figure S2.2. ^{210}Pb activity and depth-age profiles utilizing the constant rate of supply model for ATQ 206 sediment core.

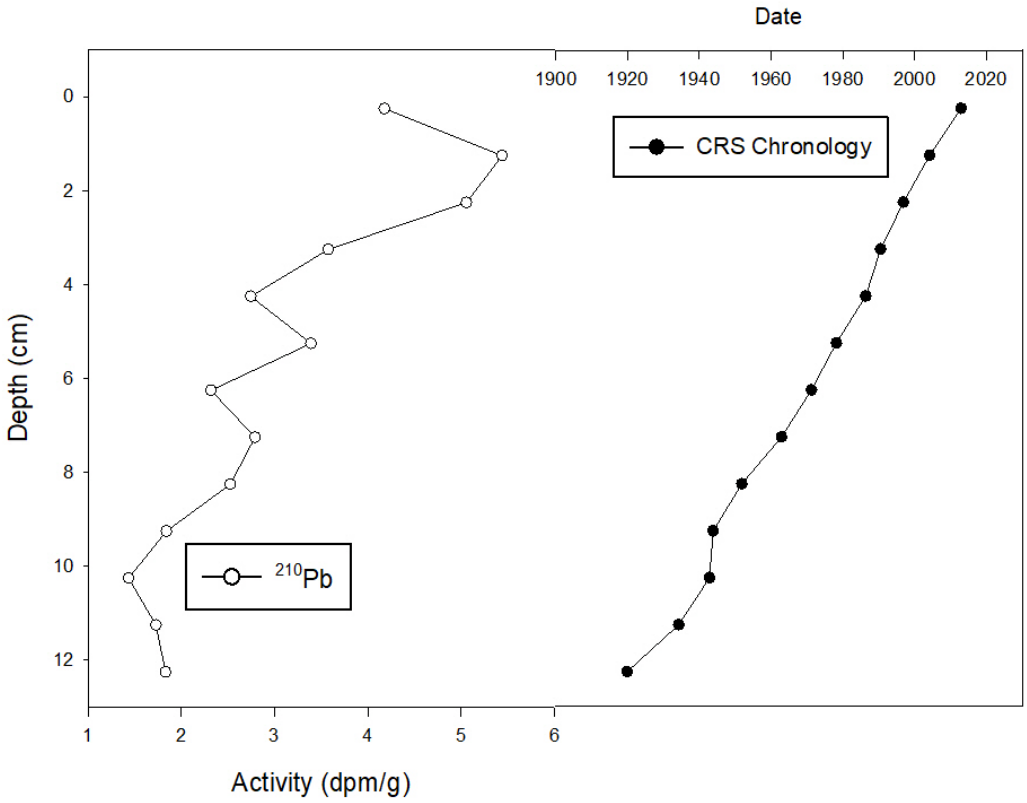

Figure S2.3. ^{210}Pb activity and depth-age profiles utilizing the constant rate of supply model for RDC 312 sediment core.

Table S2.1. Lake information from the sediment mercury accumulation meta-analysis from Chapter 2

Lake	Latitude	Longitude	Publication	Digitized (y/n)*	Focus-corrected (y/n)**	Mean accum. Rate (μg/m2/year)	Standard deviation	Trend	S	Kendall's τ	p value
2-A	68.84075	-134.102	Deison et al. 2012	N	Y	62.23	18.04	Negative	-2	-0.714	0.019
2-B	68.85356	-134.101	Deison et al. 2012	N	Y	23.88	13.58	Positive	19	0.905	0.007
Amituk	75	-93.8	Muir et al. 2009	Y	Y	1.34	0.56	Positive	27	0.700	0.020
AX-AJ	80	-87	Muir et al. 2009	Y	Y	32.55	13.79	Positive	34	0.944	<0.001
BI-02	73	-80	Muir et al. 2009	Y	Y	6.53	1.86	Positive	41	0.394	0.047
BK-AH	73.4	-119.4	Muir et al. 2009	Y	Y	2.73	0.59	No trend	-35	-0.389	0.062
Brady	58.32216667	136.681167	Engstrom et al. 1997	N	Y	11.84	2.30	Positive	36	0.462	0.033
Burial	68.402722	-159.22748	Landers et al. 2008 (WACAP)	N	Y	5.69	1.45	Positive	20	0.714	0.019
CF-11	70.3	-68.4	Muir et al. 2009	Y	Y	1.07	0.62	Positive	15	1.000	0.009
Char	74.6	-119.2	Muir et al. 2009	Y	Y	1.49	0.62	Positive	49	0.891	<0.001
Daglet	58.51916667	-137.33433	Engstrom et al. 1997	N	Y	10.23	1.99	Positive	35	0.778	0.002
Daltjørna	77.561902	14.20032	Drevnick et al. 2012	N	N	22.70	4.81	Positive	71	0.780	<0.001
DV-E	75.3	-89.5	Muir et al. 2009	Y	Y	4.02	0.66	No trend	4	0.667	0.308
Efficient	68.70228333	-149.7043	Fitgerald et al. 2005	N	Y	2.44	0.91	Positive	134	0.638	<0.001
Forgetful	68.88131667	-150.28305	Fitgerald et al. 2005	N	Y	3.16	0.83	Positive	51	0.486	0.013
Hazen	81.79931	-71.01128	Muir et al. 2009	Y	Y	21.91	2.29	No trend	-44	-0.102	0.442
Lake 53	66.494	-53.53	Bindler et al. 2001	Y	N	3.69	1.32	Positive	78	0.862	<0.001
Lake 70	66.954	-51.583	Bindler et al. 2001	Y	N	6.23	3.00	No trend	18	0.405	0.127
Matacharak	67.747846	-156.21054	Landers et al. 2008 (WACAP)	N	Y	2.33	1.00	Positive	30	0.833	0.002
MB-AC	76.2	-119.2	Muir et al. 2009	Y	Y	12.56	2.56	Positive	230	0.836	<0.001
MB-S	76.1	-119.2	Muir et al. 2009	Y	Y	6.77	0.40	No trend	0	0.000	1.000
Mcleod	63.373261	-151.08877	Landers et al. 2008 (WACAP)	N	Y	2.65	0.70	Positive	73	0.477	0.006
North	74.8	-90.1	Muir et al. 2009	Y	Y	1.35	0.53	Positive	54	0.818	<0.001
Nunatak	66.965	-49.802	Bindler et al. 2001	Y	N	8.24	1.62	Positive	17	0.810	0.016

Ossian Sarsfjellet	78.950858	12.49818	Drevnick et al. 2012	N	N	4.00	1.86	Positive	26	0.722	0.009
Perfect	68.64801667	-149.77787	Fitgerald et al. 2005	N	Y	5.85	1.61	Positive	151	0.883	<0.001
Relaxing	68.740877	-150.03749	Fitgerald et al. 2005	N	Y	2.48	0.99	Positive	197	0.853	<0.001
Rocky Basin	78.4	-77.5	Muir et al. 2009	Y	Y	2.35	1.00	Positive	10	1.000	0.03
Romulus	79.5	85.1	Muir et al. 2009	Y	Y	7.77	2.65	Positive	35	0.778	0.002
Rummy	69.08379	-123.6379	Muir et al. 2009	Y	Y	6.80	0.94	No trend	13	0.619	0.072
SHI-L4	65	-83.8	Muir et al. 2009	Y	Y	6.46	3.03	Positive	75	0.824	<0.001
SHI-L7	65.2	-85.2	Muir et al. 2009	Y	Y	20.34	5.61	No trend	6	0.167	0.602
Surprise	68.5445	-149.64868	Fitgerald et al. 2005	N	Y	3.83	2.10	Positive	270	0.900	<0.001
Vassauga	78.216667	12.933333	Drevnick et al. 2012	N	N	7.30	3.35	Positive	26	0.929	0.002
West	74.9	-109.7	Muir et al. 2009	Y	Y	8.21	4.13	Positive	27	0.761	0.006
Wonder	63.475235	-150.87638	Landers et al. 2008 (WACAP)	N	Y	2.59	1.26	Positive	26	0.929	0.002
Yterjørna	78.75	12.95	Drevnick et al. 2012	N	N	12.21	9.69	Positive	230	0.836	<0.001

Appendix B – Chapter 3

Table S3.1. Results from the percent methyl mercury analysis on a sub-sample of Ninespine stickleback from lakes on the Arctic Coastal Plain of Alaska

Lake	n	Mean % MeHg	Standard Deviation
ATQ 200	6	77.2	7.5
ATQ 201	4	73.5	8.4
ATQ 206	6	75.8	8.3
RDC 308	6	74.4	9.0
RDC 309	6	82.6	8.2
RDC 311	6	90.8	7.2

Table S3.2. Presence/Absence of different benthic macroinvertebrate taxa of lakes on the Arctic Coastal Plain of Alaska; taxon presence is indicated with an "X".

	Atqasuk Lakes			Reindeer Camp Lakes		
Taxa	**ATQ 200**	**ATQ 201**	**ATQ 206**	**RDC 308**	**RDC 309**	**RDC 311**
Brachycentridae	X	X	X	X	X	X
Ceratapogonidae			X			
Chironimidae	X	X	X	X	X	X
Cnidaria	X		X			
Corixidae				X	X	
Dytsicidae	X		X	X	X	X
Gammarus				X		X
Hirudinea		X	X		X	X
Hydrarachnidae	X	X	X	X	X	X
Hydroptilidae		X				
Limnephilidae	X	X	X		X	
Lymnaeidae			X	X		X
Notastraca	X					
Oligochaeta	X	X	X	X	X	X
Perlodidae	X	X	X	X	X	X
Physidae			X	X		X
Planorbidae		X			X	
Pleidae					X	
Sphaeridae	X	X	X	X	X	X
Tanypodinae	X	X	X	X	X	X
Tipulidae	X		X			X
Turbellaria	X					
Valvatidae		X	X	X	X	X

Appendix C- Chapter 4

Table S4.1. Results from the percent methyl mercury analysis on a sub-sample of Ninespine stickleback from lakes on the Arctic Coastal Plain of Alaska

Lake	n	Mean % MeHg	Standard Deviation
ATQ 200	6	77.2	7.5
ATQ 201	4	73.5	8.4
ATQ 206	6	75.8	8.3
RDC 308	6	74.4	9.0
RDC 309	6	82.6	8.2
RDC 311	6	90.8	7.2

Table S4.2. Fish ID and age for parasitized fish, and cumulative weight and number of *Schistocephalus punigitius* pleroceroids from each of six study lakes on the Arctic Coastal Plain of Alaska

Lake	Fish ID	Fish age (years)	Parasite cumulative weight (g)	n	Lake	Fish ID	Fish age (years)	Parasite cumulative weight (g)	n
ATQ 200	NST 217	1	0.01	1	ATQ 206	NST 178	1	0.12	1
ATQ 200	NST 273	2	0.14	1	ATQ 206	NST 183	1	0.02	1
ATQ 200	NST 274	3	0.39	2	ATQ 206	NST 186	1	0.1	1
ATQ 200	NST 275	3	0.64	3	RDC 308	NST 346	2	0.19	1
ATQ 200	NST 285	1	0.09	1	RDC 308	NST 349	3	0.27	1
ATQ 200	NST 291	2	0.14	1	RDC 308	NST 350	3	0.23	1
ATQ 200	NST 301	1	0.11	1	RDC 308	NST 352	4	0.25	1
ATQ 200	NST 307	1	0.11	1	RDC 308	NST 359	2	0.25	1
ATQ 200	NST 310	n/a	0.01	2	RDC 308	NST 361	3	0.25	1
ATQ 201	NST 104	2	0.76	3	RDC 308	NST 369	1	0.07	1
ATQ 201	NST 105	4	0.57	3	RDC 309	NST 226	1	0.2	1
ATQ 201	NST 106	4	0.58	3	RDC 309	NST 227	1	0.17	1
ATQ 201	NST 107	4	0.36	2	RDC 309	NST 228	2	0.28	1
ATQ 201	NST 108	3	0.3	1	RDC 309	NST 229	1	0.18	1
ATQ 201	NST 109	n/a	0.58	3	RDC 309	NST 230	1	0.14	1
ATQ 201	NST 110	3	0.49	2	RDC 309	NST 234	n/a	0.21	1
ATQ 201	NST 111	3	0.65	2	RDC 309	NST 235	2	0.25	1
ATQ 201	NST 112	3	0.27	1	RDC 309	NST 237	1	0.15	1
ATQ 201	NST 113	4	0.29	1	RDC 309	NST 240	1	0.17	1
ATQ 201	NST 114	3	0.25	1	RDC 309	NST 381	1	0.16	1
ATQ 201	NST 115	4	0.22	1	RDC 309	NST 394	n/a	0.45	1
ATQ 201	NST 116	3	0.62	3	RDC 311	NST 2	3	0.28	1
ATQ 201	NST 117	4	0.23	1	RDC 311	NST 3	3	0.3	1
ATQ 201	NST 118	4	0.33	1	RDC 311	NST 5	2	0.47	3
ATQ 201	NST 119	2	0.43	2	RDC 311	NST 6	2	0.44	2
ATQ 201	NST 120	3	0.49	3	RDC 311	NST 8	3	0.11	1
ATQ 201	NST 121	4	0.35	2	RDC 311	NST 11	3	0.25	1
ATQ 201	NST 122	3	0.34	2	RDC 311	NST 12	3	0.55	2
ATQ 201	NST 123	4	0.47	2	RDC 311	NST 13	2	0.08	1
ATQ 201	NST 124	2	0.41	2	RDC 311	NST 14	3	0.03	1

ATQ 201	NST 125	3	0.23	1	RDC 311	NST 17	3	0.29	2
ATQ 201	NST 126	4	0.56	3	RDC 311	NST 18	3	0.32	1
ATQ 201	NST 127	4	0.27	1	RDC 311	NST 20	2	0.27	1
ATQ 201	NST 128	3	0.33	1	RDC 311	NST 21	2	0.41	3
ATQ 201	NST 129	4	0.38	2	RDC 311	NST 22	3	0.49	2
ATQ 201	NST 130	3	0.29	1	RDC 311	NST 23	2	0.22	4
ATQ 201	NST 131	4	0.53	3	RDC 311	NST 24	4	0.69	2
ATQ 201	NST 132	3	0.59	2	RDC 311	NST 25	3	0.01	1
ATQ 201	NST 133	4	0.21	1	RDC 311	NST 26	2	0.05	2
ATQ 201	NST 134	2	0.47	3	RDC 311	NST 27	1	0.08	1
ATQ 201	NST 135	4	0.36	1	RDC 311	NST 28	3	0.15	1
ATQ 201	NST 136	3	0.38	2	RDC 311	NST 29	3	0.42	2
ATQ 201	NST 137	3	0.66	3	RDC 311	NST 30	3	0.35	1
ATQ 201	NST 138	3	0.28	3	RDC 311	NST 31	2	0.28	1
ATQ 201	NST 139	3	0.4	3	RDC 311	NST 32	4	0.31	1
ATQ 201	NST 140	3	0.49	2	RDC 311	NST 33	3	0.13	2
ATQ 201	NST 141	3	0.42	3	RDC 311	NST 34	3	0.1	1
ATQ 201	NST 142	4	0.42	2	RDC 311	NST 36	1	0.13	1
ATQ 201	NST 143	4	0.21	1	RDC 311	NST 37	3	0.29	1
ATQ 201	NST 144	3	0.2	2	RDC 311	NST 38	4	0.36	1
ATQ 201	NST 146	4	0.2	2	RDC 311	NST 39	3	0.18	1
ATQ 201	NST 147	4	0.27	1	RDC 311	NST 40	2	0.14	1
ATQ 201	NST 148	3	0.37	2	RDC 311	NST 43	2	0.3	1
ATQ 201	NST 149	3	0.37	2	RDC 311	NST 44	2	0.21	1
ATQ 201	NST 150	2	0.37	4	RDC 311	NST 45	2	0.27	1
ATQ 201	NST 151	2	0.34	2	RDC 311	NST 46	2	0.26	1
ATQ 201	NST 152	3	0.37	2	RDC 311	NST 48	2	0.22	1
ATQ 201	NST 153	3	0.44	2	RDC 311	NST 49	3	0.07	2
ATQ 206	NST 163	1	0.26	2	RDC 311	NST 50	3	0.19	1